WSRC-TR-2000-00398, Revision 0

Sludge Batch 2 (Macrobatch3) Flowsheet Studies with Simulants

D. C. Koopman
Westinghouse Savannah River Company
Aiken, SC 29808

This document was prepared in conjunction with work accomplished under Contract No. DE-AC09-96SR18500 with the U.S. Department of Energy.

DISCLAIMER

This report was prepared as an account of work sponsored by an agency of the United States Government. Neither the United States Government nor any agency thereof, nor any of their employees, makes any warranty, express or implied, or assumes any legal liability or responsibility for the accuracy, completeness, or usefulness of any information, apparatus, product or process disclosed, or represents that its use would not infringe privately owned rights. Reference herein to any specific commercial product, process or service by trade name, trademark, manufacturer, or otherwise does not necessarily constitute or imply its endorsement, recommendation, or favoring by the United States Government or any agency thereof. The views and opinions of authors expressed herein do not necessarily state or reflect those of the United States Government or any agency thereof.

This report has been reproduced directly from the best available copy.

Available for sale to the public, in paper, from: U.S. Department of Commerce, National Technical Information Service, 5285 Port Royal Road, Springfield, VA 22161, phone: (800) 553-6847, fax: (703) 605-6900, email: orders@ntis.fedworld.gov online ordering: http://www.ntis.gov/support/ordering.htm

Available electronically at http://www.osti.gov/bridge/

Available for a processing fee to U.S. Department of Energy and its contractors, in paper, from: U.S. Department of Energy, Office of Scientific and Technical Information, P.O. Box 62, Oak Ridge, TN 37831-0062, phone: (865) 576-8401, fax: (865) 576-5728, email: reports@adonis.osti.gov

Executive Summary

Sludge-only process simulations of the Sludge Receipt and Adjustment Tank (SRAT) and the Slurry Mix Evaporator (SME) cycle were conducted for the two most likely scenarios for Sludge Batch 2 (Macrobatch 3). The two scenarios are a roughly 50:50 blend of Tank 8 and Tank 40 washed sludge and Tank 40 washed sludge by itself. The testing used new simulants of Tank 8 and Tank 40 washed sludge prepared at the University of South Carolina. The washing endpoint was about 0.5 moles sodium per liter supernate. This report summarizes both the simulant preparation and process simulation activities. The rheology work requested in the Task Plan will be documented in a separate report.

Two scoping SRAT simulations were conducted for Tank 40 sludge. This was followed by a complete SRAT and SME simulation using Sludge Batch 1B acid stoichiometry (137.5%). Four scoping SRAT simulations were conducted for the Tank 8/40 blend. Three complete SRAT and SME simulations using blended sludge were then performed. One was at the recommended acid stoichiometry of 125%. The second used identical acid stoichiometry with HM levels of noble metals. The final run was at worst case noble metals and assumed complete transfer of the Formic Acid Feed Tank. Testing was completed without any major incidents. The table below summarizes the experiments more or less

chronologically. Hydrogen flow rates in excess of the design bases (0.65 lbs./hr for the SRAT and 0.23 lbs./hr for the SME) are marked in bold. Full details on the noble metals concentrations can be found in the body of the report.

Key Words: DWPF, CPC, Sludge, Tank 42, Tank 8, Tank 40, Sludge Batch 2, Macrobatch 3, SRAT, SME, Antifoam,
Catalyst, Simulant

SRAT/SME Experiment Summary Table

Run ID	Sludge	Noble Metals	Acid Stoichi-ometry	SRAT H_2, lbs./hr	SME H_2, lbs./hr	SRAT N_2O, vol. %	SME N_2O, vol. %
1A	40	Very High[2]	137.5%	**1.69**	-	1.08	-
2A	40	Low[3]	137.5%	0.0013	-	1.15	-
1B	8/40	Very High[2]	137.5%	**1.04**	-	2.17	-
2B	8/40	High[4]	137.5%	0.475	-	0.526	-
3B	8/40	High[4]	125%	0.385	-	0.718	-
4B	8/40	High[4]	110%	0.054	-	0.394	-
SB2-1	8/40	High[4]	125%	0.355	0.14	0.671	0.198
SB2-2	40	Low[3]	137.5%	0.0018	0.0010	1.12	0.00
SB2-3	8/40	HM[1]	125%	0.311	0.122	0.758	0.185
SB2-4	8/40	Worst Case[5]	290%	**6.67**	**3.00**	1.745	0.00

1 – HM technical basis for noble metal concentrations (higher than the Purex basis)
2 – Tank 8 and Tank 40 noble metals estimated by H. Elder from information in the High Level Waste database. All four noble metals exceed HM concentrations.
3 – Measured by Bibler and Fellinger on a sample of real Tank 40 sludge.
4 – Measured Tank 40 noble metals combined with H. Elder estimates for Tank 8.
5 – H. Elder estimate for Tank 8 noble metals used for both tanks.

Significant Findings

- An acid stoichiometry target of 125% is recommended for the Shielded Cells run, because it yields adequate nitrite destruction, based on runs 2B-4B, without presenting as many problems with high hydrogen generation rates.
- Noble metal concentrations predicted from the High Level Waste Database plus 137.5% acid stoichiometry led to hydrogen generation rates that exceeded the DWPF design basis in the SRAT cycle.
- Total SRAT hydrogen generation decreased nonlinearly with decreasing acid stoichiometry and noble metal content. Noble metal concentrations in these tests were higher overall than in other recent tests.
- Hydrogen generation data strongly suggest that more than one noble metal could be significantly affecting hydrogen generation. Rhodium has been considered the primary catalyst for hydrogen generation. Rhodium is generally present at an order of magnitude lower concentration than either palladium or ruthenium in the High Level Waste database.
- Foaming was not controlled by the traditional DWPF antifoam addition strategy. Recommended new strategies are at about two to three times the old levels for the SRAT cycle.
- Formate destruction in the SME product varied with acid stoichiometry making prediction of formate and nitrate ion concentrations difficult, and consequently making prediction of redox by F-3N more difficult.
- Molar carbon dioxide evolution rates tracked, but were generally greater than, hydrogen evolution rates in the second half of the SRAT cycle. The ratio of the molar generation rates ranged from near unity to about twenty. The implication is that formic acid reduction reactions may have been occurring throughout the SRAT cycle.

Reduction of mercury, nitrite, and manganese are likely complete. Either formic acid is reacting with oxygen or with other sludge solids (by poorly characterized reactions) rather than decomposing to hydrogen and carbon dioxide by catalytic decomposition.
- Nitrous oxide generation was well below the concentration needed to impact the design basis.
- Nitrite ion was destroyed in all SRAT tests.
- The mercury content of the two sludges was low, and it was essentially a non-factor in processing the sludge.
- Glasses made from the four different simulated melter feeds were all good based on the Product Consistency Test.
- The air-dried total solids content of sludge simulant was strongly effected by how the hydrous ferric oxide is precipitated. This uncertainty needs to be factored into any new simulant recipes.

Background

The Defense Waste Processing Facility, DWPF, began processing radioactive Tank 51 sludge (Sludge Batch 1A) in 1996 and continued with processing Tank 42 sludge (Sludge Batch 1B) in 1998. At the current processing rate, Batch 1B is projected to be depleted as early as June 2001. Current plans call for DWPF to begin processing radioactive sludge fed from Tank 40 at that time (Sludge Batch 2). If all goes as planned, Sludge Batch 2 will include the radioactive sludge currently in Tank 8 (in addition to the sludge already in Tank 40) before DWPF processing commences.

DWPF continues to operate under the sludge-only process flowsheet. Testing is required to demonstrate a sludge-only process for Sludge Batch 2. This document details the testing performed in support of the Sludge Batch 2 sludge-only process using non-radioactive sludge simulants. To cover unexpected contingencies, the testing included studies with Tank 40 sludge simulant and with a blend of Tank 40 and Tank 8 sludge simulants.

Introduction

SRTC/ITS received a Technical Task Request, HLW/DWPF/TTR-00-0014, "Sludge Batch 2 (Macrobatch 3) Flowsheet Studies", from Maria A. Rios-Armstrong in March of 2000. The task was accepted by Sharon L. Marra, SRT-PTD-2000-0008, on March 13. Daniel P. Lambert was designated as the Task Leader. A Task Technical and QA Plan, WSRC-RP-2000-00191, "Sludge Batch 2 (Macrobatch 3) Flowsheet Studies with Simulants", was issued and approved in mid-May of 2000. David C. Koopman was designated as the lead researcher for this task and had the overall responsibility for coordinating the activities of all participants.

Per the approved Task Plan, several process simulations were performed at different processing conditions to better define satisfactory processing parameters for the new sludge batch. The process was monitored for problems such as foaming, off-gas deposits, and for target parameters such as nitrite destruction, mercury removal, and off-gas composition and generation rate during the experiments.

These experiments duplicated expected SRAT and SME processing conditions in laboratory scale vessels. One key objective of this test program was to develop the processing parameters for the Shielded Cells verification run with actual waste samples. The parameters to be studied to meet this objective included:

- The maximum hydrogen generation rate during both the SRAT and SME processing cycles.
- The maximum nitrous oxide (N_2O) generation rate during the SRAT and SME processing cycles.
- The minimum time necessary for completing the steam stripping of mercury to reach the 0.45 wt. % mercury limit for the SRAT product.
- The correct acid addition scheme necessary to produce a melter feed with a redox of about 0.2 Fe^{2+}/SFe. Nitrate and formate ion destruction must be understood in order to predict this.

- The acid stoichiometry necessary to achieve complete nitrite ion destruction in the SRAT processing cycle (defined as a nitrite concentration of less than 1000 mg/Kg).
- The quality of the glass as predicted by the Product Composition Control System (PCCS) and measured by the Product Consistency Test (PCT).

Additional task objectives include:

- Preparation of new non-radioactive simulant sludges to approximate the expected post-washed compositions of Tank 8 and Tank 40 sludges.
- Quantifying the maximum hydrogen generation rate for a credible over-batching of the SRAT with 90 wt. % formic acid, i.e. a complete transfer of Formic Acid Tank contents.
- Making rheological measurements of the SRAT and SME products as functions of temperature and wt. % total solids.
- Supporting testing for the proposed transition to IIT747 antifoam from Dow Corning 544 antifoam.
- Performing the work within the context of the Conduct of R&D Manual.

Discussion

Overview of New Sludge Simulant Preparation

Herbert H. (Hank) Elder [May, 2000] performed an analysis of the High Level Waste Database [Hester] to predict the current compositions of Tank 8 and Tank 40 sludge. These compositions were then adjusted to the expected endpoints of the sludge washing process, about 0.5 M sodium. Radioisotopes were removed from the composition if a non-radioactive substitute was not available. Trace components with no known catalytic properties were also dropped from the recipe. A synthesis recipe was prepared for two cases – with and without insoluble sodium. A composition of a blend of Tank 8 and Tank 40 following sludge washing was also generated.

A decision was made later to proceed with the recipes without the insoluble sodium. This decision leads to the expected supernate concentration and should give more representative SRAT chemistry. The sodium content in any glass would be lower than for real waste, however, unless additional sodium species were added to the SME product. If the other choice were made, the insoluble sodium would be present in the simulant as soluble sodium salts, since no suitable insoluble sodium compound has been identified for the simulant recipes. The salts could include sodium hydroxide and sodium carbonate. This would impact the acid calculation/stoichiometry.

At the early stages of this work, it was uncertain whether or not the transfer of Tank 8 sludge to Tank 40 would be made in time for Sludge Batch 2. It was decided to be conservative and prepare Tank 40 simulant without the Tank 8 contribution. In addition, a Tank 8 simulant would be made that could be combined with the Tank 40 simulant to model various blends of the two sludges.

The recipe in Elder's report for washed Tank 8 simulant was modified slightly in its aluminum and sodium contents. Details are given in Appendix A: *Preparation of Tank 8 and Tank 40 Sludge Simulants.* This was necessary because the combined endpoints for separately washed Tank 8 and Tank 40 simulants did not match the supernate composition and aluminum content of the predicted washed blend (blended before washing).

Dr. Vincent van Brunt of the Chemical Engineering Department at the University of South Carolina, Columbia, South Carolina, was contracted to prepare approximately 300 gallons of Tank 40 sludge simulant and 300 gallons of Tank 8 sludge simulant. The details of this work are included in Appendix A. SRTC/ITS received three 55-gallon drums of both sludge simulants. Tank 8 simulant for this testing was drawn from drum #1 of the USC Tank 8 shipment. Tank 40 simulant for this testing was drawn from drum #3 of the USC Tank 40 shipment, with revised supernate as modified at TNX (to bring nitrate down to the expected concentration).

Shortly before the SRAT scoping runs were to start, an analysis of actual Tank 40 sludge became available. After meeting with the customer, it was decided to increase the nickel and manganese content of the Tank 40 simulant prior

to starting the scoping runs. The nickel content of the Tank 40 sludge solids was increased from zero to 0.35 wt. % (on an air-dried solids basis) using $NiCl_2 \cdot 6H_2O$. The manganese content of the Tank 40 sludge solids was increased from 1.26 to 2.65 wt. % using moist MnO_2 precipitated at TNX in 1998. Other differences between the simulant recipe and the initial Tank 40 waste analyses are discussed in Appendix A. A sludge blend was then prepared containing 10 kg of Tank 40 and 10 kg of Tank 8 simulant. This gave the 52% Tank 40 solids/48% Tank 8 solids (on an air-dried solids basis) ratio specified in Elder's report. During the SRAT cycle scoping runs, an evaluation of the noble metal content of the Tank 40 waste sample became available. These values were substituted for those in the Elder report after the initial two scoping runs had been completed.

Experimental

The testing was done using two sets of the experimental apparatus shown in Figure 1.

Figure 1. Schematic of Experimental Apparatus

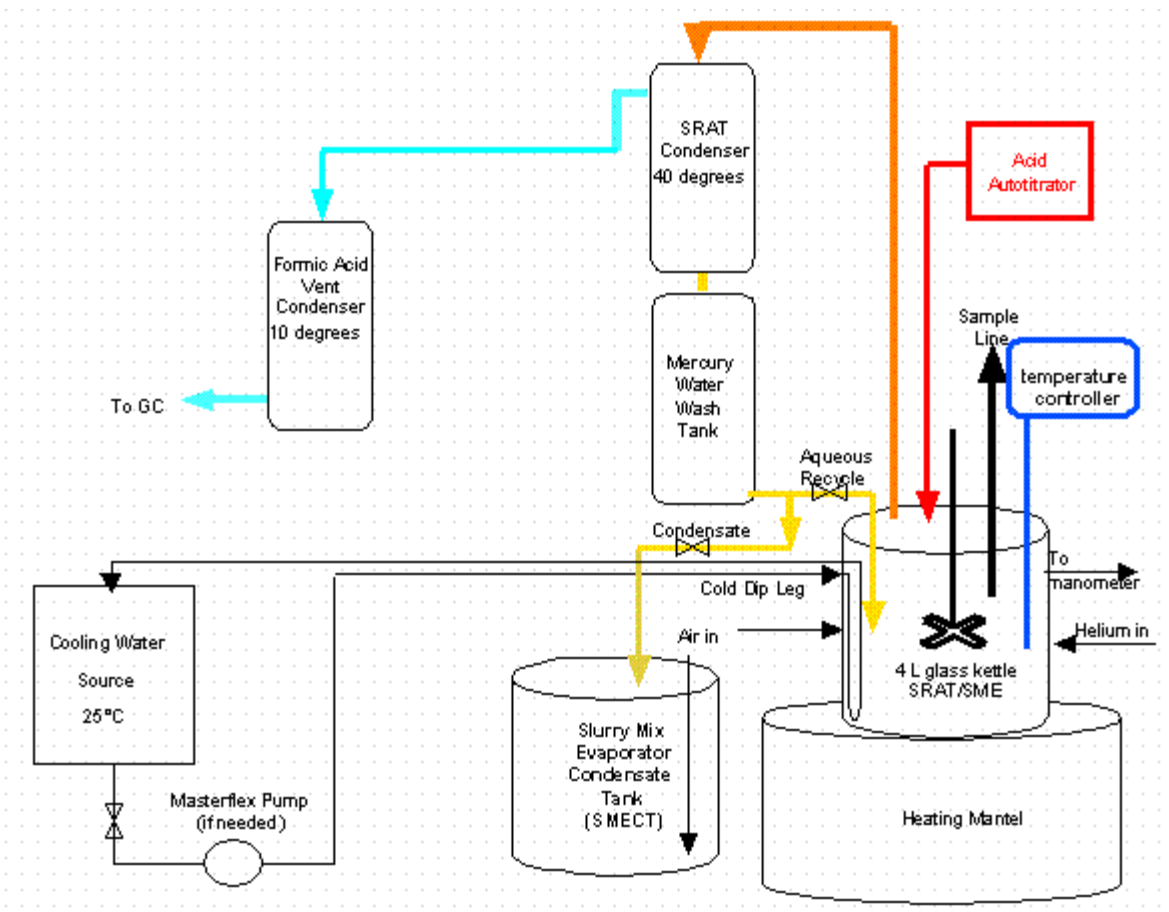

The runs were completed in the 772 labs at the Multipurpose Pilot Plant Campus (TNX). There were six four-liter vessel scoping runs simulating the SRAT cycle only. The scoping run simulations were done on extended day shifts, but still required part of a second day to complete. These runs were a prerequisite for the four variability study runs called for in the Task Plan. The variability study runs also used the four-liter vessel apparatus, but the simulation included both the SRAT and the SME cycles, and the testing was continuous from start to finish. The experimental design volumetrically scaled the DWPF vessels and flows. The duration of batch events was matched to nominal DWPF values. Simulations were at 1/9000th of DWPF scale based on a 6000-gallon DWPF sludge batch.

The SRAT cycle included all of the important DWPF processing steps. These included sludge preparation, sludge analysis, batching calculations, heat-up to 93° C, addition of first nitric acid, then formic acid, heat-up to boiling, concentration down to 6000 gallons, followed by additional boiling under reflux (twelve hours total at boiling). The key activities of the SRAT cycle included neutralization of the sludge, reduction of various metals including manganese, mercury, and noble metals, and destruction of nitrite (defined as <1000 mg/Kg nitrite ion left in solution). Key supporting data included hydrogen, carbon dioxide, and nitrous oxide generation rates; the nitrite, nitrate, and formate destruction rates; estimated oxygen depletion rate; pH, boil-up rate; and foaming tendency. A significant mass of sample was removed following the SRAT cycle for use in rheology work.

The SME cycle included the initial addition of a frit 200-water-formic acid slurry, boiling off water added with this slurry, a second addition of a frit 200-water-formic acid slurry, boiling off water until the volume is no larger than at the beginning of the cycle, cool down, and sampling. Key data included measurements of the hydrogen generation rate, carbon dioxide generation rate, glass quality, and foaming likelihood. The SME product remaining, after samples were taken for analysis and PCT, is intended to be used in future rheology work.

The scoping runs included two SRAT simulations using Tank 40 simulant and four SRAT simulations using a blend of Tank 8 and Tank 40 simulants. The significant parameters differentiating the six scoping runs are detailed in Table 1 below.

Table 1 – SRAT Cycle Scoping Run Summary

Run No.	Sludge	Date	Noble Metals	Acid Target
1A	Tank 40	7/31-8/1	note 1	137.5%
2A	Tank 40	8/7-8/8	note 2	137.5%
1B	Tank 8/40 Blend	7/31-8/1	note 3	137.5%
2B	Tank 8/40 Blend	8/7-8/8	note 4	137.5%
3B	Tank 8/40 Blend	8/10-8/11	note 4	125%
4B	Tank 8/40 Blend	8/10-8/11	note 4	110%

1. Noble metals per H. Elder's report for Tank 40 added at 110%.
2. Noble metals as analyzed by Ned E. Bibler and Terri L. Fellinger for Tank 40 added at 110%.
3. Noble metals per H. Elder's report for both tanks added at 100%.
4. Noble metals per H. Elder's report for Tank 8, and as analyzed by Ned E. Bibler and Terri L. Fellinger for Tank 40, both added at 110%.

The runs were numbered in the order that they were run for each sludge. The letter following the number denotes either Tank 40 (A) or Tank 8/Tank 40 blend (B for blend).

Based on the Tank 8/40 blend scoping runs, it was agreed that the acid target for the Task Plan variability study runs on the blend would be reduced from 137.5% to 125%. Table 2 below gives the important parameters that distinguish the four variability study runs.

Table 2 – Variability Study SRAT/SME Cycle Simulations

Run	Sludge	Date	Noble Metals	Acid Target
SB2-1	Tank 8/40 Blend	8/16-8/17	note 1	125%
SB2-2	Tank 40	8/16-8/17	note 2	137.5%
SB2-3	Tank 8/40 Blend	8/23-8/24	note 3	125%
SB2-4	Tank 8/40 Blend	8/23-8/24	note 4	290%

1. Noble metals per H. Elder's report for Tank 8, and as analyzed by Ned E. Bibler and Terri L. Fellinger for Tank 40, both added at 110%.
2. Noble metals as analyzed by Ned E. Bibler and Terri L. Fellinger added at 110%.
3. Noble metals at 100% of HM levels (mercury at predicted level).
4. Noble metals with the "worst" concentrations in either tank applied to both tanks.

The runs are numbered per the Task Plan. SB2 stands for "Sludge Batch 2", so SB2-1 is Sludge Batch 2, run #1.

SB2-1 is the most likely scenario for DWPF processing of Sludge Batch 2 waste. The acid level was the same as that used in Sludge Batch 1A, but was lower than that used in Sludge Batch 1B. SB2-2 was the next most likely scenario for DWPF processing of Sludge Batch 2 waste. It assumed that Tank 8 did not get transferred into Tank 40 prior to processing.

SB2-3 was a repetition of SB2-1 at the design envelope (HM) level of noble metals. The HM basis is documented in WSRC-TR-91-0400, Integrated DWPF Melter System (IDMS) Campaign Report – The First Two Noble Metals Operations, Hutson et al. SB2-4 was a worst case run assuming noble metals were somehow concentrated, e.g. via segregation in Tank 40. This was then compounded by assuming that the formic acid addition to the SRAT was not stopped until the entire contents of the 480 gallon tank had been fed.

Noble metals and mercury were added to the 4-liter kettle on a batch by batch basis. The original basis was H. H. Elder's report on the expected compositions of Tank 8 and Tank 40. This basis had considerable uncertainty, since it was based primarily on process knowledge. Ned Bibler and Terri Fellinger analyzed the noble metals in one of the Tank 40 sludge samples received earlier this year. Based on those results, Appendix B, it was agreed in meetings with the customer to revise the Tank 40 noble metal basis from Elder's values to those found for the actual waste sample. This change directly impacted this work between the first two pairs of SRAT scoping runs, i.e. the change came after (1A at 110% and 1B at 100% of the predicted concentrations) and before (2A, 2B at 110% of the revised predicted concentrations). The actual mercury and noble metal concentrations (on a dry solids basis) for all ten runs are given in Table 3 below:

Table 3 – Noble Metal and Mercury Concentrations in the Simulations

Run ID	Ag wt. %	Pd wt. %	Rh wt. %	Ru wt. %	Hg wt. %	Acid Stoichiometry
1A	0.320	0.241	0.0291	0.520	0.490	137.5%
2A	0.0131	0.0011	0.00077	0.00232	0.491	137.5%
1B	0.269	0.206	0.0271	0.432	0.285	137.5%
2B	0.127	0.0973	0.0147	0.205	0.294	137.5%
3B	0.127	0.0973	0.0147	0.205	0.294	125%
4B	0.127	0.0973	0.0147	0.205	0.294	110%
SB2-1	0.127	0.0973	0.0147	0.205	0.294	125%
SB2-2	0.0131	0.0011	0.00077	0.00232	0.491	137.5%
SB2-3 (HM)	0.0140	0.0790	0.0280	0.217	0.294	125%
SB2-4	0.250	0.202	0.0297	0.424	0.294	290%

SB2-3 was at 100% of HM levels for the four noble metals. SB2-4 was at 110% of the H. Elder report concentrations

for Tank 8 noble metals. That concentration was applied to both the Tank 8 and to the Tank 40 sludge, i.e. was a very conservative choice for noble metals. Runs 2A and SB2-2 used Tank 40 sludge simulant at the Tank 40 waste sample concentrations of noble metals. Runs 2B, 3B, 4B, and SB2-1 are blends of Tank 8 noble metals as predicted in the Elder report with Tank 40 noble metals as determined by Bibler and Fellinger for the waste sample. The initial mercury content of the seven blend runs already met the DWPF SRAT product spec of 0.45 wt. %, i.e. the "time necessary to steam strip mercury to 0.45 wt. %" was zero. Further discussion of mercury is included in the Results section. The initial mercury content of Tank 40 sludge required minimal predicted stripping time to bring it within specification for the SRAT product.

The nitric acid and formic acid were fed to a 93° C slurry in all ten runs. The SRAT contents were then heated to boiling and held there for at least twelve hours. Dewatering commenced immediately after going to boiling and continued until the target volume reduction was obtained. Boiling continued under reflux for the balance of the twelve hours. Processing continued into the SME cycle for the four variability study runs. There were two large frit slurry additions in the SME cycle. The addition of decontamination frit was not simulated. Slurry pH, off-gas composition, and inlet gas flow rates were monitored throughout all ten runs. SRAT samples were pulled approximately every two hours for anion analysis in all ten SRAT cycles. Samples were pulled after six and twelve hours at boiling in the SRAT cycle and at the end of the SME cycle to check for mercury during the four variability study runs (only).

Acid and Frit Addition Strategy

Concentrated formic acid (90-wt % nominal, 86.9-wt % actual) and nitric acid (50-wt % nominal, 49.2-wt % actual) were used during processing. Total acid addition was set by the acid stoichiometry selected. The acid mix was chosen to meet the targeted redox value of Fe^{2+}/SFe » 0.2. The details of the calculation are given at the appropriate point later in the report. SME frit slurry additions were recomputed during the variability study runs to take into account the mass of samples removed during the SRAT cycle. This was necessary in order to meet the target for the sludge waste in glass loading obtained from PCCS. The nominal composition of frit 200 was used as part of the calculation basis. The three components of frit slurry were actually added separately and mixed with the sludge *in situ*. This made it possible to pump out samples of SRAT product using a Masterflex pump. The water for the first frit slurry addition was used to flush the pump tubing back into the SRAT/SME vessel. *The sludge compositional data needed for redox and PCCS is summarized in Appendix A:* Preparation of Tank 8 and Tank 40 Sludge Simulants.

Not much analytical data was available on supernate adjusted Tank 40 simulant before the scoping runs started. The entire mass of supernate-adjusted Tank 40 simulant needed to complete the ten simulations described in this report was trimmed with nickel chloride and moist manganese dioxide. This occurred one time prior to any testing. A sample of the Tank 8 simulant drum had been analyzed just prior to the start of testing.

Based on simulant recipes, detailed in Appendix A, and analytical results that were available, a calculation was made of the likely compositions of Tank 40 and Tank 8/40 blend simulants. These results became inputs for redox and scaling calculations used to generate the run plans for the six scoping and four variability study simulations. Although samples of the nickel/manganese adjusted Tank 40 and blended simulants were submitted for analysis, results were not received until testing was completed. Results closely matched expectations.

Tables 4 and 5 compare the pre-run calculations of the run inputs with the analytical results of the corresponding samples. The tables are limited to quantities needed to define run parameters. More detailed descriptions of Tank 8 and Tank 40 sludges can be found in Appendix A.

Table 4 – Tank 40 Calculated vs. Measured Compositional Data

	Pre-run Calculation	Sample Result
Weight % Total Solids	16.4	16.55
Weight % Calcined Solids	12.3	13.35
Base Equivalents at pH = 5.5	0.449	0.449
Nitrite Concentration, mg/L	6400	8030
Nitrate Concentration, mg/L	5200	5510

The sample results are generally within typical ranges for good agreement, i.e. approximately 90% of the measured values within approximately 10% of the expected values. A calcine factor of 78.5% had been measured prior to trimming with nickel and manganese. The new measurement for the calcine factor is 80.7%. A running history of analytical data during supernate nitrate adjustment of this sludge argues strongly against accepting the 8030 mg/L nitrite value as accurate. See Appendix A, *Preparation of Tank 8 and Tank 40 Sludge Simulant*, for further details.

Table 5 – Tank 8/40 Blend Calculated vs. Measured Compositional Data

	Best pre-run Calculation	Sample Result
Weight % Total Solids	15.4	15.85
Weight % Calcined Solids	12.0	13.2
Base Equivalents at pH = 5.5	0.439	-
Nitrite Concentration, mg/L	8500	8160
Nitrate Concentration, mg/L	3800	4120

The sample results again are generally within expectations. A calcine factor of 83%, as predicted by the sample result, is extremely unlikely. Six measurements of the calcine factor were made on the three drums of Tank 8 simulant received (two per drum). The average was 78% and the spread was small. The Tank 8 drum results, combined with the data for Tank 40 described above, suggest a calcine factor of about 79% is more likely to be typical of the blend simulant than 83%. No direct titration of the Tank 8/Tank 40 blend was performed. The best pre-run calculation was the average of separate titrations at TNX of the Tank 40 and Tank 8 simulants used to prepare the blend. Results for a sample of Tank 8 simulant submitted to ADS for titration to pH 7 and 5.5 have not yet been received.

Data for the simulant production at USC and the ten test runs were recorded or incorporated into two lab notebooks. These are WSRC-NB-2000-00140, "Macro Batch 3 Simulant" (runs 1A, 2A, 4B, SB2-2, and SB2-3), and WSRC-NB-11-00141, "General DWPF Support Activities" (runs 1B, 2B, 3B, SB2-1, and SB2-4). Scale calibrations were checked daily and recorded in separate log books. Air pipettes for the 1 ml NaOH additions to the IC samples were checked by date, and the delivered masses were recorded as back-up. Testing generally went smoothly, except for some helium supply pressure upsets and leak problems (in the building, not the apparatus) during the early scoping runs.

Results

Material Balance

A large amount of data became available during the SRAT or SRAT/SME simulations. This included:

- mass and analysis of the starting sludge titration results for the formic and nitric acids
- mass of simulated flush water
- mass of water used to fill the Mercury Water Wash Tank (MWWT)
- volumes/masses of both acids added in the SRAT cycle
- masses and times for samples removed
- masses and times for antifoam solution additions

- mass of condensate recovered from the Formic Acid Vent Condenser (FAVC)
- final mass within the MWWT
- mass of frit-water-formic acid added during the SME cycle
- helium and air purge inlet volumetric flow rates
- off-gas composition as analyzed by the GC
- slurry temperature
- slurry pH
- agitator rpm and motor torque
- and, in the case of the four variability study runs, masses of all of the rig components (glassware and metal) that could potentially come in contact with sludge or condensate both before and after the run.

Following the run, additional data became available including:

- run sample results for anions during the SRAT cycle
- sample results for the cation breakdown of the SRAT and SME products
- mercury content of the SRAT and SME products and of the SRAT six hours into boiling
- total, soluble, and insoluble solids in the SRAT and SME products.

SRAT and SME product samples were filtered and the supernate pH was checked and compared to the kettle pH readings at those times in the simulation. Kettle pH probe calibration drifts during the run, and this gives additional points of comparison. A visual inspection of the MWWT occasionally revealed a small amount of mercury adsorbed on the glass surface. SME product samples were made into glass and the Product Consistency Test was performed.

As part of Section 4 of the Conduct of Research and Development Manual, WSRC-IM-97-00024, Rev. 2, material balances were constructed for all ten simulations to test the reproducibility and precision/accuracy of the data obtained. In essence, the material balances attempted to capture two main facts. First, that the evolution of gases corresponds to a loss of slurry mass. Second, that acid-base neutralization reactions produce water at the expense of species that were previously considered to be solids ("solids" being defined as anything that isn't water, e.g. nitric acid). In addition, it was assumed that mercury(II) is reduced and removed via steam stripping during the SRAT cycle.

The large quantity of data was insufficient to account for all possible terms that might be incorporated into a material balance. One example was oxygen consumption by various reactions postulated to be occurring during processing. For example, NO was expected to consume oxygen to form NO_2. Oxygen was also anticipated to be consumed by some formic acid decompositions that do not produce hydrogen. The SRAT/SME vessel was under a continuous, metered air purge. Large decreases in oxygen flow in the off-gas were seen and measured, however small increases or decreases in the GC measurement of oxygen could not be differentiated from random noise.

Material balances were nevertheless attempted. They captured the following terms:

- all measurable additions and removals of non-gaseous masses, e.g. sludge, water, acids, antifoam, samples, and frit
- loss of nitrite and formate ion as measured by ion chromatography
- loss/gain of nitrate ion as measured by ion chromatography
- mass of carbon dioxide evolved (integrated from the gas flow rate and GC data)
- mass of hydrogen evolved (integrated from the gas flow rate and GC data)
- mass of nitrous oxide, N_2O, evolved (integrated from the gas flow rate and GC data).

Sustained formate losses tended to occur in the runs with higher acid stoichiometries. IC data coupled with mass balance data showed a continuously declining mass of formate in the system. The mass of formate lost was a function of acid stoichiometry, time, and perhaps other factors. The formate concentration data were fit to pseudo-first order kinetics. Based on this, the final SRAT product formate concentration was predicted. This will be discussed further in the hydrogen and carbon balance sections below. More subtle changes were seen in the nitrate ion data after adjusting the nitrate concentration for conversion of nitrite to nitrate. This will be discussed in the nitrogen balance sections below. Total SRAT and SME product solids were predicted, and these were compared to sample data. The discussion

below separates the Tank 40 results from the Tank 8/40 blend results.

Table 6 below gives results of material balance predictions of the wt. % total solids in the SRAT and SME products of the ten runs. The poorest prediction, a 7% difference relative to the measured value, was found in SB2-4 (290% acid and worst case noble metals). In all ten runs, the predicted mass of the final slurry (SRAT product for the scoping runs, SME product for the variability study runs) slightly exceeded the mass actually recovered. This suggests that the simple material balance used to track data needed more terms to account for losses in solids content. The predicted and measured wt. % total solids data did not show as clear a trend as the slurry mass data. This is detailed in Table 6.

Table 6 – Wt. % Total Solids Predictions and Measurements

Run	SRAT-Predicted	SRAT-Measured	SME-Predicted	SME-Measured
1A	16.8	17.9	-	-
2A (like SB2-2)	18.7	18.4	-	-
1B	16.8	17.0	-	-
2B	17.4	16.9	-	-
3B (like SB2-1)	17.2	16.5	-	-
4B	17.4	16.5	-	-
SB2-1	17.3	16.4	44.1	44.6
SB2-2	18.9	18.8	48.1	49.2
SB2-3	17.5	16.5	44.4	44.1
SB2-4	20.0	18.7	45.0	47.3

Measured values were the average of two separate measurements made from the same 125-ml sample. In spite of the simplifications required to produce the material balance model, it appeared to be capturing the major factors occurring during processing. If not, the agreement between predicted and measured total solids would not be this good. The SME product prediction benefits from the addition of large quantities of glass frit. It is particularly difficult to reconcile the "high" SRAT prediction for SB2-4 with the "low" SME prediction. Some of these discrepancies can probably be attributed to variations in slurry sampling and analytical uncertainty.

Although there were some things that differed from material balance to material balance, the following assumptions were made in all ten cases:

- 100% destruction of nitrite in the SRAT cycle
- 30% conversion of nitrite to nitrate in the SRAT cycle (close to typical)
- 100% loss of carbonate in the SRAT cycle (may be typical)
- 100% loss of mercury in the SRAT cycle
- 100% loss of the hydroxide present in the sludge recipe as NaOH (typical)
- perfect mixing – samples are identical to the mean kettle composition
- 0% loss of water vapor in the FAVC off-gas
- Tank 40 sludge is as-measured: 16.55 wt. % total solids
- Tank 8/40 blend sludge is as-measured: 15.85 wt. % total solids
- antifoam and its decomposition products are nonvolatile
- formate ion loss would be modeled using the IC data

- any nitrate ion loss indicated by IC data would be ignored initially and then compared to sample data
- the nitric acid and formic acid did not vary in molarity throughout the testing period (sufficient was made at the beginning to complete all tests).

Discussions on the nitrogen balance and on the hydrogen-carbon balance below will discuss some of these assumptions further. The Tank 40 sludge simulant was originally estimated to be approximately 16.4 wt. % total solids based on drum samples of simulant combined with the mass of additional nickel and manganese that were added to enrich these two components. The Tank 8/40 blend simulant had been estimated to be 15.4 wt. % total solids, assuming 16.4% for the Tank 40 component. Dropping the Tank 8/40 blend starting solids to 15.4-15-5% from the 15.85% as-measured value would have produced a net improvement in the SRAT material balance predictions in Table 6 above (six better and one worse). Though such a small change might have been justified (and could have been attributed to a slightly biased sample), it was not made. This report used measured values directly whenever they were available over predictions, even when the predictions were themselves based on closely similar measurements. (If a sample could obviously be determined as "bad", then this position would be reevaluated. That was not an issue in preparing the material balances.)

Tank 40 Testing – SRAT Cycle

Three SRAT cycles were completed using Tank 40 sludge simulant. The first of these had very high levels of noble metals (scoping run 1A). The other two (scoping run 2A and SB2-2) were essentially identical in plan and had very low levels of noble metals. Scoping runs were not run in round-the-clock mode. Consequently, the SRAT cycle was interrupted at some point, shut down, and then restarted the next day. All three runs targeted 137.5% acid stoichiometry and a redox of Fe^{2+}/SFe equal to 0.2. Tank 40 sludge was visually observed to be unusually viscous.

Preliminary measurements put the yield stress of the Tank 40 sludge simulant used in these tests about one order of magnitude higher than other simulant sludges such as Tank 42 and Tank 8. This difference was even more obvious during acid addition. Nearly all signs of visible mixing disappeared at intermediate pH values. While 270 rpm was adequate to get good mixing following acid addition, speeds as high as 450 rpm were not appreciably mixing the sludge during acid addition. (Speeds above 450 rpm would have been tried, but the increasing angular deflection of the agitator shaft at 460-480 rpm threatened to bring the agitator into direct contact with other vessel internals.)

Very large bubbles, approaching one-inch in diameter, were observed during periods of gas evolution. This was most easily observed during the acid addition period of the SRAT cycle, when there was not a simultaneous evolution due to boiling. The large size of the bubbles was tentatively attributed to the high viscosity of the simulant.

Hydrogen-Carbon Balance

The hydrogen-carbon balance relates to hydrogen evolution and formate ion destruction, both key operational concerns for DWPF. Hydrogen and carbon will be discussed together, since the catalytic decomposition of formic acid can produce both hydrogen and carbon dioxide gases. The major findings are as follows. The sum of carbonate and formate lost from the sludge was comparable to the amount of carbon dioxide produced. The amount of formate lost was much greater than what can be explained based on reduction of mercury and manganese, conversion of nitrite to N_2O, and hydrogen generation. Reaction paths for formate destruction that involve the consumption of oxygen appear to be required to explain the observations.

Masses of gases evolved during either the SRAT or SME cycle were determined the same way. The procedure was as follows:

- Analyze the pre-run and post-run calibration data for the GC.
- Correct the raw GC run data based on the calibration data (linear scaling with time).
- Scale the known, MKS-controlled, helium flow using the corrected GC compositions to produce instantaneous flows of the other gases.
- Integrate the individual instantaneous gas flows using Simpson’s Rule to obtain the total volume produced in a specified period of time.

- Convert the volume, in standard cubic centimeters, to gram moles or grams.
- Multiply by the run scale factor (9000) to put the number on a DWPF basis.

Table 7 below gives total production mass and maximum production rate of both hydrogen and carbon dioxide for the three Tank 40 runs. Hydrogen data from WSRC-RP-98-00149, the equivalent study for Sludge Batch 1B, were included for comparison. *The DWPF design basis upper limit in the SRAT cycle for hydrogen is 0.65 lbs./hr.*

Table 7 – Hydrogen and Carbon Dioxide Summary for Tank 40 SRAT Tests

	Mass H_2, lb.	Max. Rate, H_2, lbs./hr	DWPF H_2 Limit, lbs/hr	Mass CO_2, lb.	Max. Rate, CO_2, lbs./hr
1A	5.36	**1.69**	0.65	1170	520
2A	0.014	0.0013	0.65	570	960
SB2-2	0.015	0.0018	0.65	600	590
Tank 42 (125%)	-	0.001	0.65	-	-
Tank 42 (137.5%)	-	0.004	0.65	-	-

The maximum hydrogen generation rate for scoping run 1A exceeded the DWPF design basis of 0.65 lb./hr. Decreasing palladium and ruthenium by a factor of approximately 200 coupled with decreasing the rhodium by a factor of 38 apparently led to the three order-of-magnitude drop in the maximum hydrogen generation rate from 1A to 2A and SB2-2.

Carbon dioxide is not linked to a design limit, but its evolution gives an idea of the conversion of carbonate and formate ions and formic acid into gas during the SRAT cycle, and consequently not in the melter. Whether or not the presence or absence of each of the various sludge anions has a negative effect on melt rate has not been clearly established. It is generally believed that some of the anions in the melter feed don't decompose in the cold cap, and instead reach the melt pool, decomposing there.

Figure 2 shows the SRAT production rate of hydrogen scaled to DWPF for the three Tank 40 simulant tests. The precision of the data for scoping run 2A and SB2-2 was limited by truncation at the third decimal place in the raw GC volume percent data. The 2A and SB2-2 DWPF-scale flow rates were multiplied by 100 to get them off the time axis. In all figures that follow, the scoping run down time has been essentially removed (generally 8-12 hours). The time axis zero was placed at the end of formic acid addition for comparison purposes. The data below were converted to DWPF scale. The point at which there was a secondary maximum in N_2O evolution during scoping run 1A is shown by an arrow. This maximum can be seen in Figure 4 on page 22. There appeared to be a marked increase in hydrogen generation associated with the nitrous oxide maximum.

Figure 2. Tank 40 - Hydrogen Generation

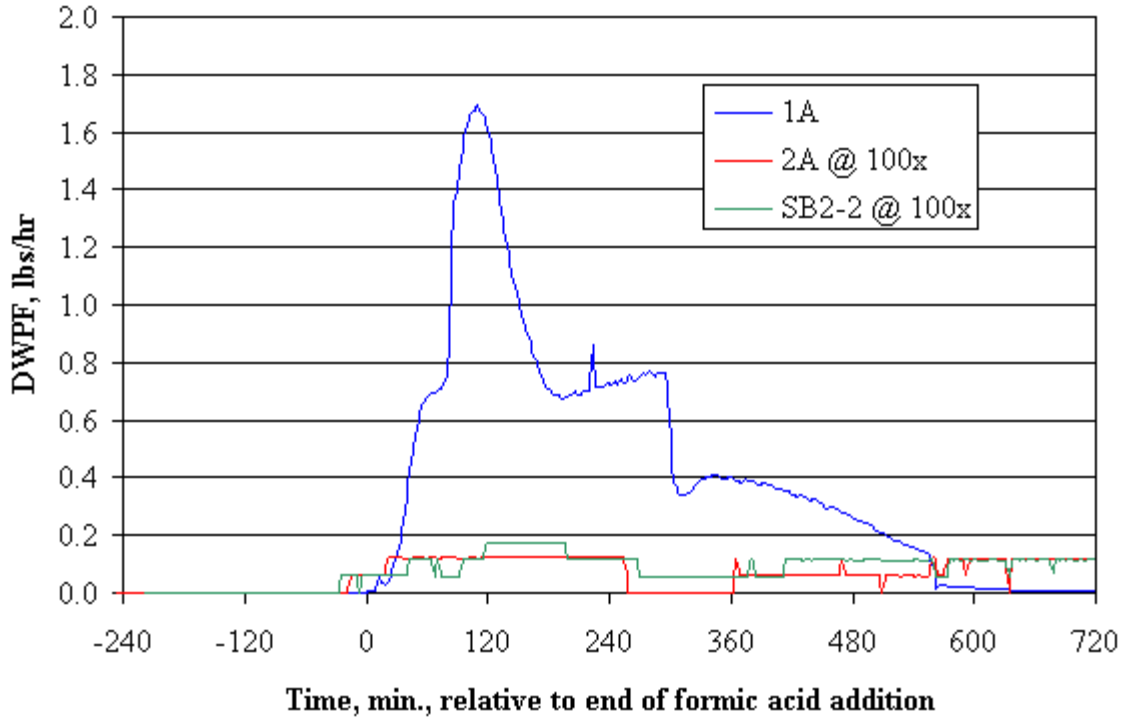

Figure 3 below shows the equivalent SRAT production rate of carbon dioxide for the same three runs.

Figure 3. Tank 40 - Carbon Dioxide Generation

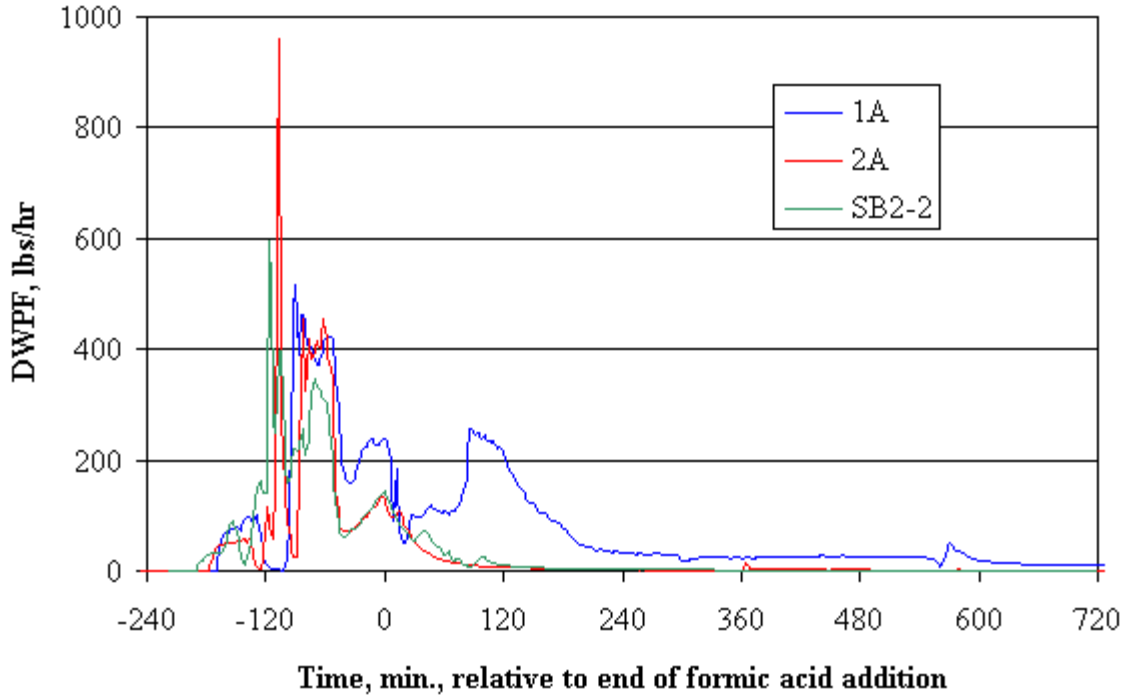

Carbon dioxide generation is generally associated with pH changes during acid addition (carbonate destruction) and with formic acid reactions (reduction, decomposition). There was considerable similarity in the carbon dioxide data

during acid addition. Scoping Run 1A, however, with its higher noble metal content produced considerably more carbon dioxide during the boiling portion of the SRAT cycle. This was when the majority of the extra 400 pounds CO_2 in Table 7 were produced. Agreement between scoping run 2A and SB2-2 was quite good. This was expected since the two runs were prepared identically. Problems with mixing during formic acid addition, coupled with the need to periodically reduce formic acid addition rate, undoubtedly account for some of the differences observed.

Carbon dioxide produced during nitric acid addition must come from the carbonate content of the sludge. The large spikes and dips at about -120 minutes may have been due to the exchange of the nitric acid feed tube for the formic acid feed tube (and resulting disruption in the air purge flow). Formic acid addition generally took 100-110 minutes. Going to boiling took about 25 minutes.

The available mass of carbonate in one Tank 40 sludge batch can be converted into about 265 lbs. of carbon dioxide. The relevant reactions for this sludge simulant are:

$$Na_2CO_3 + 2H^+ \rightarrow 2Na^+ + CO_2 + H_2O \quad \text{(C-1)}$$
$$CaCO_3 + 2H^+ \rightarrow Ca^{2+} + CO_2 + H_2O \quad \text{(C-2)}$$
$$SrCO_3 + 2H^+ \rightarrow Sr^{2+} + CO_2 + H_2O \quad \text{(C-3)}$$

The balance of the carbon dioxide produced must come from destruction of either formate ion or molecular formic acid. Various formic acid consuming reactions have been postulated for the SRAT cycle including:

$$HgO + HCOOH \rightarrow Hg^0 + CO_2 + H_2O \quad \text{(F-1)}$$
$$2HNO_2 + 2HCOOH \rightarrow N_2O + 2CO_2 + 3H_2O \quad \text{(F-2)}$$
$$MnO_2 + HCOOH \rightarrow MnO + CO_2 + H_2O \quad \text{(F-3)}$$
$$2HNO_2 + HCOOH \rightarrow 2NO + CO_2 + 2H_2O \quad \text{(F-4)}$$
$$2HCOOH + O_2 \rightarrow 2CO_2 + 2H_2O \quad \text{(F-5)}$$
$$HCOOH \rightarrow CO_2 + H_2 \quad \text{(F-6)}$$

Reaction F-4 was impossible to track with the current GC. The reaction of formic acid with oxygen, F-5, was included since the slurry was saturated with air, and the formation of hydrogen by the last reaction may depend on whether a hydrogen radical encounters another hydrogen or an oxygen molecule. In addition there was a large drop in the oxygen flow rate in the off-gas during formic acid addition. The last reaction is believed to need a catalyst, such as rhodium or one of the other noble metals, in order to proceed at an appreciable rate. Reaction F-3 is presumably followed by the following manganese dissolution reaction

$$MnO + 2HCOOH \rightarrow Mn^{2+} + 2HCOO^- + H_2O$$

but the acidic species doesn’t need to be formic acid, and no gas generation is expected.

Total conversion of Tank 40 mercury requires only 10 lbs. of formic acid and produces 9.6 lbs. of carbon dioxide. The mass of Tank 40 manganese, however, exceeds that of mercury by about a factor of five, and its molecular weight is only about one-fourth as large. Manganese has the potential to destroy 204 lbs. of formic acid and produce 195 lbs. of carbon dioxide by F-3. However, it is not known what fraction of the manganese is reduced from oxidation state (IV) to (II) during these SRAT cycles. Nitrous acid is also not necessarily reduced by formic acid. It can be converted into nitric acid instead as discussed in the nitrogen balance section below, reaction N-3.

Since hydrogen was measured, Table 7, the equivalent amount of carbon dioxide produced by reaction F-6 was calculated. Data was also taken on the formate content of the SRAT slurry during processing. The measured loss of formate in the SRAT can be converted into an equivalent mass of carbon dioxide produced. Table 8 gives a summary of the various contributing factors as equivalent pounds of carbon dioxide. Carbon dioxide values per hydrogen and nitrous oxide evolved were calculated from integrations of the two gas flow rates combined with reactions F-2 and F-6 above to compute the equivalent carbon dioxide evolution. The oxygen consumption term was calculated from net

decrease in oxygen flow rate relative to the purge air oxygen flow supplied. All runs had at least one period of unquestionable oxygen consumption clearly distinguishable from background noise in the data. The equivalent mass of carbon dioxide produced was estimated using equation F-5.

Table 8 – Carbon Balance as CO_2 for Tank 40

Factor (as equiv. lb. CO_2)	Scoping Run 1A	Scoping Run 2A	SB2-2
Carbonate lost (100%)	265	265	265
Lost Formate – IC	+ 1530	+ 270	+ 270
Sum of likely lost CO_2	1795	535	535
vs. CO_2 by GC	1170	570	600
Lost Formate Factors:			
100% Mn reduction	200	200	200
100% Hg reduction	10	10	10
Per H_2 evolved	120	0.3	0.3
Per N_2O evolved	+ 27	+ 23	+ 26
Sum of Formate factors:	360	230	240
Extra per O_2 consumed:	+ >600	+ >400	+ >390
Revised Formate Sum:	>960	>630	>630

There was relatively good agreement (within ~10%) between scoping run 2A and variability study run SB2-2 for the equivalent carbon dioxide calculated from total destruction of carbonate and lost formate as determined by IC . There was also good agreement between the lost carbonate plus formate and the GC measured CO_2 for this pair of essentially identical SRAT cycles. Based on this agreement, it was concluded that an assumption of relatively complete carbonate destruction was valid. Accurate anticipation of the formate loss, and consequently the accurate prediction of the melter feed formate concentration, is important in predicting the unadjusted redox of the melter feed.

The agreement between formate loss plus carbonate loss with the GC measurement was poor (not within 50%) for scoping run 1A. The lost formate alone greatly exceeded the carbon dioxide mass as measured at the GC. This was unexpected and remains unexplained. Mobile Lab and ADS reported similar formate numbers near the end of the SRAT cycle for this run.

The known contributors for formate conversion to carbon dioxide, given in the lower half of Table 8, were inadequate to explain the IC formate loss during run 1A, but came close in 2A and SB2-2. (Compare numbers in blue. The IC loss is a trend from seven to eight samples taken starting after acid addition and then periodically during the SRAT cycle until it ended.) Several scenarios have been postulated to explain such data. One scenario has manganese being reduced by formic acid, then re-oxidized by nitrous or nitric acid, re-reduced, etc. until processing stops or one acid is consumed. The nitrous acid would be entering the SRAT in the SRAT condenser reflux stream. It would be generated continuously there by absorption of various nitrogen oxides. If most of the nitrite is destroyed during acid addition (no reflux, since not boiling), then it is hard to get this process going later on.

A second scenario has the formic acid participating in other reduction reactions similar to F-1 and F-2 that have not yet been identified as significant to the SRAT acid calculation. A third hypotheses is that the formic acid or formate reacts with dissolved oxygen to produce carbon dioxide and water, reaction F-5. In this scenario the hydrogen atom liberated from the formate carbon encounters either another hydrogen atom to produce hydrogen or encounters an oxygen molecule to produce a highly reactive intermediate that goes to water in an acidic solution. Alternatively, the formic acid breaks down into water and carbon monoxide, and the CO reacts with oxygen. Reaction F-5 was the basis for the calculation of CO_2 formed from oxygen consumption in Table 8.

Reaction F-4 yields NO as well as CO_2, and the NO could react with oxygen to explain some of the observed oxygen consumption (see reaction N-5 below). The initial nitrite concentration was the same for all three batches, so this

reaction is at best a partial explanation for the extra lost formate. Further investigation into the mode of formic acid/formate loss would seem to be warranted, but it appears almost certain that formic acid and oxygen are reacting together. Such studies might involve using various isotope tagged formic acid feeds with a modified GC, e.g. GC mass spec combination, that could distinguish various hydrogen, carbon, and oxygen isotopes.

An attempt was made to extract an oxygen loss rate from the GC data. There are some small unresolved issues between the GC calibration and the MKS flow controller delivered flow. The current hypotheses to explain these follows. Helium is the current internal standard. Helium elutes quickly, and hydrogen is not far behind. Obtaining an accurate helium value is consequently difficult, because of severe constraints on the retention time window (narrow and cannot overlap hydrogen). A possible solution/correction would be to use krypton as the internal standard. Krypton would elute not too long after nitrogen allowing retention of a three minute sampling cycle. Eliminating helium would also remove its potential interference with the hydrogen measurement. Although krypton is more expensive than helium, the simulations do not use a large amount of internal standard, and krypton is less prone to leaking than helium.

The present GC issues limit the accuracy of the oxygen consumption determination. However a lower bound can be placed on oxygen consumption. Unfortunately, not all consumed oxygen would be involved in formate destruction. Oxygen is also consumed in the conversion of NO to NO_2. Thus, if oxygen consumption were accurately known, it would place an upper limit on carbon dioxide produced by reaction with formate ion or formic acid. All that the actual data allows is to place an "upper limit" on carbon dioxide derived from a "lower bound" on oxygen consumed (obviously not an ideal situation). Keeping that in mind, two rows were added at the bottom of Table 8 above. These reflect the potential impact of an oxygen-formate reaction term on carbon dioxide production. It would be hoped that the last row in Table 8 has a comparable or larger number than the formate loss determined by IC.

It is clear from Table 8 that lower bound oxygen consumption (given as pounds CO_2 made) represents a potentially major factor in formate consumption and carbon dioxide generation. It greatly exceeded the identified factors listed in Table 8 in formate destruction potential, unless something like the proposed manganese oxidation state cycle was occurring. Oxygen consumption provided ample margin for obtaining closure on runs 2A and SB2-2. There appears to be little hope of obtaining carbon balance closure on scoping run 1A. Even neglecting carbonate destruction, which is obviously not the right thing to do, left a 30% gap in closure between the computed formate lost and the carbon dioxide evolved. Formate data for run 1A came from both the Mobile Lab and ADS. Consequently, the formate data is unlikely to be the source of the poor closure. It would be interesting to repeat one of these experiments in the future, plus the related analysis, with a different internal standard gas and see whether or not the closure improves.

Nitrogen Balance

Nitrogen containing species are tracked for nitrite ion destruction, nitrate ion concentration versus time, and N_2O as a gas phase component. The significant findings include the near complete destruction of nitrite in a short period of time using 137.5% acid stoichiometry and the near constant mass of nitrate ion once nitrite ion is destroyed.

The nitrogen balance section is concerned with nitrite ion, nitrate ion, and the various evolved nitrogen oxide gases. The following reactions are pertinent to an acidic medium:

$H_3O^+ + NO_2^- \rightarrow HNO_2 + H_2O$	(N-1)
$2HNO_2 + 2HCOOH \rightarrow N_2O + 2CO_2 + 2H_2O$	(N-2)
$3HNO_2 \leftrightarrow HNO_3 + 2NO + 2H_2O$ (concentrated solutions)	(N-3)
$2HNO_2 \leftrightarrow NO_2 + NO + H_2O$ (gas phase, $K_{20°C} = 1.56$/atm)	(N-4)
$2NO + O_2 \rightarrow NO_2$ ($T < 140°C$)	(N-5)
$2NO_2 + H_2O \rightarrow HNO_2 + HNO_3$	(N-6)
$2NO_2 \leftrightarrow N_2O_4$ (gas phase: 90% NO_2, 10% N_2O_4 at 100°C, 1 atm)	(N-7)
$2HNO_2 + HCOOH \rightarrow CO_2 + 2NO + 2H_2O$	(N-8)

Reaction N-1 takes nitrite ion from the sludge supernate and converts it to nitrous acid which in turn is either attacked

by formic acid N-2 or decomposes thermally N-3. Of the gaseous oxides, N_2O is considered rather *unreactive*, NO is considered *moderately reactive*, NO_2 (and N_2O_4 by inference) is considered *rather reactive* in Cotton and Wilkinson's Advanced Inorganic Chemistry. NO_2 is a brown-colored gas at high concentrations. The adsorption of NO_2 into water can give a blue to green colored solution initially which changes colors through orange to an ultimately clear solution. (The GC used in this testing only detects N_2O from the evolved gases listed above, and the measurement is made downstream of the FAVC.)

Brown gas evolution from the SRAT was observed in all ten SRAT simulations. Thus either or both of reactions N-4 and N-5 were probably occurring. During scoping run 1A, it was noticed that the top layer of liquid in the MWWT appeared to be tinted green (as though something were diffusing into the stagnant liquid from the vapor space). A liquid sample was taken from the vapor-liquid interface region. Not long after the sample was taken, the color was lost (both in the sample and in the MWWT). This was taken as a visual demonstration that reaction N-6 was occurring. This phenomenon was noticed during formic acid addition period, when the NO_2 was most obvious. Although this phenomenon was not observed during boiling, it is quite reasonable to expect that small amounts of evolved NO or NO_2 were converted back into nitrous and nitric acid and recycled to the SRAT while the SRAT was being refluxed. Reaction N-8 was postulated by Hsu [1990, 1992] to explain the simultaneous evolution of carbon dioxide and NO/NO_2. It differs from N-2 in requiring only one formic acid molecule to reduce two nitrite ions.

The Tank 40 SRAT cycle data indicate that nitrite ion was essentially 100% destroyed in runs 1A, 2A, and SB2-2. It was also destroyed relatively quickly, generally falling to <100 ppm within the first four hours at boiling. This rapid destruction made determination of a destruction rate impractical (insufficient data with non-trivial nitrite concentrations). The evolved N_2O accounted for only 8-10% of the nitrite loss. Assuming that the other ~90% of the nitrite goes ultimately to NO per N-4 and N-5 in a single pass (no recycle return of nitrous acid), then only about 50 pounds of oxygen are required for the reaction step converting NO to NO_2. This is only a small fraction of the oxygen consumed per Table 8. Figure 4 below shows the DWPF-scaled N_2O generation rate for the three Tank 40 SRAT cycles:

Figure 4. Tank 40 - Nitrous Oxide Generation

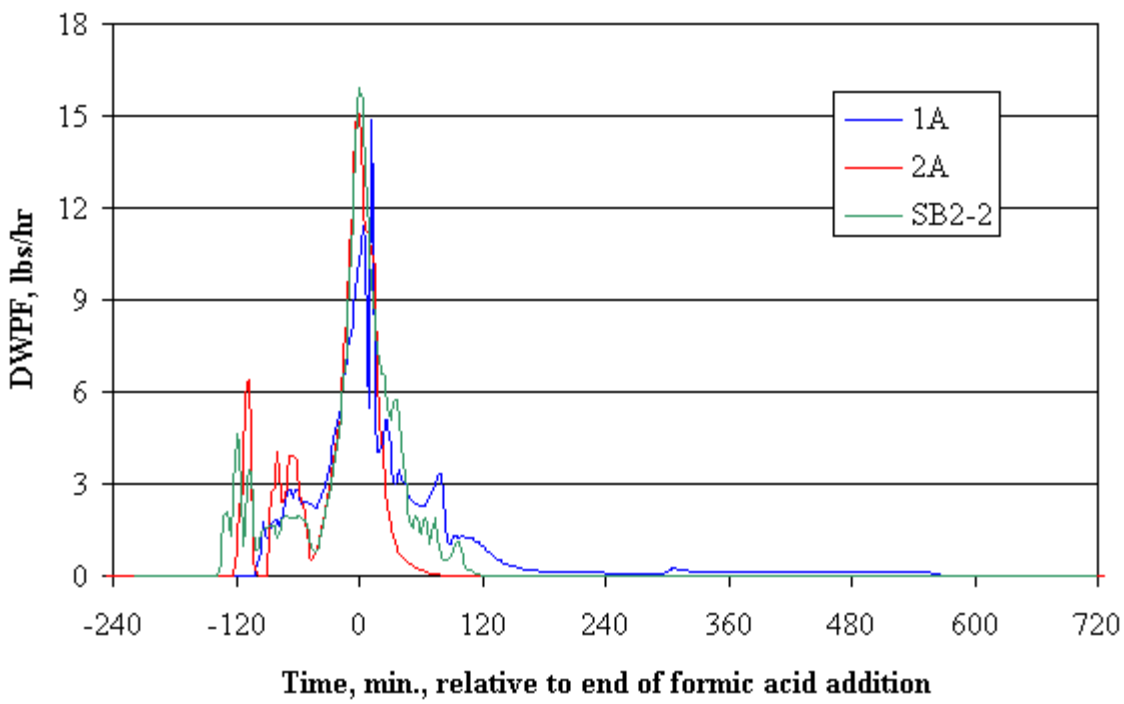

The three traces were remarkably similar given the enormous difference in noble metal concentrations between runs. A

reasonable hypothesis would be that noble metals do not effect N_2O evolution, although the reverse is suspected to be false, i.e. that nitrite destruction, or its lack, does affect noble metal activation as catalysts. In scoping run 1A, as well as in the Tank 8/40 blend tests, there was a surge in hydrogen generation rate associated with a secondary maximum in N_2O production. This peak is marked in Figure 4, and is also marked on Figure 2 (showing the hydrogen generation rate). Although palladium and ruthenium are considered poorer catalysts, they were present at 8 and 18 times higher concentrations than rhodium respectively. It is possible that more than one of these species became active near the end of formic acid addition, when hydrogen first began to appear, and that a different combination became active somewhat later leading to the increased hydrogen generation rate. The Tank 40 data alone does not offer any evidence as to which noble metals might be important.

The assumption of a 30% conversion of nitrite to nitrate was consistent with the IC data from samples pulled after two to four hours of boiling in the SRAT cycle. (30% is derived assuming the remaining 90% of the nitrite not lost as N_2O goes to nitrate by reaction N-3 above, i.e. 1/3 of 90% of the initial nitrite moles are converted into nitrate moles.) Predicted and measured nitrate immediately following dewatering are given in Table 9 below. This point was chosen because the SRAT slurry volume was essentially the same in all runs, and any denitration loss during reflux had yet to occur.

Table 9 – Predicted vs. Measured Nitrate Following Tank 40 SRAT Dewatering

Run	Predicted Nitrate, mg/L supernate	Measured Nitrate, mg/L supernate
1A	15,119	14,432
2A	14,946	14,940
SB2-2	15,628	24,700[1]

1. This entire run's sample results ran 5-9000 mg/L above expectation.

The nitrate results for SB2-2 were not consistent with other nitrate data obtained during this testing, and many results exceed what would appear to be the maximum possible nitrate the sludge could possibly have. A somewhat closer agreement was obtained between the SRAT final product sample and predicted result, 22,500 mg/L vs. 17,233 mg/L, respectively. The source of these differences will likely remain unresolved.

The grams of nitrate in the kettle appeared to remain fairly constant (once nitrite conversion was complete) in runs 2A and SB2-2 based on the IC data. This was not the case with run 1A. Following nitrite conversion, there was a gradual decline in the indicated grams of nitrate as calculated from the sample results. Approximately one-third of the nitrate ion appeared to have disappeared by the end of the SRAT cycle (based on the NaOH-quenched samples analyzed by ADS). However, when the final SRAT product was analyzed by Mobile Lab, they reported 17,100 mg/L nitrate, while the material balance prediction was 17,200 mg/L assuming no loss of nitrate. (Simultaneously taken formate data agreed well between measurements by either lab and model predictions.) Consequently, the possible loss of one-third of the nitrate ion was not conclusive. This will not be studied further, since it occurred in a non-repeated scoping run using unlikely noble metal concentrations.

Table 10 below provides the requested information on the maximum N_2O generation rate during the Tank 40 testing. Results for Tank 42 at 125% and 137.5% acid from WSRC-RP-99-00149 are again included for comparison.

Table 10 – Nitrous Oxide Results Summary for Tank 40

	Mass N_2O, lb.	Max. Volume % N_2O	Max. Rate, N_2O lbs./hr
1A	13.4	1.08	14.8
2A	11.7	1.15	15.0
SB2-2	13.1	1.12	15.9
Tank 42 (125%)	-	0.204	5.411
Tank 42 (137.5%)	-	2.442	45.102

Agreement between 2A and SB2-2 was reasonable for a laboratory experiment, considering the numerical integration needed to produce total mass and typical fluctuations in GC readings (a maximum rate almost always occurs at a fluctuation above the general trend). The concentrations of N_2O were well below the 20-volume % basis for DWPF flammability calculations.

Steam Stripping of Mercury

Tank 40 simulant was trimmed with mercury to a level (0.491 wt. %) per the High Level Waste database calculations by H. Elder. This concentration just exceeded the SRAT product design maximum of 0.45 wt. % on a dry solids basis. Mercury analyses were not obtained for the scoping runs. Three samples were analyzed from SB2-2 for mercury. The first sample came at the mid-point of the twelve hour SRAT cycle boiling period, the second sample came at the end of the SRAT cycle, and the third sample came at the end of the SME cycle. ADS reported sample results in mg mercury/g slurry. Table 11 summarizes the calculated initial mercury concentration and the three ADS results.

Table 11 – Mercury Results for Tank 40 Run SB2-2

Predicted initial Hg content	4740 mg mercury/g slurry
SRAT mid-point sample	<100 mg mercury/g slurry
SRAT product sample	<100 mg mercury/g slurry
SME product sample	<100 mg mercury/g slurry

The results would seem to indicate that the mercury was effectively removed by steam stripping in the early phases of the SRAT cycle. All of these sample results may be unrealistically low based on discussions with researchers who have performed similar measurements in the past. Their observation was that it was hard to reduce the mercury concentration below roughly 1000 mg mercury/g slurry.

The initial appearance of elemental mercury following reduction was monitored during the testing. Colloidal mercury usually forms a film that can be maintained at the vapor-liquid interface. During GFPS testing with Sludge Batch 1B simulant, a gray film formed that spread to cover the entire vapor-liquid interface. Various observations were made during the testing. A gray film was observed in both runs 2A and SB2-2. The amount was small. A black film was also observed at other times during these runs, including in the SME cycle of SB2-2. It is nearly impossible to detect the film when there is a lot of foam formation, which may explain why none was reported during scoping run 1A.

Foaming

All Sludge Batch 2 testing used IIT747 antifoam. Antifoam was diluted to 10% effective strength. Each antifoam addition was followed by a water flush of equivalent volume. This simulates using a 5% antifoam solution. Foaming was a problem in the Tank 40 testing. An initial dose of 100 ppm antifoam prior to acid addition was supplemented with two additional 50 ppm doses during acid addition in 1A. An initial dose of 100 ppm was supplemented with a second 100 ppm dose during acid addition in 2A. SB2-2 started with an initial dose of 150 ppm antifoam. A second

addition of 50 ppm was needed to get through acid addition.

Problems with getting through acid addition using a 100 ppm antifoam addition were first observed in the GFPS test of IIT747 antifoam in September, 1999 [Koopman]. It was not clear at the time whether the problem was unique to the antifoam or was related to problems with the formic acid pump which delayed completion of formic acid addition. Supporting evidence that the 100 ppm initial dosage was inadequate for acid addition came during abbreviated SRAT cycles performed as part of the melt rate study [WSRC-NB-99-00170]. It became accepted practice to start at 150-200 ppm antifoam rather than 100 ppm. The melt rate study runs had no mercury or noble metals.

There was one event during the Tank 40 SRAT cycle acid addition phase of run SB2-2 worth noting. While attempts were being made to get the formic acid to mix into the sludge, there was a brief surge in gas pressure associated with some foam formation. This brief pressure surge forced water out of the manometer used to track vessel pressure. An estimate of the pressure needed to do this at the time was made, and a pressure of about 6-8 inches water was sufficient (there wasn't very much water in the manometer initially).

Foaming problems persisted into the boiling phase of the SRAT cycle. A fresh 100 ppm addition of antifoam was made as the SRAT went to boiling, regardless of how much antifoam had been added during acid addition. There were six additional antifoam additions made in scoping run 1A before the SRAT cycle was completed. Five were an extra 50 ppm, and one was an extra 100 ppm addition. One of the extra 50 ppm additions was made the morning the run resumed after having been shut down for the night. Only one additional antifoam addition was made in scoping run 2A (low noble metals). That was a 50 ppm addition the morning the run resumed after being shut down overnight. SB2-2 received a 100 ppm addition prior to going to boiling and took another 50 ppm almost as soon as boiling actually started. No further antifoam was needed to complete the SRAT cycle. SB2-2 was not shut down during the SRAT cycle.

Total antifoam additions for the three SRAT cycles (1A, 2A, SB2-2) were 650 ppm, 350 ppm, and 350 ppm (respectively) versus 200 ppm prototypical. Qualitative agreement was good between 2A and SB2-2 (identically batched sludge, acid, and noble metals). Actual antifoam additions during testing would seem to be characterized by *as little as was needed to make it through the run*. It is not recommended that DWPF try to run with such a small margin of error, estimated to be about 50 ppm or less, relative to too little antifoam.

Tank 40 Testing – SME Cycle and Redox for SB2-2

Acid Additions and Redox

A spreadsheet has been developed to calculate the nitric and formic acid addition required to reach a redox target for a given sludge mass, sludge composition, and acid stoichiometry. All Tank 40 simulant tests had a redox target of $Fe^{2+}/SFe = 0.2$. The formate and nitrate concentration of the SB2-2 SME product were also measured. This was used to calculate (F-3N) in moles/liter. The results are summarized in Table 12 below:

Table 12 – Redox Summary for Tank 40

	Target Redox, $Fe^{2+}/\Sigma Fe$	Predicted Redox By F-3N, $Fe^{2+}/\Sigma Fe$
SB2-2	0.20	0.16

The "Predicted Redox By F – 3N" above was calculated using

$$Fe^{2+}/\Sigma Fe = 0.217 + (0.253*F - 0.739*N)*(45 \text{ wt. \%/wt. \% total solids of SME product})$$

where F and N are the measured formate and nitrate ion concentrations in the SME product in units of molarity. The equation was taken from the Excel spreadsheet being used to calculate expected redox in DWPF. The difference

between the target redox and that predicted by the SME product anions was due to uncompensated losses to the two anions during processing.

SME Cycle Gas Generation Rates

The Tank 40 variability study run, SB2-2, was continued through a SME cycle. Table 13 summarizes the key quantities measured during the SME cycle. No nitrous oxide was detected.

Table 13 – Tank 40 SME Cycle Gas Evolution Summary

	Hydrogen	Carbon Dioxide	Nitrous Oxide
Maximum Concentration, vol. %	0.0049	0.621	0.0
Maximum Generation Rate, lb./hr	0.0010	2.751	0.0
Total Mass, lb.	0.0068	7.2	0.0

The DWPF design basis limit for hydrogen in the SME cycle is 0.23 lbs./hr. These hydrogen values are well below the design basis limits. The mass of carbon dioxide evolved was only about 1% of that evolved during the SRAT cycle, 600 lbs., see Table 8.

Figure 5. Tank 40 SME Gas Generation Rates

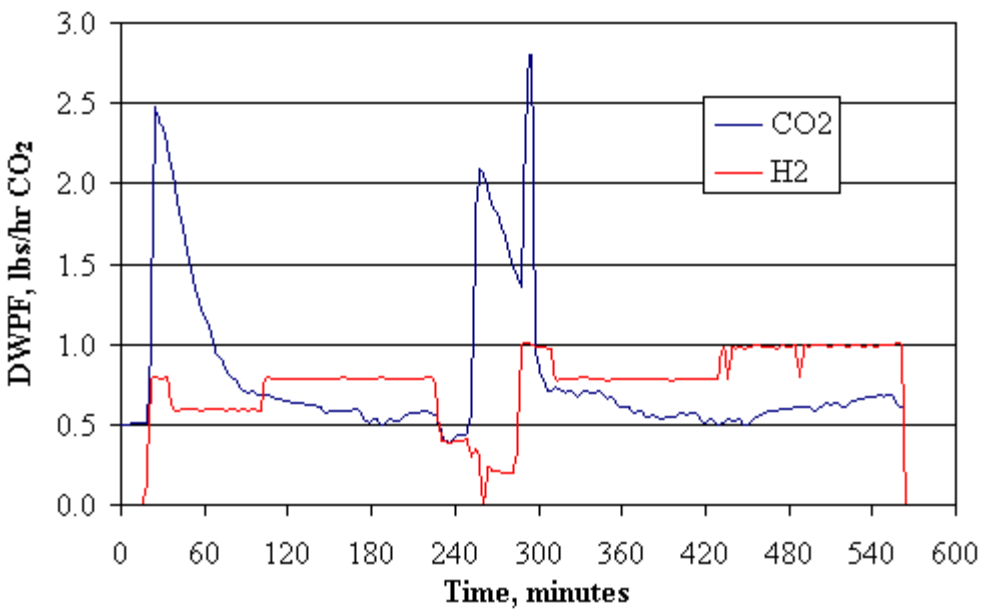

The hydrogen flow rate data was dominated by the presence of a single significant digit in the GC data file, e.g. gradual transitions from 0.003 volume % to 0.004 volume % show as stair step jumps in flow rate. The arrows denote the period when the kettle was cool because of the mass of frit and water added, followed by the heat-up time to return to boiling.

SME Product Acceptability Tests

The glass produced from SB2-2 SME product was tested to determine its leach rate for Na, Li, B, and Si versus the EA Glass Standard. The leach rates for these cations were much lower than the EA Glass Standard. The PCT results are summarized in Table 14 below.

Table 14 – Product Consistency Test Results for Tank 40 Glass, g/L

	Na	Li	B	Si
EA	14.9	9.77	18.9	4.26
SB2-2	0.671	0.745	0.567	0.426

PCCS calculations were performed for the Tank 40 sludge composition, Appendix H. The maximum frit 200 permitted by the current liquidus constraint was 76.3 wt. %. The maximum frit 200 permitted by the homogeneity constraint was 81.2 wt. %. The variability study run, SB2-2, targeted sludge oxides at 23.7 wt. % and frit 200 at 76.3 wt. % in the recipe calculations.

SME Cycle Foaming

Foaming was not an issue during the SME cycle of SB2-2. A prototypical initial addition of 100 ppm IIT747 antifoam was made prior to going to boiling after the first frit addition. Foaming was not a problem during the dewatering following either of the two frit additions. There was probably some residual antifoam from the SRAT cycle still active at the start of the SME cycle, since only about an hour elapsed between the end of the SRAT cycle and the beginning of the SME cycle.

Tank 8/40 Blend Testing – SRAT Cycle

Seven SRAT cycles were completed using a blend of Tank 8 and Tank 40 sludge simulants. Four of these runs were scoping runs (1B-4B), and three were variability study runs (SB2-1, SB2-3, and SB2-4). Scoping run 1B and variability study run SB2-4 had very high levels of noble metals (for different reasons), Table 3. Scoping run 3B and variability study run SB2-1 were essentially identical in plan. *SB2-1 is considered the base case for blend processing and the planned strategy for the Shielded Cells run.* Scoping runs 2B and 4B were at higher and lower acid stoichiometry respectively than 3B and SB2-1.

Variability study tests were run continuously until the completion of the SME cycle. Scoping runs were not conducted in round-the-clock mode. Consequently, the SRAT cycle was interrupted at some point, shut down, and then restarted the next day. Six runs targeted a redox of Fe^{2+}/SFe equal to 0.2. The last variability study run, SB2-4, assumed a complete transfer of the Formic Acid Feed Tank to the SRAT. SB2-4 acid stoichiometry had nitric acid comparable to runs 3B, SB2-1, and SB2-3. Only formic acid changed. The net result was about 290% acid stoichiometry versus 125% in 3B, SB2-1, and SB2-3. SB2-3 differed from SB2-1 in that it used HM levels of the noble metals Ag, Pd, Rh, and Ru.

The blend of Tank 8 and Tank 40 sludge simulants was less viscous than Tank 40 alone, but more viscous than Tank 42 sludge simulant tested in 1999. Poor mixing was generally not an issue during the tests with the blended sludges. Three of the four scoping runs had a 3-inch diameter Rushton flat blade radial flow impeller in the lower position (1B, 2B, 3B), whereas the Tank 40 scoping runs and blend run 4B were made with a 3.625-inch diameter Rushton type. All variability study runs were made with 3.625-inch diameter Rushton impellers in the lower position. Any effects of impeller size on the blend runs were too subtle to be detected.

Hydrogen-Carbon Balance

The background for this section is given under Tank 40 Testing: Hydrogen-Carbon Balance above. Many of the significant findings are similar to those for Tank 40. The sum of carbonate and formate lost from the sludge was comparable to the amount of carbon dioxide produced. The amount of formate lost was much greater than what can be explained based on a combination of reduction of mercury and manganese, conversion of nitrite to N_2O, and hydrogen generation. Reaction paths for formate destruction that involve the consumption of oxygen again appear to be required to explain the observations. In addition it was found that hydrogen could be generated at a rate in excess of the design basis at high acid stoichiometries (≥135%).

Table 15 below gives the total production mass and maximum production rate of hydrogen and carbon dioxide for the seven Tank 8/40 blend runs. Hydrogen data from WSRC-RP-98-00149, the equivalent study for Sludge Batch 1B, are

again included for comparison. *The DWPF design basis upper limit in the SRAT cycle for hydrogen is 0.65 lbs./hr.*

Table 15 – Hydrogen and Carbon Dioxide Summary for Blend SRAT Tests

Run (% acid)	Mass H_2, lb.	Max. Rate, H_2, lbs./hr	DWPF H_2 Limit, lbs/hr	Mass CO_2, lb.	Max. Rate, CO_2, lbs./hr
1B (137.5%)	3.26	**1.04**	0.65	1190	525
2B (137.5%)	2.65	0.475	0.65	1050	583
3B (125%)	1.70	0.385	0.65	1070	560
4B (110%)	0.29	0.054	0.65	815	543
SB2-1 (125%)	1.95	0.355	0.65	1130	597
SB2-3 (125%)	1.43	0.311	0.65	920	501
SB2-4 (290%)	34.86	**6.67**	0.65	2600	521
Tank 42 (125%)	-	0.001	0.65	-	-
Tank 42 (137.5%)	-	0.004	0.65	-	-

Runs 1B and SB2-4 exceeded the design basis hydrogen generation rates. The estimated noble metal composition for the Tank 8 component of the blend dominated all but run 1B (where Tank 40 and Tank 8 estimates were comparable). SB2-4 used the High Level Waste database estimates for Tank 8 noble metals for both the Tank 8 and the Tank 40 portions of the blend The noble metal loadings in both runs 1B and SB2-4 may be unrealistically conservative.

The nominal case, SB2-1, had a maximum hydrogen generation rate of about one-half the design basis. The result from essentially identical run 3B was at 60% of the design basis. If the noble metal content of the actual waste sample is comparable to that in the simulants, then it is possible that hydrogen evolution during the Shielded Cells run might exceed 25% of the lower flammability limit.

Figure 6 shows the SRAT generation rate of hydrogen scaled to DWPF for the four blend scoping runs. Hydrogen was initially detected following a large peak in N_2O generation (refer to nitrogen balance section below and Figure 12). 1B, with about double the noble metal content of the other scoping runs, had a large generation rate of hydrogen shortly after nitrite destruction was essentially complete. 2B and 3B began producing hydrogen at about the same time as 1B, but at a much lower rate initially. 2B started late and was shut down for the night at about the 150 minute mark (two-and-a-half hours into boiling). Unfortunately, this processing interruption to the experiment may have adversely affected the overall hydrogen generation process, since the second significant drop in N_2O production came later than was typically observed. The other scoping run shutdown interruptions occurred much later in the SRAT cycle. This makes the process of comparing run 2B to the other runs more challenging.

Figure 6. Tank 8/40 Blend - Hydrogen Generation

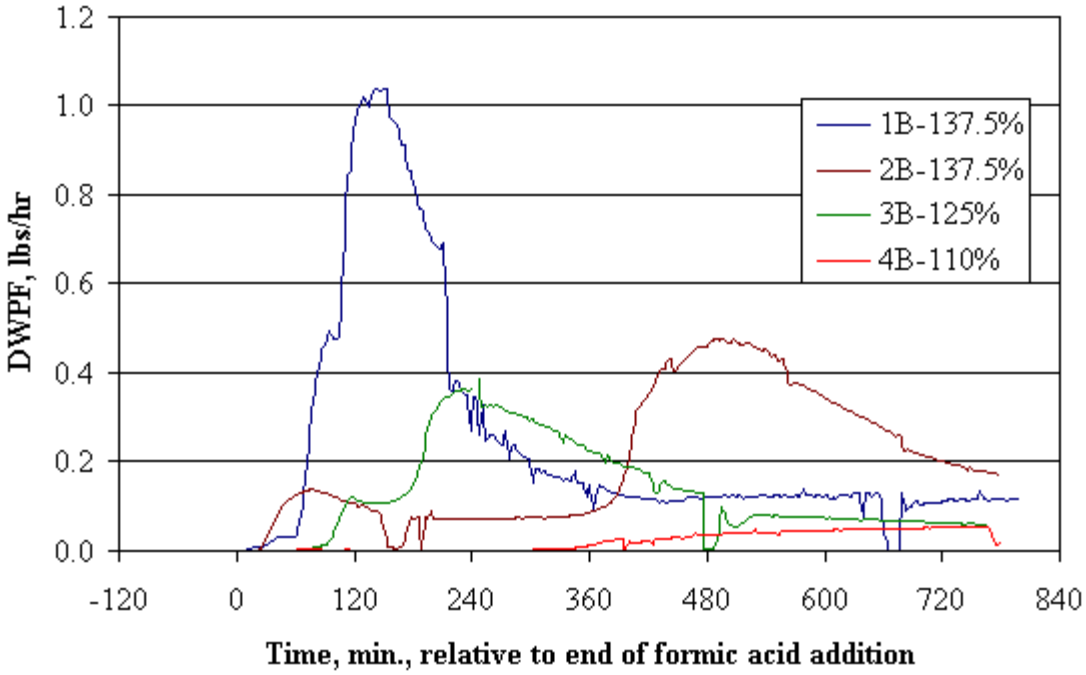

Broadly, it appeared that the approximately 50% reduction in noble metals for runs 2B-4B vs. 1B led to about a 50% reduction in maximum hydrogen rate at constant acid. Simultaneously, it appeared that reducing the acid stoichiometry also led to lower maximum rates. Nitrite ion was still at 490 mg/L at the 480 minute mark in 4B, while nitrite was less than 100 mg/L at the 120 minute mark in the other three runs. Run 4B nitrite ion destruction rate and hydrogen generation rate were similar to runs in the 1/240th scale Glass Feed Preparation System made in 1999 using Tank 42 simulant at 137.5% acid [Koopman]. Additional details can be found in Appendix F: *Supplemental Data from the Test Runs*.

Figure 7 compares the hydrogen generation rate data for the three runs at 125% acid: 3B, SB2-1, and SB2-3. 3B and SB2-1 were batched identically, while SB2-3 used 100% HM levels of the four noble metals.

Figure 7. Tank 8/40 Blend - Hydrogen - 125% Acid

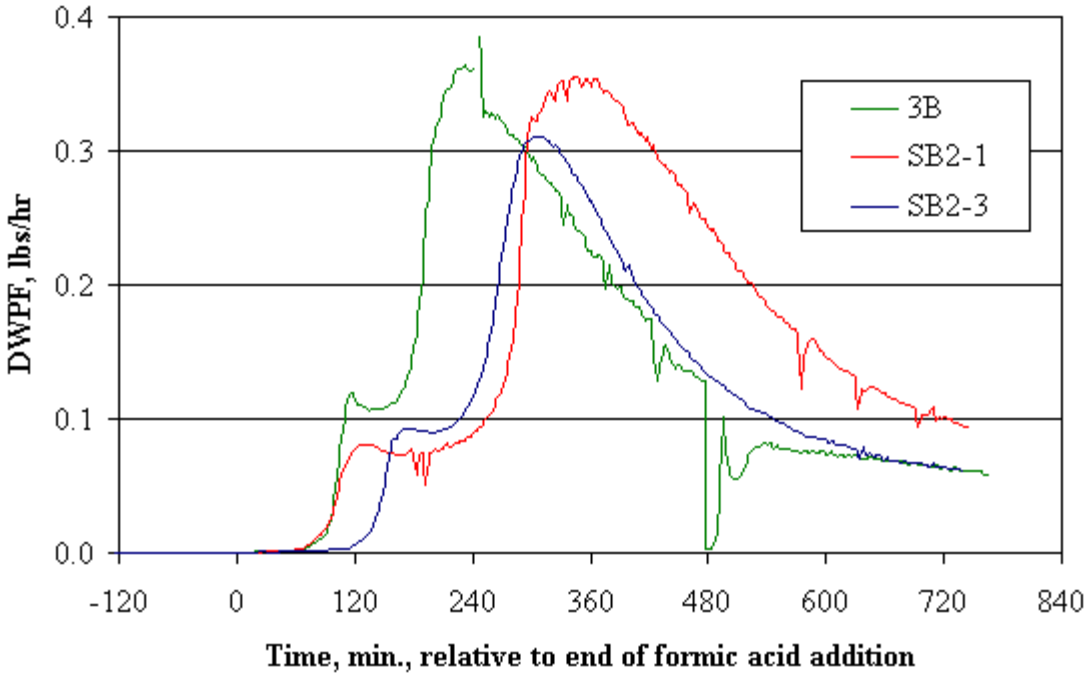

Hydrogen generation was again observed to be associated with two features in the evolution of N_2O. After a large initial peak in N_2O production, hydrogen began to be detected. After a second lesser peak, marked on Figure 13, the hydrogen generation rate rose to its maximum value. A noteworthy feature of Figure 7 is that SB2-3 has almost double the rhodium content of the other two runs. In spite of this the hydrogen mass produced and the maximum rate were both lower than in the other two runs (numbers in Table 15 above). On the other hand, ruthenium concentrations were almost identical (0.205 wt. % vs. 0.217 wt. % for SB2-3), while palladium concentrations were very similar (0.097 wt. % vs. 0.079 wt. % for SB2-3). Since the mass of hydrogen produced in SB2-3 is 81-88% of that in the other two runs, and the palladium content is 81% as high, it would be tempting to associate palladium with the boost in hydrogen generation observed. The ruthenium is so close in concentration and the uncertainty in the gas generation data too large to rule out ruthenium or a combination at this point.

Such a hypotheses concerning the other noble metals does not contradict what was observed for 1B and 2B above, since the relative decreases in palladium, rhodium, and ruthenium were all comparable (47-54%). It may be that rhodium activates first, shortly after acid addition, but is limited in its ability to make hydrogen by its smaller mass. After the second N_2O peak, there may be a second noble metal that becomes active, e.g. ruthenium or palladium, and is associated with the increase in hydrogen generation rate. If nitrite ion destruction is delayed, as in 4B, this noble metal may remain inactive or become only weakly active. The importance of balancing the overall acid stoichiometry with constraints on hydrogen generation rate remains quite evident.

The similarity of the initial hydrogen generation rate of about 0.1 lb./hr in the 90-150 minute period is also hard to explain if rhodium is the only active species. Depending on how rhodium crystallizes, it is possible to form roughly similar active surfaces from solutions differing by a factor of two in rhodium content. The run logs indicated that nothing particularly different was done between runs SB2-1 and SB2-3. The only intentional difference beyond using HM levels of noble metals was the use of irradiated IIT747 antifoam in SB2-3. Irradiation appears to have had only a minimal impact on the antifoam [Lambert]. The total antifoam added in the three 125% acid runs was the same, but it was added more gradually to 3B than it was in the other two runs. It is not possible to rule out the possibility that the antifoam affected a surface process like crystal growth. Results of such an interaction would be unpredictable.

Both palladium and ruthenium are closer in concentration between the three runs than rhodium. If the "simplest solution is the best" principle were to be applied, then palladium or ruthenium would be favored over rhodium as the

primary catalyst. Note also in Figure 6, for run 1B, where all the noble metals were doubled, that the height of the initial generation rate appeared to be about 0.5 lb./hr (wasn't there long). This observation tends to support the idea that more of some noble metal (which one is unclear) does effect the initial hydrogen generation rate during the period between the two N_2O peaks.

Work at the University of Georgia in the 1991-2 period looked at the noble metals individually. Some abstracted quotes from that work are included in Appendix C: *Excerpt Material from the University of Georgia Reports on Noble Metals*. Their findings indicated that rhodium would be active initially, even when nitrite was present, but that its activity would fall once nitrite was fully consumed (actually when nitrite was completely absent from their model system). They showed ruthenium gaining in activity in runs with no nitrite. Data reported on palladium were admitted to be contradictory with regards to its activity in the presence of nitrite, but palladium was reported to be active once nitrite was eliminated.

Taking the UGa work at face value, the initial hydrogen generation rate would be due to rhodium and/or palladium. The limiting step in the generation rate may not be catalyst concentration, in which case having twice as much rhodium in the HM run becomes a non-factor. Most of the perceived likely factors contributing to the generation rate (bulk fluid mass transfer, gas-solid diffusion, etc.) would be roughly linear in either formic acid concentration or catalyst concentration. Presumably, formic acid concentration was about equal in all the 125% acid runs. Consequently, these collectively controlled factors suggest that the role of rhodium was not dominant.

That would seem to imply that palladium is initially controlling (taking as given that ruthenium has zero activity until near total nitrite destruction is achieved). However, there is no reason to suppose that rhodium is inactive in this period. Following the second N_2O generation rate maximum may come a shift from a rhodium-palladium co-catalyzed system to a ruthenium-palladium co-catalyzed system (taking as given that the rhodium experiences a drop in catalytic activity once nitrite is consumed).

Figure 8 gives the carbon dioxide generation rate for the four scoping runs.

Figure 8. Tank 8/40 Blend - Carbon Dioxide Generation

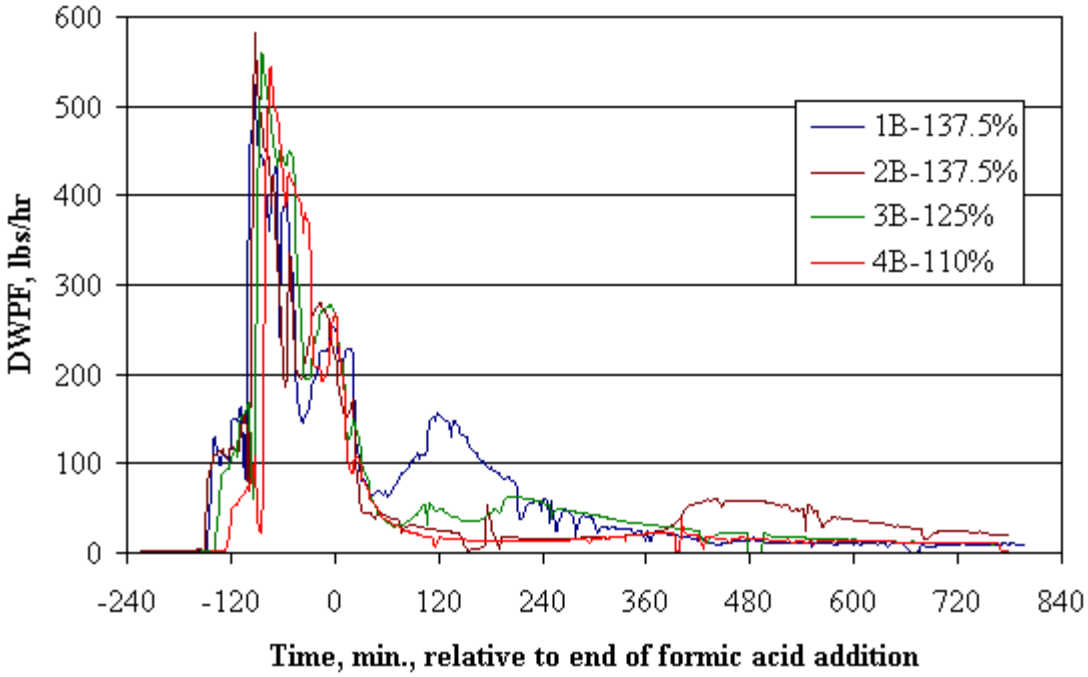

Figure 9 gives a more detailed view of how similar 1B and 2B were during acid addition and going to boiling. These two runs were both at 137.5% acid stoichiometry but at different levels of noble metals. The similarities help establish the reproducibility of the data being taken.

Figure 9. Tank 8/40 Blend - Carbon Dioxide Generation (Detail)

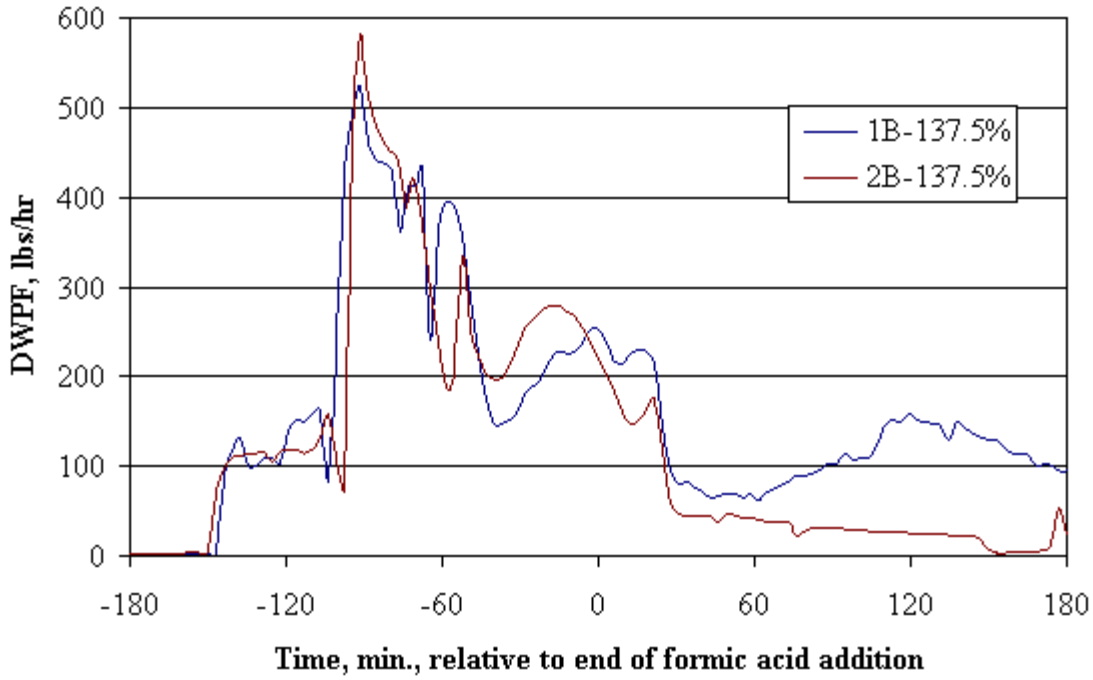

There was incredible similarity in the timing and magnitude of the peaks (appear to be at least seven) seen during acid addition. Multiple maxima, often partially superimposed by the time they reached the FAVC, were generally observed in the CO_2 generation rate during acid addition. It was only after the 1B run had gone to boiling, and started making markedly more hydrogen, that the two carbon dioxide generation curves diverged significantly. There were only two carbonates present in significant quantity by recipe: sodium carbonate and calcium carbonate. There was also a small amount of strontium carbonate. This seems to be too short a list to explain the diversity of features seen during acid addition, just as the mass of CO_2 that could be produced from carbonate was inadequate to explain the mass of CO_2 being produced. The mass of CO_2 produced from mercury reduction was quite small, but it may have been detected as a peak superimposed on the other features.

CO_2 was initially observed before the start of nitric acid addition, during the heat-up from room temperature to 93° C. This CO_2 was thought to be derived from the carbonate-bicarbonate-carbonic acid-CO_2+H_2O system, but it is presently unclear how significant CO_2 can be formed in a basic solution by thermal decomposition.

The total mass of CO_2 being formed during acid addition exceeded that expected from full destruction of the sludge carbonate. It appeared that much of the structure in Figure 9 came from the activation of various formic acid reductions as the pH of the system fell.

Figure 10 and 11 show the comparable data for the three runs at 125% acid.

Figure 10. Tank 8/40 Blend - Carbon Dioxide - 125% Acid

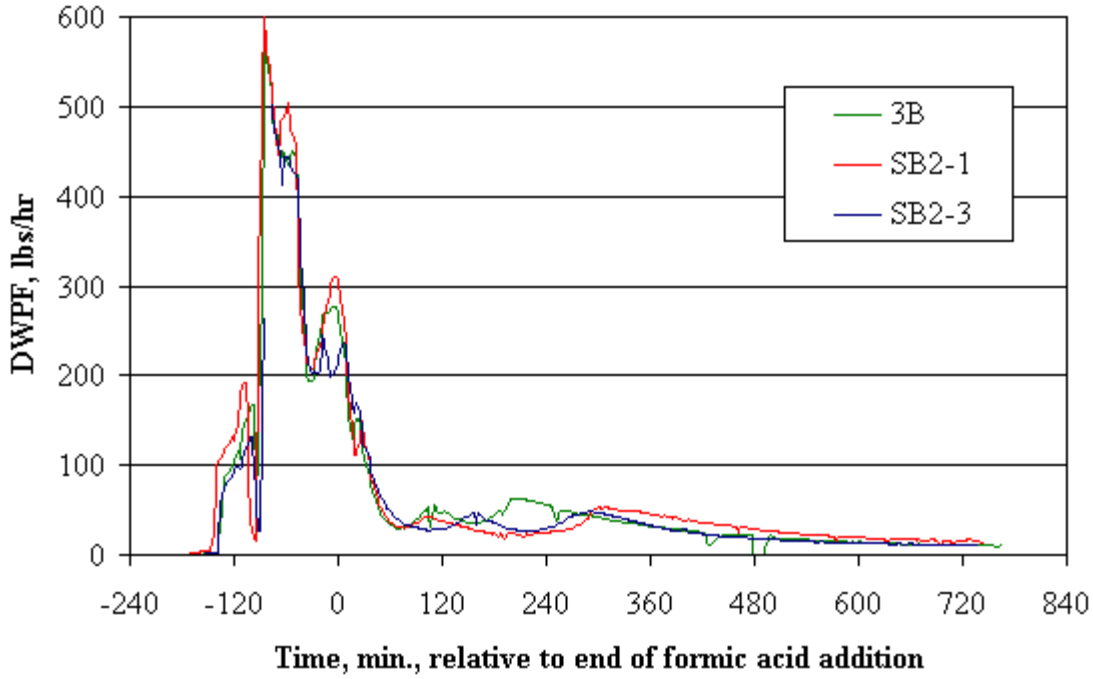

Figure 11. Tank 8/40 Blend - Carbon Dioxide - 125% Acid (Detail)

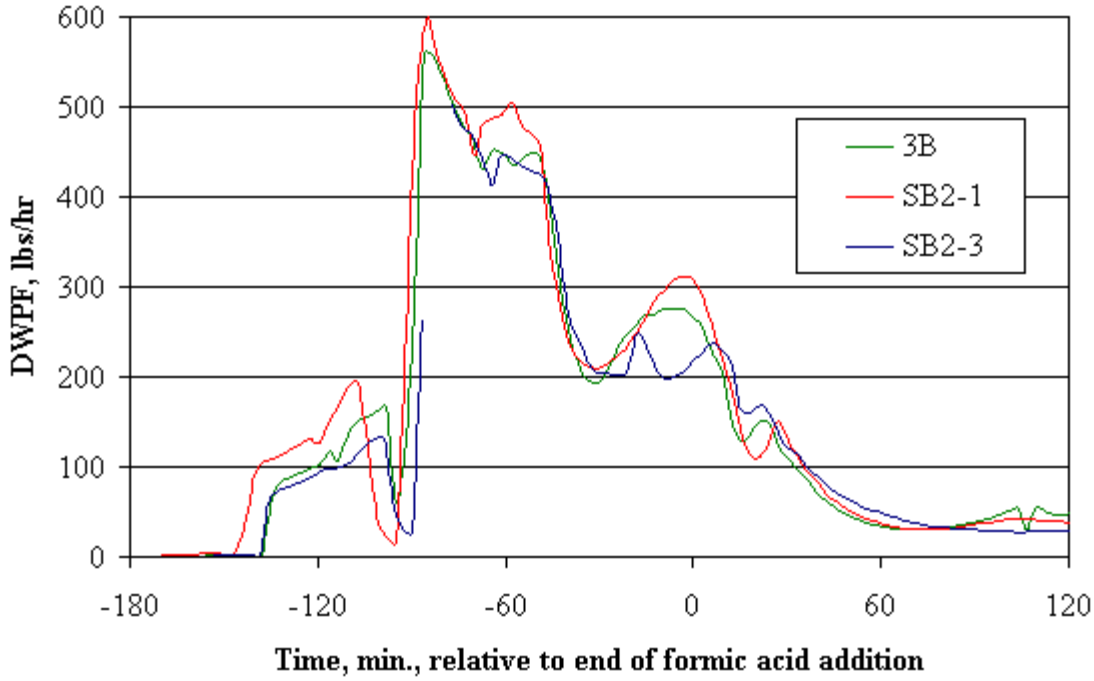

The similarities in the CO_2 results at constant acid were even stronger than those observed for the set of four scoping runs. Much of the ~10% lower total CO_2 production in SB2-3 may have been due to an upset in the GC readings that occurred at about -90 minutes, just as the CO_2 generation rate was going to maximum.

The available mass of carbonate in one Tank 8/40 sludge batch can be converted into about 290 lbs. of carbon dioxide. Although the total is similar to Tank 40, there is a shift from $CaCO_3$ based carbonate in Tank 40 to Na_2CO_3 based carbonate in Tank 8. Carbonate from Na_2CO_3 made up less than 3% of the carbonate in Tank 40 simulant, but

accounted for about 25% in the blend simulant. The relevant reactions for this sludge were given in the Tank 40 sludge results discussion earlier.

Total conversion of mercury requires only 6 lbs. of formic acid and produces 5.6 lbs. of carbon dioxide. The mass of manganese, however, exceeds that of mercury by about a factor of nine. Manganese has the potential to consume 186 lbs. of formic acid and produce 178 lbs. of carbon dioxide during reduction from oxidation state (IV) to (II). However, it is not believed that manganese is fully reduced during the SRAT cycle. Table 16 gives a summary of the various factors contributing to CO_2 formation for the four scoping runs. All values are in equivalent lbs./hr of CO_2. Table 17 gives a summary of the same factors for the variability study runs.

Table 16 – Carbon Balance as CO_2 for Tank 8/40 Blend Scoping Runs

Factor (as equiv. lbs. CO_2)	Scoping Run 1B	Scoping Run 2B	Scoping Run 3B	Scoping Run 4B
Carbonate lost (100%)	290	290	290	290
Lost Formate – by IC	+ 1090	+ 800	+ 580	+ 360
Sum of likely lost CO_2	1380	1090	870	650
vs. CO_2 by GC	1190	1050	1070	815
Lost Formate Factors:				
100% Mn reduction	180	180	180	180
100% Hg reduction	6	6	6	6
Per H_2 evolved	71	58	37	6
Per N_2O evolved	+ 47	+ 24	+ 23	+ 24
Sum of Formate factors:	304	268	246	216
Extra per O_2 consumed:	+ >480	+ >410	+ >540	+ >500
Revised Formate Sum:	>780	>680	>780	>720

There was fair agreement (within 20%) between the equivalent carbon dioxide from total destruction of carbonate and formic acid/formate ion lost as determined by IC and the carbon dioxide total measured by GC for the four scoping runs. As was seen for Tank 40, the usual factors (Hg, Mn, H_2 evolution, N_2O evolution) fell short of explaining the formate consumption measured by IC. The differences here, however, are much larger than those seen for the 2A and SB2-2 Tank 40 runs, perhaps due to the significantly higher noble metal concentrations here. As mentioned under the Tank 40 discussion above, allowing formic acid conversion with oxygen to CO_2 and water offers one possible path to carbon balance closure. However, unidentified reduction reactions could as easily be occurring that do not produce hydrogen.

Table 17 – Carbon Balance as CO_2 for Tank 8/40 Blend Variability Runs

Factor (as equiv. lbs. CO_2)	SB2-1	SB2-3	SB2-4
Carbonate lost (100%)	290	290	290
Lost Formate – by IC	+ 570	+ 440	+ 2100
Sum of likely lost CO_2	860	730	2390
vs. CO_2 by GC	1130	920	2600
Lost Formate Factors:			
100% Mn reduction	180	180	180
100% Hg reduction	6	6	6
Per H_2 evolved	43	31	770
Per N_2O evolved	+ 26	+ 33	+ 30
Sum of Formate factors:	255	250	986
Extra per O_2 consumed:	+ >560	+ >330	+ >500
Revised Formate Sum:	>820	>580	>1500

There was fair agreement (within 25%) between the equivalent carbon dioxide from total destruction of carbonate and formic acid/formate ion lost as determined by IC and the carbon dioxide measured at the GC for the three variability study runs. GC results for 3B and SB2-1 agreed well. IC results for 3B and SB2-1 agreed well. These two facts bear on the reproducibility of results, which appears to be better than the carbon material balance closure (a higher level of precision than accuracy). Both GC and IC predict a lower destruction rate for formic acid in SB2-3 (HM noble metals) than in SB2-1 (nominal case).

The issue of which SRAT product would lead to the best melter feed was not answered by this analysis. An investigation into the processes consuming the formic acid would be required to determine whether extra formic acid leads to a more reduced melter feed, and that lies beyond the scope of this work. If, however, the extra formic acid being converted into CO_2 as the % acid stoichiometry increases is due to reduction reactions with sludge, then this might imply that acid stoichiometry should be increased until the hydrogen generation rate becomes a limiting issue. It appeared that the gas generation rates in these tests were considerably higher than those observed during GFPS runs with Tank 42 simulant in 1999. Data from those tests was not fully analyzed – not in the scope of the antifoam task plan. The data is still available, however, and could be analyzed at some future date.

The consistent differences between the cumulative GC total and the carbonate/formate total for carbon dioxide were not readily explained. The GC and the MKS flow controllers were recently calibrated and checked. Any area bias on the GC was corrected during the analysis. The formate samples were immediately diluted with 1 ml of 1 M NaOH to quench any ongoing reactions. Sample masses were recorded before and after this dilution, so that necessary sample result conversions could be made. The formate sample was filtered before analysis, but the wt. % insoluble solids in the kettle was reasonably well known at the time of each sample. The number of times that one total came out higher than the other split 30:70 on the ten runs. The numerical integration of the GC data may have introduced a larger than expected error, since the GC data was not very smooth. (But, recall that numerical integration tends to be error smoothing as opposed to numerical differentiation which exaggerates errors.) As mentioned earlier, one possible cause of the differences could be within the GC at the high concentrations of CO_2 being measured (two to three times that in the calibration gas standard).

The four measurable contributors to formate loss are again inadequate to explain the IC based formate loss, as was also the case in the Tank 40 test runs (compare the blue numbers). They only account for roughly half of the observed formate loss. Hypothetical scenarios to explain that were covered earlier in the Tank 40 discussion. An oxygen loss rate bound was extracted from the GC data. The two rows at the bottom of Tables 16 and 17 above reflect the potential impact of this term alone and when combined with the other four contributors. Uncertainty in the true oxygen feed flow makes these numbers approximate. Oxygen consumption could be twice as large as estimated in many of the ten runs. Nevertheless, it appears that oxygen consumption must be somehow linked to formate destruction, either directly or indirectly.

Nitrogen Balance

The nitrogen balance reactions were discussed in the Tank 40 discussion earlier. It was found that nitrite ion was readily destroyed over the range of acid stoichiometries studies, 110-137.5%. Nitrate ion mass appeared to remain relatively constant once nitrite destruction was complete.

The Tank 8/40 blend SRAT cycle data indicate that nitrite ion was essentially 100% destroyed in all tests. It was generally destroyed quickly, falling to <100 mg/Kg within the first four hours at boiling except in run 4B (110% acid). The observed N_2O accounts for only 6-9% of the nitrite loss. Figure 12 below shows the DWPF-scaled N_2O generation rate for the four Tank 8/40 blend scoping run SRAT cycles:

Figure 12. Tank 8/40 Blend - Nitrous Oxide Generation

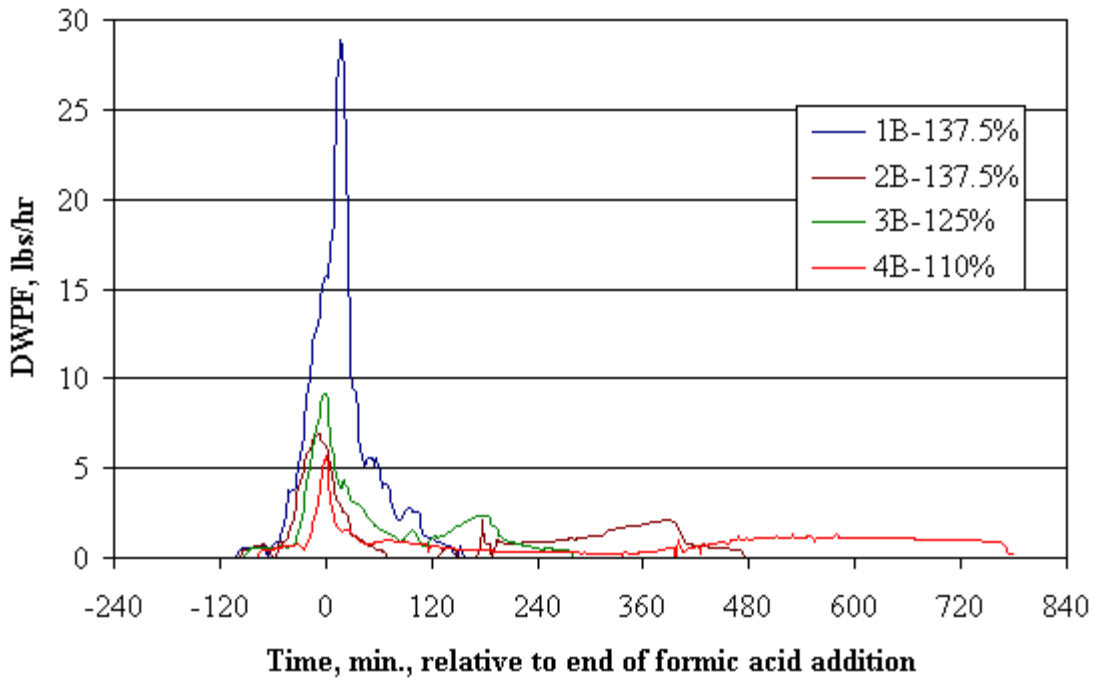

Each curve was characterized generally by two clearly distinct maxima, one just after the completion of acid addition and a second, smaller one later. There was considerably more variation than was seen in Figure 4, the corresponding Tank 40 plot. That plot, however, had all three runs at 137.5% acid. Since noble metals had seemingly no effect on the Tank 40 data, where there was a two order-of-magnitude swing in noble metal concentration, some other factor must presumably be responsible for the change that occurred from 1B to 2B at constant acid and roughly two-fold change in noble metals. Figure 13 gives the data for the two comparable SRAT cycles at 125% acid and the HM noble metal run, SB2-3, at 125% acid.

Figure 13. Tank 8/40 Blend - Nitrous Oxide - 125% Acid

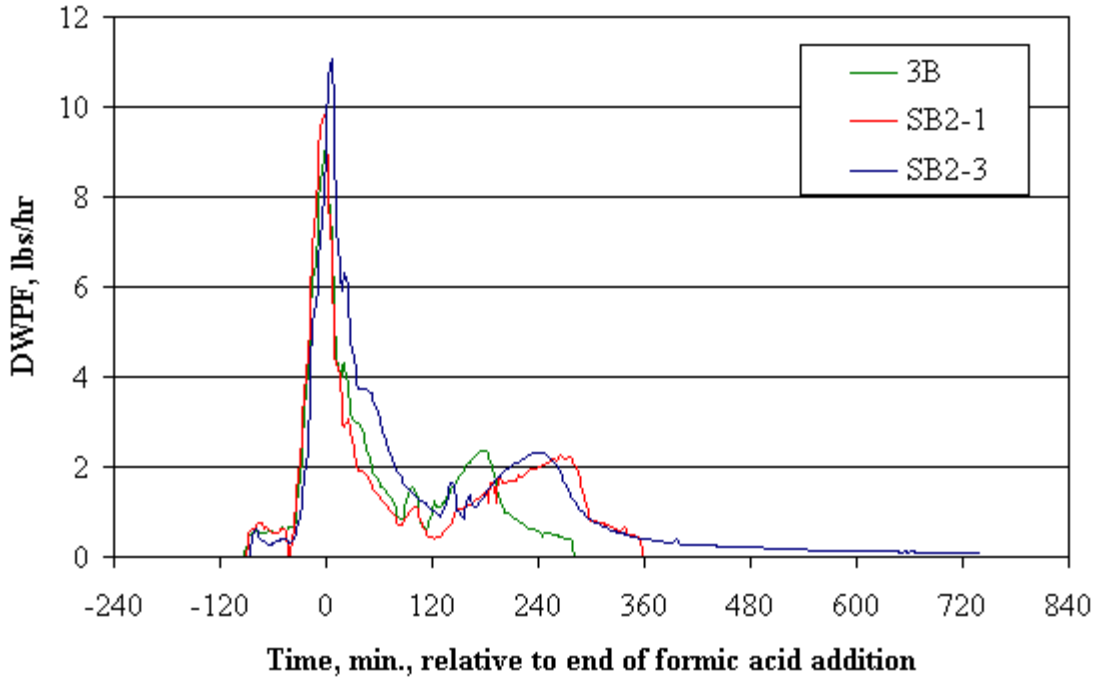

The three curves were extremely similar again, much like Figure 4, and not as much like Figure 12. The primary and secondary maxima are clearly visible. As discussed under the hydrogen-carbon balance above, the onset of hydrogen detection came with the initial, larger maximum, but an increase in hydrogen generation rate was associated with the secondary maximum.

The correspondence in time between various gas evolution/consumption effects is better seen in a plot like Figure 14 for SB2-1, the nominal case (additional similar plots can be found in Appendix F: *Supplemental Data from the Test Runs*). The flowrates have been scaled as indicated in the legend so that features in each are visible.

Figure 14. Composite SRAT Gas Generation Plot for SB2-1

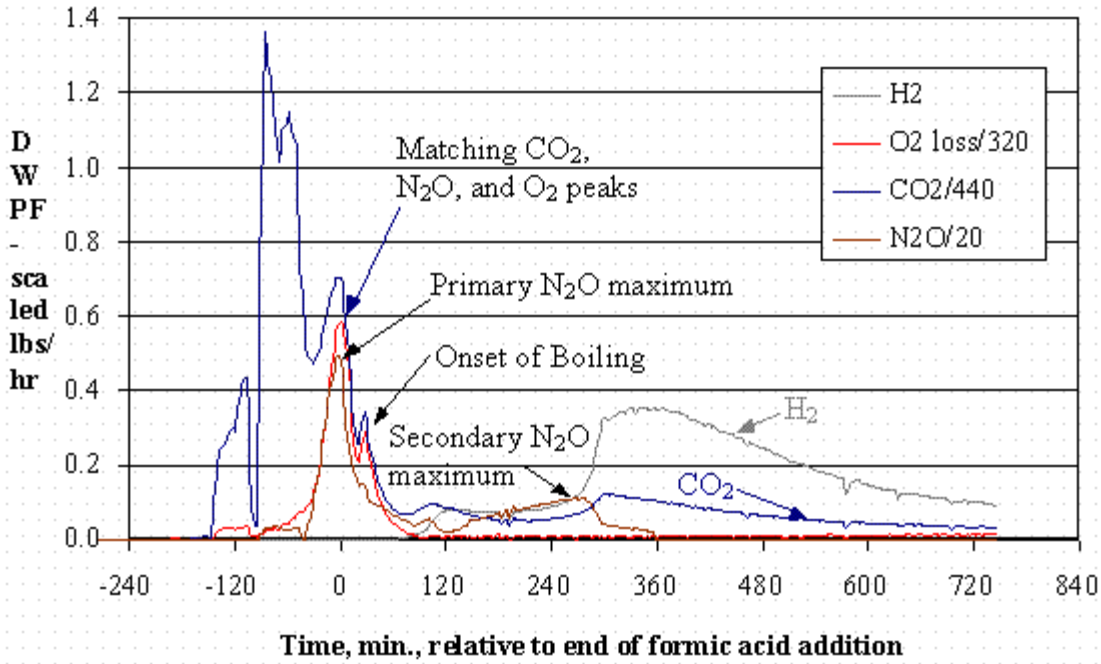

The zero consumption point for oxygen was somewhat arbitrary, and that entire curve could shift upwards. On a molar basis the flows in Figure 14 have O_2 and CO_2 at 20x H_2 and N_2O at 1x H_2. Two CO_2 peaks line up with two O_2 consumption peaks (at -10 minutes and at +30 minutes). The peak heights were more similar than an integration to areas would have been. (The matching N_2O peak at about -10 minutes represents only 1/20th as many moles/hour). Since the postulated formate consumption reaction is

$$2HCOOH + O_2 \rightarrow 2CO_2 + 2H_2O \qquad \text{(F-5)}$$

there appears to be more than enough oxygen consumption occurring to support this reaction during this time period and still have some left over for the nitrite destruction by

$$4HNO_2 \leftrightarrow 2NO_2 + 2NO + 2H_2O \qquad \text{(N-4)}$$
$$2NO + O_2 \rightarrow NO_2 \qquad \text{(N-5)}$$

It was not possible to track this reaction chain with the current instrumentation and equipment configuration. In the period from 180 to 720 minutes the carbon dioxide and hydrogen followed very similar curves, but the molar CO_2 generation rate was about six times higher. (Oxygen consumption was particularly hard to extract in this region – too close to the presumed feed flow). Apparently about 5/6th of the formate destruction occurring in this period was by reactions that did not produce hydrogen (the ratio appeared to hold nearly constant over quite a long period of time). (During scoping run 4B at 110% acid, the molar generation rate ratio of carbon dioxide to hydrogen may have exceed twenty – see Appendix F for more details).

The primary maximum in N_2O production was also correlated with one of the increased oxygen consumption rate periods. Oxygen is not necessary to convert nitrite to nitrous oxide. One inference would be that NO is evolved simultaneously with N_2O in a parallel reaction path, and that it is the NO that is consuming the oxygen. If so, the secondary maximum in N_2O production (at about +240 minutes) might also have been expected to have been accompanied by a detectable rate of oxygen consumption. No such change in oxygen consumption rate above the background noise was detected.

The analysis of the gas data leads to this seeming contradiction, that oxygen consumption is correlated with carbon dioxide most of the time, and that oxygen consumption is correlated with N_2O evolution most of the time. But oxygen consumption is not associated with either all of the time. More precise measurements would be needed to begin resolving the issues inherent in the above statements.

The assumption of a 30% conversion of nitrite to nitrate was consistent with the IC data after two-four hours of boiling in the SRAT cycle. (30% is derived assuming that about 90% of the nitrite converts nitrate in a molar ratio of 1/3 per the reaction described in the Tank 40 discussion.) Predicted and measured nitrate after dewatering are given in Table 18 below:

Table 18 – Predicted vs. Measured SRAT Nitrate Following Blend Dewatering

Run	Predicted Nitrate, mg/L supernate	Measured Nitrate, mg/L supernate
1B	15,056	12,198
2B	16,069	16,474
3B	14,797	17,000
4B	13,139	13,600[1]
SB2-1	14,787	18,800[2]
SB2-3	14,336	11,900
SB2-4	10,944	11,400

1. Nitrite only about 85% destroyed at this point.
2. This result appears to be an aberration.

The nitrate measurement result in Table 18 for SB2-1 followed a 14,100 mg/L result before dewatering, and was followed by a 16,800 mg/L two hours later. Analysis of the corresponding SRAT product occurred on a different day. The predicted and measured results were 16,150 and 16,200 mg/L respectively. Such close agreement was equally unusual.

A more realistic sense of improved closure between measured and predicted nitrate was seen in scoping run 1B where the SRAT cycle mid-run samples were 10,000-12,000 mg/L nitrate, and the final SRAT product sample was 18,000 mg/L (first set by ADS, SRAT product by Mobile Lab), and the predicted SRAT product was 16,600 mg/L. Agreement between the two labs was seldom within 10% on nitrate.

The grams of nitrate in the kettle appeared to remain fairly constant (once nitrite conversion was complete) in runs 1B, 2B, 3B, 4B, SB2-1, and SB2-3 based on the IC data. This was not the case with run SB2-4. Following nitrite conversion, there was a gradual decline in the indicated grams of nitrate as calculated from the IC sample results. Approximately 10-30% of the nitrate ion appeared to have disappeared by the end of the SRAT cycle based on the NaOH-quenched run samples analyzed by Mobile Lab. However, when the final SRAT product was analyzed by Mobile Lab, they reported 12,800 mg/L nitrate, while the material balance prediction (assuming no nitrate loss) was 13,350 mg/L. Consequently, as with the similar Tank 40 finding, the possible loss of 10-30% of the nitrate ion is not conclusive. An attempt to devise a scenario to explain these measurements by attributing the deviations to the kettle sampling system has not yet led to a plausible explanation (almost any conceivable quality of sample ought to be closer in nitrate to the predictions than what was measured, especially if the concentration is not changing appreciably, and noting that the nitrate is concentrated in the supernate phase).

Table 19 below provides the requested information on the maximum N_2O generation rate during the Tank 8/40 blend testing. Results for Tank 42 from WSRC-RP-99-00149 are again included for comparison.

Table 19 – SRAT Nitrous Oxide Results Summary for Tank 8/40 Blend

	Mass N_2O, lb.	Max. Volume % N_2O	Max. Rate, N_2O lb./hr
1B	23.7	2.17	28.7
2B	12.1	0.526	6.87
3B (like SB2-1)	11.6	0.718	9.14
4B	12.0	0.394	5.65
SB2-1 (nominal)	13.1	0.671	9.82
SB2-3	16.6	0.758	11.0
SB2-4	15.2	1.745	22.9
Tank 42 (125%)	-	0.204	5.411
Tank 42 (137.5%)	-	2.442	45.102

Agreement between 3B and SB2-1, the two "identical" SRAT cycles was reasonable for a laboratory experiment, and considering the numerical integration needed to produce the total mass plus the typical fluctuations in GC readings (a maximum rate almost always occurs at a fluctuation above the general trend). The concentrations of N_2O are well below the 20-volume % basis for DWPF flammability calculations.

Steam Stripping of Mercury

Tank 8/40 blended simulant was trimmed with mercury to 0.294 wt. %. That does not exceed the SRAT product design maximum of 0.45 wt. % on a dry solids basis. Mercury analyses were not obtained for the scoping runs. Three samples were analyzed from each of SB2-1, SB2-3, and SB2-4 for mercury. The first set of samples came at the mid-point of

the twelve hour SRAT cycle boiling period, the second set of samples came at the end of the SRAT cycle, and the third set of samples came at the end of the SME cycle. ADS reported sample results in mg mercury/g slurry. Table 20 summarizes the calculated initial mercury concentration and the three ADS results.

Table 20 – Mercury Results for Tank 8/40 Blend Runs

	SB2-1	SB2-3	SB2-4
Predicted initial Hg content	2864 μg/g	2860 μg/g	2859 μg/g
SRAT mid-point sample	3197 μg/g	775 μg/g	1072 μg/g
SRAT product sample	376 μg/g	724 μg/g	1085 μg/g
SME product sample	136 μg/g	904 μg/g	841 μg/g

Mercury should not be an issue at the projected sludge feed concentration. At 300-700 lbs. steam/lb. mercury stripped, the expected mercury content of all the samples would be nearly zero in these units, even at the SRAT mid-point sample (~1400 grams steam boiled versus 1.3 g of mercury batched). The SB2-3 and SB2-4 results suggest that the mercury may have become trapped (encapsulated by sludge particles?). The above results are not readily interpreted. The data could be qualitatively marking the concentration range for mercury below which it is difficult to remove mercury by steam stripping. Alternatively, these may be very poor quality sample results. The data support either conclusion and possibly other hypotheses as well.

There were some visual observations of films during the blend testing just as there were during the Tank 40 testing described earlier. The only gray film was reported during SB2-3, the run with HM levels of noble metals. Black films were reported during SB2-1, SB2-4, and possibly also during SB2-3 (everyone thought so, but agreed it was hard to tell). The blend scoping runs (1B-4B) were characterized by foaming problems (see below), and floating colloidal mercury could well have been formed but not observed.

Foaming

All Sludge Batch 2 testing used IIT747 antifoam as described for Tank 40 earlier. Foaming was a problem in the Tank 8/40 blend testing. The four scoping runs attempted to follow the DWPF prototypical antifoam addition strategy, 100 ppm before acid addition and 100 ppm before going to boiling. This strategy was revised for the three blend variability study runs. The actual antifoam additions required to complete the seven blend SRAT cycles are summarized in Table 21 below:

Table 21 – Antifoam Additions to Tank 8/40 Blend SRAT Cycles

(Additions in ppm)	1B	2B	3B	4B	SB2-1	SB2-3	SB2-4
Before acid addition	100.	100.	100.	100.	200.	200.	200.
During acid addition	50.	50.		50.			
Before boiling	100.	100.	100.	100.	500.	500.	500.
During boiling	50.	100.	100.	50.			50.
During boiling	50.	100.[1]	100.	50.			50.
During boiling	50.	100.[1]	100.	50.			50.
During boiling	50.	100.[1]	100.				
During boiling	50.[1]	50.[1]	100.[1]				
Antifoam Addition Total	500.	700.	700.	400.	700.	700.	850.
% Acid Stoichiometry	137.5	137.5	125.	110.	125.	125.	290.

1. Antifoam additions made on second day of discontinuous SRAT cycles.

Some historical problems with the DWPF prototypical antifoam addition strategy were discussed in the Tank 40 foaming section earlier. Based on the four scoping runs and discussions with DWPF, it was decided to try 700 ppm in the variability study runs using two additions, one before acid addition, 200 ppm, and one before boiling, 500 ppm. This strategy appeared to work fine during SB2-1, the nominal blend run at 125% acid. This strategy also worked fine during SB2-3, 125% acid and HM noble metals. The biggest difference between SB2-1 and SB2-3 from a foaming/antifoam perspective was that the IIT747 antifoam used in SB2-3 was irradiated at $1.1*10^6$ rad/hr from a cobalt-60 source for 37 minutes [Lambert]. Only minor foam formation was observed during this run, using the revised antifoam addition strategy.

Although it initially appeared that noble metals might be adversely affecting antifoam performance, there was more evidence that avoiding excessive acid addition might have been the key to extending antifoam life. Noble metal concentration was identical for runs 2B, 3B, 4B, and SB2-1. It was roughly twice as high for 1B and SB2-4. Run 1B managed to conclude with the second smallest total antifoam addition, but SB2-4 required the largest antifoam addition. Run 4B with only 110% acid required the least antifoam to complete. Actual antifoam additions would seem to be characterized by *as little as was needed to make it through the run*, except in the case of SB2-1 and SB2-3. It is not recommended that DWPF try to run with such a small margin of error, estimated to be about 50 ppm or less, relative to the minimum required amount of antifoam.

Tank 8/40 Blend Testing – SME Cycle and Redox

Acid Additions and Redox

A spreadsheet has been previously developed to calculate the nitric and formic acid additions required to reach a redox target for a given sludge mass, sludge composition, and acid stoichiometry. All but one Tank 8/40 blend simulant tests had a redox target of $Fe^{2+}/SFe = 0.2$. The formate and nitrate concentration of the SB2-1 SME product were also measured. This was used to calculate (F-3N) in moles/liter. The results are summarized in Table 22 below:

Table 22 – Redox Summary for Tank 8/40 SME Product

	Target Redox, Fe^{2+}/SFe	Predicted Redox By F-3N, Fe^{2+}/SFe
SB2-1	0.2	0.16
SB2-3	0.2	0.19
SB2-4	No Target	0.45

The "Predicted Redox By F – 3N" above was calculated using

$$Fe^{2+}/SFe = 0.217 + (0.253*F - 0.739*N)*(45 \text{ wt. \%/wt. \% total solids of SME product})$$

where F and N are the formate and nitrate ion concentrations of the SME product in units of molarity. The difference between the target redox and that predicted by the SME product anions was due to uncompensated losses to the two anions during processing. Formate and nitrate ion results for SB2-3 and SB2-4 both looked low based on the results through the SRAT cycle plus material balance calculations (the large amount of gas evolution in the SB2-4 SME cycle was never fully incorporated into the material balance).

Appendix E gives the various sample results for the four SME cycles. After SB2-1 and SB2-2 were completed, it was judged that the product did not look concentrated enough for the Task Plan rheology measurements. The run plan had

basically tried to hold the SME product volume equal to the initial SRAT product volume. In runs SB2-3 and SB2-4 the SME product was concentrated somewhat further. The potentially alarming conclusion is the low weight percent total solids of these melter feeds. They ran about 45 wt. % total solids. This can be traced back to the low initial wt. % total solids of the SRAT feed sludge. If the uranium in the real waste, plus the insoluble sodium deleted from the simulant recipe, brings the sludge solids loading back up to 17-17.5 wt. %, then there ought to be a corresponding increase in the SME product. If the real waste behaves rheologically like the simulants used in this testing, then the real waste might be very difficult to handle and process due to high viscosity. A separate report will be prepared describing the simulant rheology work that occurred in parallel with this work.

SME Cycle Gas Generation Rates

The three Tank 8/40 blend variability study runs, SB2-1, SB2-3, and SB2-4, were taken through the SME cycle. Similar quantities were derived from the GC data as were derived for the SRAT cycle. These results are given in Table 23 below.

Table 23 – Tank 8/40 Blend SME Cycle Gas Evolution Summary

Hydrogen	SB2-1	SB2-3	SB2-4
Maximum Concentration, vol. %	0.682	0.582	2.85
Maximum Generation Rate, lbs./hr	0.140	0.122	3.00
Total Mass, lb.	0.659	0.623	9.06
Carbon Dioxide			
Maximum Concentration, vol. %	16.6	14.9	8.62
Maximum Generation Rate, lbs./hr	89.3	77.8	235.
Total Mass, lb.	107.	110.	600.
Nitrous Oxide			
Maximum Concentration, vol. %	0.198	0.185	0.0
Maximum Generation Rate, lbs./hr	0.961	0.965	0.0
Total Mass, lb.	0.350	0.680	0.0

The two runs at 125% acid were at over one-half of the maximum design basis flow for hydrogen in the SME cycle of 0.23 lbs./hr. SB2-4 with 290% acid exceeded the design basis hydrogen flow by a factor of thirteen. Figure 15 shows the hydrogen flow rate at DWPF scale during the three SME cycles. The lack of N_2O in the SB2-4 run may simply mean that the concentration was too small to be detected. Hydrogen evolution during SB2-4 was almost continuously above the DWPF design basis limit (except when cooled down during the second frit slurry addition).

Figure 15. SME Hydrogen Generation in Blend Runs

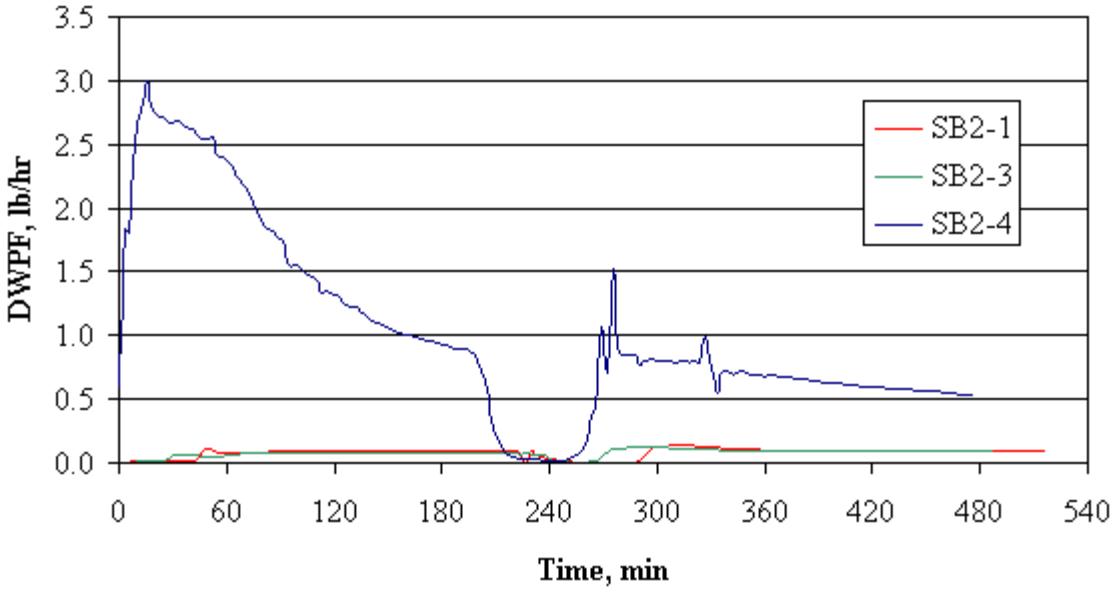

Figure 16 gives the SME carbon dioxide generation rate at DWPF scale for the Tank 8/40 blend variability study runs. The behavior of the two 125% acid stoichiometry runs, SB2-1 and SB2-3, was very similar. SB2-4, as described in Table 23 above, produced about six times as much carbon dioxide as the other two runs. Spikes in the gas generation rate following the second frit addition are associated with the onset of boiling (and rapid displacement of accumulated gas in the kettle).

Figure 16. SME Carbon Dioxide Generation in Blend Runs

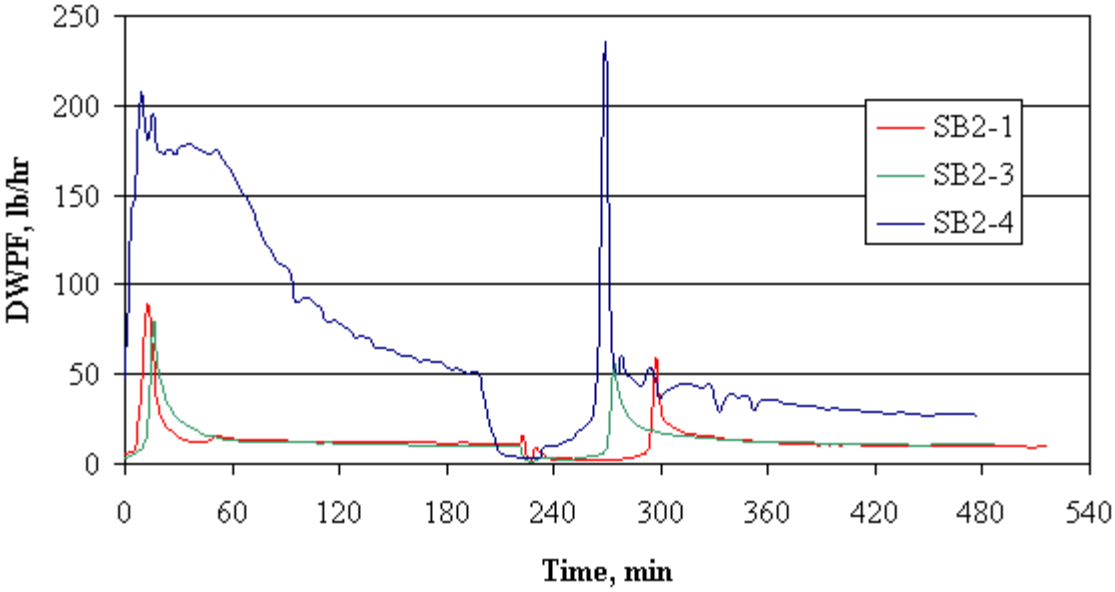

Figure 17 gives the SME nitrous oxide generation rate at DWPF scale.

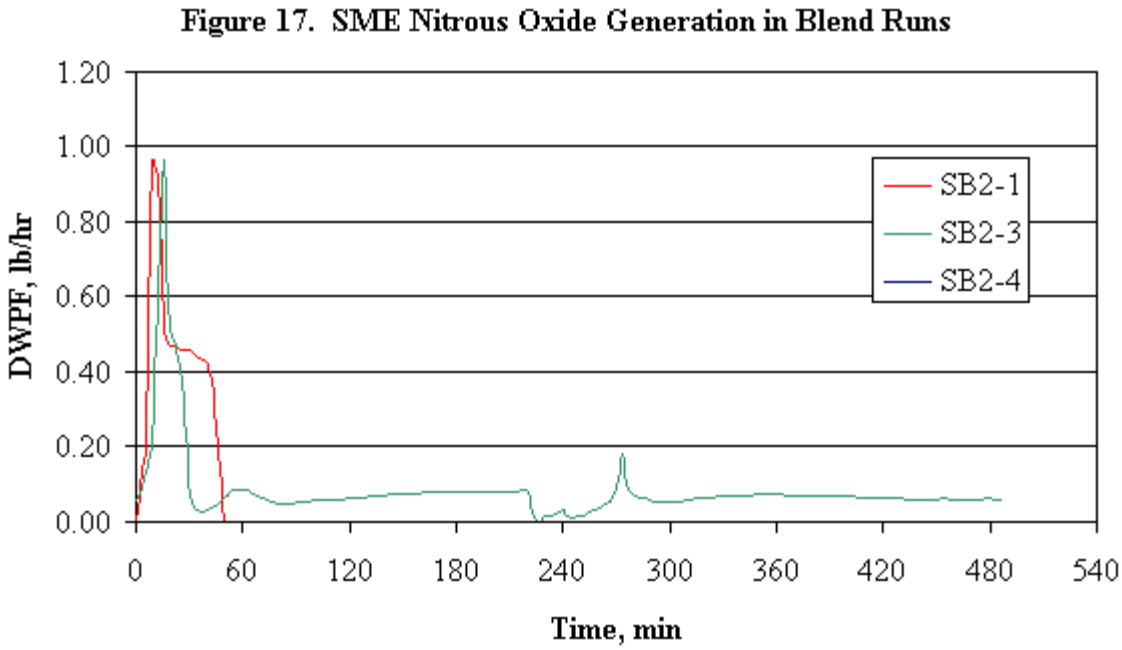

It is evident from the traces in Figure 17 that nitrous oxide was frequently below the detection limits of the GC during all three runs. No nitrous oxide was detected during the SB2-4 SME cycle. Data obtained frequently had only a single significant figure. Roughly comparable masses of N_2O had been produced during the three corresponding SRAT cycles, Table 19.

SME Product Acceptability Tests

The glass produced from SB2-1, -3, and -4 SME products were tested to determine their leach rates for Na, Li, B, and Si versus the EA Glass Standard. The leach rates for these cations were much lower than that of the EA Glass Standard. The PCT results are summarized in Table 24:

Table 24 – Product Consistency Test for Tank 8/40 Glasses, g/L

	Na	Li	B	Si
SB2-1	0.613	0.712	0.540	0.413
SB2-3	0.602	0.695	0.505	0.391
SB2-4	0.649	0.759	0.565	0.398
EA	14.9	9.77	18.9	4.265

PCCS calculations were performed for the blended sludge composition, Appendix H. The maximum frit 200 permitted by the current liquidus constraint was 74.8 wt. %. The maximum frit 200 permitted by the homogeneity constraint was 79.1 wt. %. The three blend variability study runs targeted sludge oxides at 25.2 wt. % and frit 200 at 74.8 wt. % in the recipe calculations.

SME Cycle Foaming

Antifoam additions in the SME cycle were done prototypically during the three variability study runs. An initial dose of 100 ppm of antifoam was added to the SME sludge after the first frit 200-water-formic acid addition and before

boiling. Foaming was not observed during the SB2-1 SME cycle. Foaming was not observed during the SB2-3 SME cycle. During SB2-4, an additional 50 ppm of antifoam was required during the first frit addition dewatering step to control foaming, and an additional 450 ppm of antifoam was ultimately added during the second frit addition dewatering period to control foaming.

Tank 8/40 Blend Testing – The Case of SB2-4

Graphical data for SB2-4 have been omitted from the discussion of Tank 8/40 blend testing up until this point, although numbers have been included in the various tables. SB2-4 was characterized by more of everything than the other runs, more hydrogen evolution, more carbon dioxide evolution, more formate destruction, etc.

By the end of the SB2-4 SRAT cycle there were a number of unusual observations not made in any of the other nine test runs. A reddish ring was observed all around the kettle at the end of the SRAT cycle. The kettle was reported to have had a mirrored look to it. (I thought the kettle wall looked more like the reflections you get from a soap bubble, sort of a rainbow-like effect, superimposed on the brown sludge. The kettle was definitely not shiny in the metallic sense of the word.) The sludge itself, which had initially been sort of tan to dark orange in color, turned to a very dark brown color during processing. It is not clear what this signified. Perhaps a dark solid species precipitated onto the surface of some of the lighter colored particles, producing a net darker appearance.

Figure 18 below is a composite plot of scaled gas generation rate data at DWPF scale for the SB2-4 SRAT cycle.

Figure 18. SB2-4 SRAT Composite Gas Generation Plot

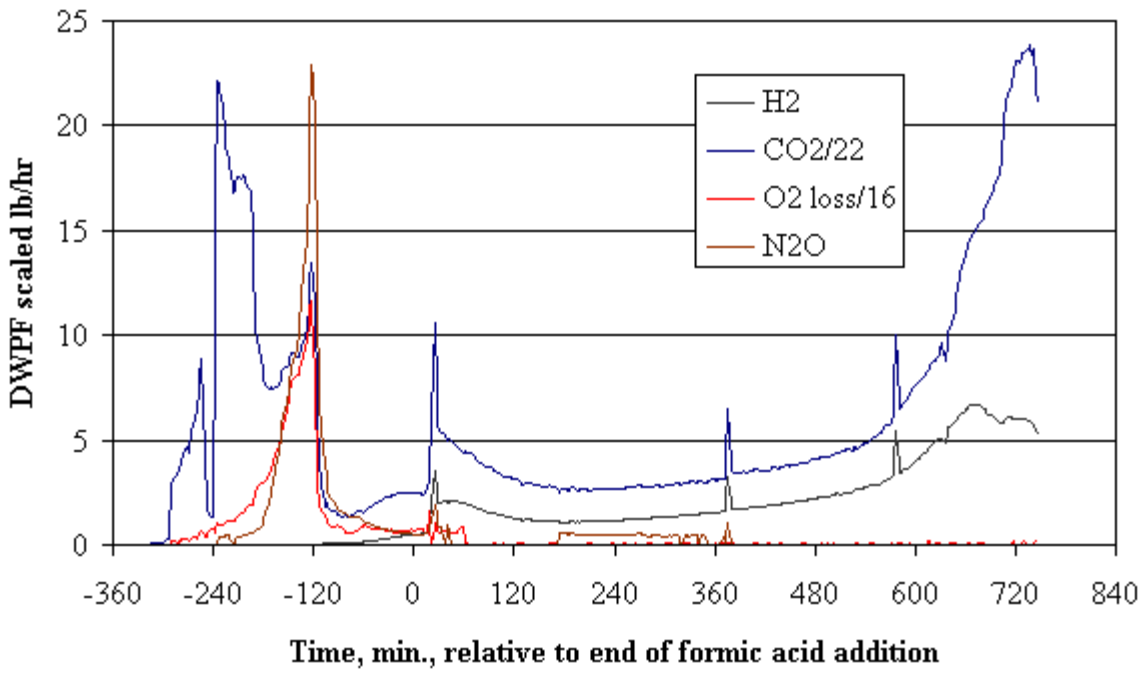

The carbon dioxide and hydrogen generation rates, and the oxygen consumption rate, were scaled to an equimolar basis, i.e. 5 lb./hr scaled CO_2, 5 lb./hr scaled O_2 loss, and 5 lb./hr scaled H_2 represent the same molar flows. Only N_2O was not scaled to hydrogen, because its second maximum between 180 and 360 minutes would have been hard to see. Over much of the SRAT cycle boiling period, the carbon dioxide generation rate was about double the hydrogen generation rate. This ratio is much closer to unity than the six to one ratio observed for SB2-1. It could be argued that this effect was due to nearly tripling (2.6x) the formic acid content of the SRAT, since

(about three times as much acid)*(about 1:6 H_2:CO_2) = (about 1:2 H_2:CO_2).

Consequently this may be another piece of the puzzle that will eventually lead to an unraveling of what the formic acid

is doing in the SRAT cycle after the nitrite and mercury are gone. The feature in the hydrogen data at about 660 minutes is also interesting. It appears that the hydrogen generation rate has hit a maximum and is starting to fall. Simultaneously, there appears to be a surge in the carbon dioxide generation rate leading to about a four to one ratio between the two. SRAT nitrite destruction was so thorough that there was no N_2O detected in the SME cycle, unlike SB2-1 and SB2-3.

Recommendations

Shielded Cells Run

The following recommendations are made for the Shielded Cells run using Tank 8/40 blend:

- Based on the noble metal concentrations in the simulant testing, the acid stoichiometry target should be 125%. At this acid level, hydrogen generation rates in the SRAT and in the SME cycles were slightly above 50% of the two DWPF design basis maxima, and there was no radiolytic hydrogen contribution to the flows.
- IIT747 antifoam should be added shortly before acid addition at a concentration of at least 200 ppm, and again prior to going to boiling at 500 ppm.
- An additional 100 ppm of antifoam should be added with the first frit addition before any SME cycle dewatering.
- Attempt to watch the degree of mixing during formic acid addition. The quality of mixing was visually observed to worsen during the period around pH 7 in the simulant testing.

Revised Antifoam Addition Strategy

Based on this testing, the following minimal antifoam addition strategy was developed for Tank 8/Tank 40 blend sludge simulant.

> Use 200 ppm of IIT747 antifoam prior to acid addition, use 500 ppm of IIT747 antifoam prior to boiling in the SRAT, and use 100 ppm of IIT747 antifoam prior to boiling in the SME. Refresh the antifoam every 8-12 hours.

It is believed that noble metals were a contributing factor in having to raise the antifoam concentration during boiling in the SRAT cycle. When actual Tank 8 noble metals are determined, and if they are found to be considerably lower in concentration than in this testing, then it may well be that a much lower antifoam concentration would be sufficient. The 200 ppm recommendation for acid addition will remain. Foaming during acid addition has been seen with several simulants, both with and without noble metals and mercury, using IIT747 antifoam at only 100 ppm.

Should the need arise to process Tank 40 separately, then the following minimal antifoam addition strategy is recommended.

> Use 200 ppm of IIT747 antifoam prior to acid addition, use 200 ppm of IIT747 antifoam prior to boiling in the SRAT, and use 100 ppm of IIT747 antifoam prior to boiling in the SME. Refresh the antifoam every 8-12 hours.

Future Work

Hydrogen Study and SRAT Acid Calculation

It appears that Tank 8/40 simulant mixed with varying concentrations of noble metals produced measurably different hydrogen generation rates. There was a lot of compelling data that indicated that noble metals other than rhodium were contributing to hydrogen generation. There was also a suggestion in the scoping run data that noble metals may be affecting the IIT747 antifoam life or effectiveness (in the variability study runs, an attempt was made to dampen foaming into a non-issue). The tendency to foam appeared to be greater in runs with higher noble metal concentrations during the scoping runs. It is recommended that a study be developed which determines which noble metals are active,

and when they are active.

Coupled with the catalytic questions are a series of questions concerning the fate of formic acid lost during the SRAT cycle. Why does formic acid decompose to hydrogen to varying degrees without the formation of identical quantities of carbon dioxide (apparently a matching molar production rate has only been observed in runs under an inert atmosphere)?

The SRAT acid calculation uses the assumptions that 75% of the nitrite ion destruction occurs due to formic acid reduction, while the data in this report suggest a percentage in the 5-10% range (if only the path to N_2O is viable for formic acid reduction of nitrite). If, however, the NO is not only generated by both of the following reactions, that don't require formic acid as a reducing agent,

$$3HNO_2 \leftrightarrow HNO_3 + 2NO + 2H_2O \qquad \text{(N-3)}$$
$$2HNO_2 \leftrightarrow NO_2 + NO + H_2O \qquad \text{(N-4)}$$

but is also generated by [Hsu: 1990, 1992]:

$$2HNO_2 + HCOOH \leftrightarrow CO_2 + 2NO + 2H_2O \qquad \text{(N-8, F-4)}$$

then additional formic acid is being consumed in nitrite destruction than can be tracked with the existing equipment. (N-3 and N-4 are documented in outside literature. An outside literature reference for N-8 was not pursued.) Thermodynamic modeling might give some insight into the relative equilibrium constants of some of these proposed parallel reaction paths in acidic aqueous solutions.

The SRAT acid calculation also uses one of the following assumptions:

- that 60% of the manganese is reduced as:

  $$MnO_2 + 2H^+ \text{ ? } Mn^{2+} + O_2 + H_2$$

- that 40% of the sludge manganese is reduced by (WSRC-RP-90-0554):

  $$MnO_2 + 3HCOOH \text{ ? } Mn^{2+} + CO_2 + H_2O + 2HCOO^-$$

Either assumption is consistent with a 1.2 moles acid/mole manganese factor in the acid calculation. The latter reaction seems to be a relatively more likely scenario, given the vast excess of CO_2 being produced relative to hydrogen during this testing plus the net consumption of oxygen observed. It is probably worth checking the Mn^{+2} concentration of the SRAT contents as a function of time during major testing programs like this one in the future. Manganese and nitrite combined can account for something like a quarter of the "stoichiometric acid" requirement.

Suggested Improvements in the Experiment

There is a great deal of information contained in the gas chromatograph data when coupled with the helium internal standard flow which is controlled by an MKS flow controller. The helium internal flow standard is introduced into the SRAT. The helium experiences all of the same dynamic effects as the vessel contents experience as the SRAT goes to boiling. This produces an apparent surge in the volumetric percentages and in the generation and/or flow rates of all the gases being monitored as they are displaced by water vapor within the SRAT vapor space. As mentioned in the text, it might be prudent to test an alternative internal standard such as krypton. The internal standard could also be introduced downstream of the SRAT condenser.

If there were no real change in actual generation rates, then the calculated generation rates based on the GC and standard flow shouldn't spike. That is, all gases in the equipment vapor spaces should respond similarly in a dynamic

sense (assuming they are initially well-mixed) when the SRAT goes to boiling. Then all the gas compositions should jump by an identical ratio, and the calculation of the generation rates should eliminate the spikes. This doesn't happen. There is still a spike in the calculated gas generation data at the onset of boiling. Although this could be due to the release of trapped gases in the sludge as boiling begins, it is not clear that that is the case. The standard gas could be fed in just upstream of the FAVC inlet and mixed with the off-gas in an inline mixer. This should give a better quantified flow rate of the standard gas past the GC as a function of time.

The gas data being obtained does not appear to be capable of adequately explaining all of the observed phenomena. This report really pushes what can be deduced from the current GC data. For example, trying to use oxygen consumption to infer NO production or formic acid destruction or identifying other unidentified processes is clearly at its limit. A GC mass spec or some other instrument could upgrade the capability in this area. Direct measurement of SRAT gas composition would also be superior to measuring downstream of the FAVC. All large process changes are being dampened by the large volumes that the gases must pass through before being measured.

Potential future experiments could seek to develop an understanding of the likely answers to questions such as:

- How is the balance of the formic acid being destroyed that does not seem to be related to hydrogen, mercury, manganese, and nitrite?
- Is formic acid reacting with nitrite (or HNO_2) by the path that isn't being tracked going to NO (and how could it be tracked separately from the reaction with nitric acid that also produces NO)?
- Is formic acid reacting with oxygen?
- Are there significant reduction reactions occurring, perhaps with other sludge components, that are not being captured in the acid balance?
- Does the additional off-gas produced by additional acid significantly change the way the sludge will perform when it reaches the melter?
- Since the gas generation reactions were clearly not finished at the twelve hour point in the SRAT, how long should the SRAT cycle be at a minimum to produce better melter performance?

An on-line rheometer could give valuable insight into how much thicker the sludge gets during acid addition than it is at the beginning or end of acid addition. The changes seen with the Tank 40 simulant were enormous, but remain unquantified.

Orion sells a combination ORP, conductivity, pH, and temperature probe with an internal reference as a single unit. Currently, testing uses a pH probe and a separate temperature probe, and does not measure conductivity or oxidation-reduction potential. It is not known whether existing probes could withstand process conditions, or whether measurements would need to be made off line. (There could be an issue with cumulative sample mass at the bench-scale, but that would not be an issue at $1/240^{th}$ scale in the Glass Feed Prep System in Thermal Fluids Lab.) ORP measurement might permit distinguishing between CO_2 peaks due to carbonate conversion versus formic acid decomposition.

Acknowledgments

Continued availability of skilled technicians is critical to this work. The high reproducibility of some of the results reported here can only be attributed to a group of people who are being extremely conscientious in seeing that the raw sludge is well-mixed before putting it in the kettle, that the instruments are calibrated, that the target boil-up rate is being maintained, and so on. It would be a serious loss to the program to see rapid turnover in this resource. The author wishes to thank the following people for their assistance in this effort:

- M. Frances Williams, for many hours of technical coverage and GC upkeep.
- Vickie Williams, Jon DuVall, Sammie King, Mary Moss, Tony Burckhalter, and Richard (Nick) Odom for their hard work in assembling the apparatus, conducting the process simulation experiments, and handling the samples

that are the basis for this report. This included having to work many hours of overtime.
- David Best and Erich Frickey of Mobile Lab for their speedy analysis of run samples.
- The Analytical Development Section for their work on the pre-test, scoping run anion, and variability study mercury samples.
- W. E. Daniel for help in understanding and using the spreadsheets that generate scaling calculations and redox calculations for the bench-scale tests, for help in linking these spreadsheet results into the run plans, and for help with small problems that arose with the apparatus.
- Kevin Brown for his contributions on the PCCS work.
- Irene Reamer for her contributions on the PCT work.
- Lewis F. Landon, Daniel P. Lambert, and Sharon L. Marra for their support and guidance.
- Drs. Darsh Wasan and Alex Nikolov of IIT for their insights on antifoam.

References

1. Cotton, F. A. and Wilkinson, G, Advanced Inorganic Chemistry – A Comprehensive Text, 3rd Edition, John Wiley and Sons, Inc., 1972.
2. R. E. Eibling, **Nitric Acid – Formic Acid Compatibility in DWPF (U)**, WSRC-RP-92-1247, October 20, 1992.
3. H. H. Elder, Sludge Batch 2 Qualification Strategy and Simulant Composition, HLW-SDT-2000-00128, Rev. 0, May 9, 2000.
4. T. L. Fellinger, C. L. Crawford, K. M. Marshall, and N. E. Bibler, Confirmation Run of the DWPF SRAT Cycle Using the Sludge-Only Flowsheet with Tank 42 Radioactive Sludge and Frit 200 in the Shielded Cells Facility (U), WSRC-RP-98-00329, June 3, 1998.
5. J. R. Hester, **High Level Waste Characterization System**, WSRC-TR-96-0264, December, 1996.
6. C. W. Hsu, **DWPF Formic Acid Requirement (U)**, WSRC-RP-90-0554, July 5, 1990.
7. C. W. Hsu, Defense Waste Processing Facility Nitric Acid Requirement for Treating Sludge (U), WSRC-RP-92-1056, September 4, 1992.
8. N. D. Hutson, J. R. Zamecnik, M. E. Smith, D. H. Miller, and J. A. Ritter, **Integrated DWPF Melter System (IDMS) Campaign Report – The First Two Noble Metals Operations (U)**, WSRC-TR-91-0400, June 6, 1991.
9. N. D. Hutson, Revision of Batch 1 Sludge Composition for Integrated Cold Runs in the Defense Waste Processing Facility (U), WSRC-TR-95-0079, February 16, 1995.
10. R. B. King, A. D. King, Jr., N. K. Bhattacharyya, Y. -H. Lim, G. Vemparala, V. Vemparala, and L. Colletti, "Technical Report to the Westinghouse Savannah River Laboratory, Aiken, South Carolina, on **Elucidation of Noble Metal/Formic Acid Chemistry During DWPF Feed Preparation**", Reports 1-11, March 1991-January 1992 (one per month).
11. D. C. Koopman, Comparison of Dow Corning 544 Antifoam to IIT747 Antifoam in the 1/240 SRAT (U), WRSC-TR-99-00377, Rev. 0, December 17, 1999.
12. D. P. Lambert, Testing of Irradiated and Nonirradiated IIT747 Antifoam in Simulated Sludge Processing (U), WSRC-RP-2000-00788, Rev. 0, October 25, 2000.
13. D. P. Lambert and C. S. Boley, Tank 42 Sludge-only Process Development for the Defense Waste Processing Facility (DWPF) (U), WSRC-RP-98-00149, Rev. 0, April 30, 1998.
14. Mellor's Modern Inorganic Chemistry, as revised by G. D. Parkes, Longman, Green, and Co., Ltd., 1961.
15. M. R. Poirier, Specification for the Procurement of Tank 40 and Tank 8 Sludge Feed Simulants, SRT-WHM-2000-004, Rev. 0, 1, and 2, June 29, 2000.
16. W. R. Wilmarth, C. J. Coleman, J. C. Hart, W. T. Boyce, and C. C. Diprete, **Characterization of Tank 40H Supernate and Hydroxide Washing of Sludge**, WSRC-TR-2000-00353, Rev. 0, October 6, 2000.

Appendix A: Preparation of Tank 8 and Tank 40 Sludge Simulants

The demand for sludge simulant had essentially depleted the available stocks of Tank 51 simulant produced by Optima Chemicals for Sludge Batch 1A testing (this simulant had also been used as the starting point for Tank

42 simulant for Sludge Batch 1B testing). With demands for multi-gallon quantities of melter feed for Hydragard testing, for use in the new Mini-melter, for melt rate testing studies, etc. on the increase, a decision was made to obtain larger volumes of Tank 8 and Tank 40 simulants than could be economically prepared at bench-scale at TNX.

Defining the Simulant Composition

Herbert H. (Hank) Elder [2000] was given the task of estimating the present-day compositions of both Tank 8 and Tank 40 waste from the High Level Waste Database [Hester], and then estimating the composition of Tank 8 and Tank 40 wastes following washing. After these initial calculations, Hank generated a pair of recipes for each sludge simulant in a post-washed state. One recipe excluded and one recipe included the presence of "insoluble" sodium in real waste, i.e. sodium that cannot be removed by continued washing.

None of the recipe sodium compounds, other than zeolites (which were not used in the new simulants), have been shown to produce an insoluble sodium species during simulant preparation. To make up the difference between soluble and insoluble sodium with soluble species, including NaOH and Na_2CO_3, would impact the SRAT acid calculation in a non-conservative fashion. These recipes excluded radioisotopes like uranium and thorium, as well as cerium and lanthanum. Strontium was included at a small concentration, but a non-radioactive isotope was used. Predicted cesium concentrations were so small that no non-radioactive cesium was included in the recipe.

The absence of uranium presented a dilemma. There is no good chemical simulant, other than using depleted uranium itself. This has been determined to be impractical at the present time. Uranium is present in significant quantities, especially in Tank 8 sludge. The decision that was made was equivalent to replacing uranium with water in the recipe. In this manner the grams iron per gram simulant, grams aluminum per gram simulant, grams noble metal per gram simulant, etc. could be made equivalent to the same quantities per gram of real sludge. The wt. % total solids in the sludge would be lower, however, due to the absence of uranium (and thorium). This would be expected to lead to lower viscosity simulants. Also, directly comparing real and simulated waste samples that report a quantity relative to the mass of air-dried solids would be inconsistent with this synthesis strategy.

Table A.1 gives the sludge elemental concentrations on a calcined solids basis as determined by Hank Elder (only the baseline washing case shown):

Table A.1 – Estimated Washed Sludge Elemental Composition - Calcined Basis

	Tank 8	Tank 40
Al	8.90	8.31
Ba	0.24	0.24
Ca	2.04	3.17
Ce	0.24	0.49
Cr	0.24	0.27
Cu	0.15	0.19
Fe	24.45	34.30
K	0.28	0.42
La	0.14	0.24
Mg	0.12	0.16
Mn	2.74	1.42
Na	13.37	13.37
Ni	2.80	0.00
Pb	0.07	0.38
Si	0.76	1.08
Th	0.00	0.19
U	13.38	3.51
Zn	0.27	0.36
Zr	0.47	0.68

The sodium equivalence between the two sludges was forced by Hank in the washing calculation. Significant features included the negligible nickel content of Tank 40 along with its low manganese content. Calcium was fairly high in Tank 40. Magnesium was low in both compositions. Noble metal concentration estimates were more difficult. The next table describes the best estimates for the noble metals from Hank Elder's study given as either ppm metal oxide or ppm metal in the total simulant solids.

Table A.2 – Noble Metals in the Sludge Simulant

	Tank 8	Tank 40
HgO	887	5096
AgO	2440	3297
Pd	1833	2262
Rh	270	-
Ru	3850	4752

No rhodium prediction was generated for Tank 40, because there was no available data. A decision was made to use the Tank 8 estimate of rhodium concentration for both tanks until a better value became available.

Using the data in Table A.1, Hank prepared recipes for Tank 8 simulant, Tank 40 simulant, and a blend of Tank 8 and 40 simulant. (Actually Hank prepared a high and a low sodium recipe for each.) The recipe was in the format of Nick Hutson's 1995 recipe for Batch 1 sludge [1995]. In other words it gave the masses of the various chemicals to add at various stages in the simulant preparation recipe for a 1000 gallon batch rather than the expected composition of the sludge product. Hank's recipes indicated that the Phase I precipitate (manganese, iron, nickel, and a portion of the calcium) would be assumed to contain MnO_2, $Fe(OH)_3$, $Ni(OH)_2$ and $CaCO_3$ in any further calculations.

The recipe for the washed Tank 8/Tank 40 blend was predicted to produce a product slightly different from what would be obtained by blending washed Tank 8 and washed Tank 40. The difference was essentially confined to sodium, potassium, and aluminum. The reason for this was related to the washing calculation. The recipes for

simulant blend assumed mixing before final washing. The attempt to mix after washing each tank individually was giving a somewhat different end point. At the time when a decision was needed, it was agreed that Tank 8 would not be processed alone, but that Tank 40 might be processed without Tank 8. Therefore, the washed Tank 40 recipe was left unaltered. The Tank 8 recipe was adjusted slightly so that a blend of the adjusted washed Tank 8 simulant with the washed Tank 40 recipe would produce a slurry that matched the recipe for washed Tank 8/Tank 40 blend.

Table A.3 projects the calcined composition of Tank 40 simulant prepared per the low sodium (no insoluble sodium) variation of the Tank 40 recipe with the predicted composition of calcined Tank 40 waste. The composition assumes no sodium or potassium remain in the sludge following the intermediate wash (following iron and nickel nitrate precipitations by NaOH, which followed precipitation of MnO_2 from $Mn(NO_3)_2$ and $KMnO_4$.) Actually there is some potassium present in addition to the amount used to calculate its simulant composition below. Similarly, there is some sodium and some nitrate that survives the intermediate washing. The equivalence of calcium between the two tables apparently represents an undiscovered error in the original calculations.

Table A.3 – Comparison of Tank 40 Predicted and Simulated Calcined Waste

	Tank 40	Tank 40 Simulant
Al	8.31	9.28
Ba	0.24	0.26
Ca	3.17	3.17
Ce	0.49	0.00
Cr	0.27	0.30
Cu	0.19	0.19
Fe	34.30	37.71
K	0.42	0.09
La	0.24	0.00
Mg	0.16	0.17
Mn	1.42	1.55
Na	13.37	8.89
Ni	0.00	0.00
Pb	0.38	0.42
Si	1.08	1.18
Th	0.19	0.00
U	3.51	0.00
Zn	0.36	0.39
Zr	0.68	0.74

Otherwise, the numbers vary from column to column by about 10% allowing for round-off in the original tables. This is the impact of removing the excluded radioactive species. It is not clear why the simulant potassium is lower than the Tank 40 prediciton. The next table compares the same quantities for Tank 8 waste and the adjusted recipe for Tank 8 simulant.

Table A.4 – Comparison of Tank 8 Predicted and Simulated Calcined Waste

	Tank 8	Tank 8 simulant
Al	8.90	11.89
Ba	0.24	0.31
Ca	2.04	2.79
Ce	0.24	0.00
Cr	0.24	0.32
Cu	0.15	0.17
Fe	24.45	32.15
K	0.28	0.01
La	0.14	0.00
Mg	0.12	0.16
Mn	2.74	3.61
Na	13.37	9.76
Ni	2.80	3.69
Pb	0.07	0.28
Si	0.76	1.00
Th	0.00	0.00
U	13.38	0.00
Zn	0.27	0.35
Zr	0.47	0.62

Copper, potassium, and lead appear to have been adjusted incorrectly from the expected waste composition of Tank 8 to the simulant recipe, but the difference is probably within the uncertainty of the original numbers. Most simulant species are at about 130% of the predicted waste composition. This is due to the elimination of the radioactive species. Sodium is relatively low in the simulant because the "no insoluble sodium" recipe was followed. Tank 40 needed to be blended with Tank 8 simulant in the ratio of 52:48 on an air-dried (or "as produced" as simulant) solids basis to produce the projected simulant for waste blend given by Hank's calculations.

The two recipes were also used to calculate the compositions of air-dried sludge simulants based on the final chemical species projected. This information was needed to complete the tables for expected sludge composition at the end and for the expected sludge composition after the initial precipitation and washing in the sludge simulant recipe specification.

Obtaining New Simulants

A contract was entered into with Dr. Vincent van Brunt of the Department of Chemical Engineering at the University of South Carolina in Columbia. The simulant preparation was performed in the Filtration Research Engineering Demonstration unit, or FRED, located on the USC campus. Based on conversations with Dr. van Brunt, the recipe was re-scaled for a 300 gallon batch size. This was issued initially as SRT-WHM-2000-004, Rev. 0 [Poirier]. The simulant was purchased in cooperation with the Alternative Salt Process development group, who wanted some sludge simulant for cross-flow filtration tests. It was agreed that each lot of 300 gallons would be split equally between Alt Salt and DWPF. SRTC purchased the chemicals needed to make the sludge and had them shipped to USC.

The simulant preparation start date was adversely impacted by the availability of stainless steel drums. The site specifications for drums were under review at the time that an order needed to be placed to meet schedule. Once drums were received, however, they were quickly transferred to USC, and the preparation of Tank 40 simulant was begun. SRTC monitored all chemical additions during the Tank 40 and Tank 8 simulant preparations. All species' weights added were essentially identical to the recipe within the limits of the scales being used. Scales were checked with known weights to confirm their accuracy.

Preparation of Tank 40 Simulant

USC performed the precipitation of MnO_2 from $Mn(NO_3)_2$ and $KMnO_4$, followed by the precipitation of $Fe(NO_3)_3$ by NaOH, and the addition of $CaCO_3$. At this point the slurry pH was measured and found to be acidic. Additional NaOH was added to bring the pH up to 10-11. It was noted by USC and confirmed visually by the author that mixing became very difficult as the pH entered the region of 6-8. As the pH continued to rise, the slurry became more fluid again. USC washed the simulant per the recipe using the cross-flow filter to produce the decant stream. The slurry was sampled and analyzed by USC. Table A.5 summarizes the results.

Table A.5 – Tank 40 Simulant After Washing Phase

	Acceptance Range	Data
Mn	1.81-2.00	2.11, 2.21, 1.99, 2.17
Fe	43.36-47.92	51.4, 54.1, 52.1, 54.0
Ca	3.48-4.26	3.81, 4.09, 3.70, 4.13
Wt. % Soluble Solids	0.15-0.2 wt %	0.15 wt. %

Attention immediately focused on the consistently high Mn and Fe results relative to the expected values of 1.9, 45.6, and 3.87 % for Mn, Fe, and Ca. The ratios were nearly correct, but the absolute numbers suggested something was wrong with the anion side of the recipe.

Some quick and dirty experiments confirmed that the calculated compositions, which used $Fe(OH)_3$ as the iron salt, were very sensitive to the actual composition of the "hydrous ferric oxide", or $Fe_2O_3 \cdot xH_2O$. Since the above samples were air-dried to 115° C, tests were run at TNX on simply precipitated hydrous ferric oxide, with no manganese or calcium. The tests measured the mass of air-dried hydrous ferric oxide as a function of temperature between 25° and 115° C. This test was reasonable for Tank 40, since the recipe contained no nickel to co-precipitate with the iron. (Calcium carbonate was considered to be an insoluble species added just prior to washing, but probably not impacting the iron composition.) [The reader is directed to: D. C. Koopman, Iron Precipitation from Aqueous Ferric Nitrate Neutralized with Sodium Hydroxide (U), WSRC-PTD-2000-00025, June 16, 2000, for more details.]

The testing suggested that $0.5 < x < 1.5$ was a better estimate of the iron composition than the $x = 3$ (same as $Fe(OH)_3$) used to generate the specification. The revised cation concentration expected values became 2.22, 53.5, and 4.54 for Mn, Fe, and Ca respectively at $x = 1$. Calcium looked a little low, but the spec tolerance was more generous for this species.

USC was given permission to proceed with the recipe. The remaining trim chemicals were added, and the final slurry was mixed and sampled. Because of the issue with the iron, it was not noticed that sodium nitrate was relatively high in the washed precipitate (in fact it appeared to exceed the soluble solids specification all by itself based on IC anion results). Soluble solids were determined by a direct measurement not dependent on species. Sample results for the final Tank 40 sludge simulant cations looked pretty much as expected once the correction for the hydrous ferric oxide was applied. The same could not be said for the nitrate anion.

Because of schedule issues within the Alt Salt program, and the lack of an immediate plan that could be guaranteed to correct the nitrate without ruining the simulant, it was decided to accept the simulant as made. Any adjustments would be made at TNX after receipt.

Four drums of simulant were shipped to SRTC and two were kept at USC for filtration tests. The net produced

was just 227 gallons of simulant at an SG of 1.11 and about 16 wt. % total solids. ITS received 60% of this, or 137 gallons, split among three drums. Drums were weighed at TNX upon receipt, and the USC weights were confirmed. The drums were sampled, and plans to deal with the high nitrate content were formulated. It was immediately noted that the simulant was unusually bright in color, more of a dark orange than a brown. This was tentatively attributed to the lack of nickel and low manganese dioxide content of the simulant (nickel hydroxide is dark green and manganese dioxide is nearly black).

Preparation of Tank 8 Simulant

USC proceeded into the preparation of Tank 8 simulant. The specification was revised (or at least the Tank 8 portion was), however, to assume that the iron would precipitate as $Fe_2O_3 \cdot 0.5H_2O$. The specification was also revised to put a hold point into the washing step to confirm the nitrate concentration. The initial precipitation elements would be evaluated on a ratio to iron basis rather than an absolute basis to remove the uncertainty in the value of x in the iron. Finally the specification was revised to let SRTC specify the final mass of sodium nitrate that would be added to the slurry during the final chemical additions. Also it became clear that the volume that would be produced would be closer to 270 gallons than 300 gallons if the wt. % total solids came out at about 15%. A decision was made to not increase the chemical additions throughout the recipe to increase the amount of final product.

Ca, Mn, and Ni relative to iron were all where they were expected to be following the precipitation step (ratios within 3% of target). Washing the sample by a 50-fold dilution and then reanalyzing the solids gave Ca/Fe 12.3% lower than expected. Mn and Ni relative to iron were 8.7 and 6.4% lower than expected respectively. The results were still within specified tolerances and USC proceeded to wash the sludge.

USC was required to wash until the ratio of nitrate ion to iron ion was less than 0.023 on a mass basis. Ultimately, USC washed to 0.027, then continued washing to 0.018 for the above ratio. Based on this result, the sodium nitrate addition was reduced from 4.335 pounds to 1.5 pounds during the final phase chemical additions. In spite of this, when the final product sample was analyzed by USC, the nitrate content was found by USC to be 10% higher than expected. USC was instructed to remove 15% of the supernate and replace it with water. This decision was made because it is easier to add chemicals to increase concentrations than it is to remove chemicals and reduce concentrations. The product was accepted and reanalyzed. Nitrite and chloride ion each fell by roughly 15%, but nitrate ion was reported to increase. This simple result shows the difficulty of controlling the outcome of the simulant preparation process. Sodium results were ambiguous in the total solids, but were clearly lower in the supernate by about 20%.

USC produced about 245 gallons of Tank 8 simulant at about 14.9 wt. % total solids and an SG of 1.1. ITS received about 141 gallons of this. This concluded the work involving the University of South Carolina-Columbia. The table below shows the elemental results for the Tank 8 simulant drums (3) that came to TNX for ITS compared to the original recipe given in Table A.4 above on a calcined basis (where the effects of the condition of the hydrous ferric oxide are irrelevant):

Table A.6 – Tank 8 Calcined Solids, Measured vs. Predicted Compositions

	Tank 8 predicted composition	Tank 8 simulant recipe	Drum 1 simulant sample	Drum 2 simulant sample	Drum 5 simulant sample
Al	8.90	11.89	11.4	12.35	11.9
Ba	0.24	0.31	0.316	0.240	0.229
Ca	2.04	2.79	2.625	2.99	2.91
Ce	0.24	0.00	-	-	-
Cr	0.24	0.32	0.226	0.305	0.290
Cu	0.15	0.17	0.159	0.176	0.168
Fe	24.45	32.15	35.45	33.40	32.40
K	0.28	0.01	<0.01	<0.018	<0.018
La	0.14	0.00	-	-	-
Mg	0.12	0.16	0.144	0.167	0.167
Mn	2.74	3.61	2.465	3.66	3.58
Na	13.37	9.76	6.29	7.57	7.37
Ni	2.80	3.69	3.43	3.70	3.66
Pb	0.07	0.28	0.148	0.118	0.113
Si	0.76	1.00	0.997	1.20	1.19
Sr	not calc'd	0.11	0.102	n/a	n/a
Th	0.00	0.00	-	-	-
U	13.38	0.00	-	-	-
Zn	0.27	0.35	0.297	0.286	0.274
Zr	0.47	0.62	0.583	0.408	0.448

There was an unusual result here and there in the table above, but the general agreement was excellent between the expected recipe compositions and the three sets of average drum sample results. The notable exception was sodium, which was 27% below expectation on the overall drum average. A result 15% lower was expected based on the USC supernate decanting that followed all chemical additions. The 15% expected difference will eventually be made up before further tests are run.

The following table gives the breakdown of the IC determinable anions in the Tank 8 sludge. The original estimate was somewhat arbitrary, since precise concentration data at the start of the USC supernate decanting was not available. Also, a value for x in $Fe_2O_3 \cdot xH_2O$ was not estimated for the Tank 8 simulant (most elemental data was taken on a calcined solids basis, not an air-dried solids basis).

Table A.7 – Anion Content of Tank 8 Sludge Simulant Supernate

Anions, mg/Kg	Original Estimate	Pre-Decanting Sample	Post-Decanting Estimate	Drum 1 Sample	Drum 2 Sample	Drum 5 Sample
Nitrate	1300	1590	1200	1660	1350	1400
Nitrite	10500	11700	9400	8900	10000	10000
Chloride	1700	2240	1600	1980	1910	2100
Sulfate	1600	1600	1400	1400	-	-
Phosphate	230	<10.0	210	<10.0	-	-
Fluoride	8	<10.0	7	<10.0	-	-

The phosphate apparently was not present in the aqueous phase. Other results were generally consistent with a decant of 10-15%, except for the Drum 1 nitrate. It is postulated that the differences in nitrite/nitrate between Drum 1 and Drums 2 & 3 were due to the samples being analyzed on different days, rather than to real

differences in the supernate composition.

Tank 40 Adjustments and Trimming

An adjustment program was started at TNX to decrease the supernate nitrate content of the three Tank 40 simulant drums. The target was to reduce the nitrate to 55% of its initial concentration. Once this was accomplished, the other soluble species, especially including sodium hydroxide, sodium nitrite, and sodium chloride, would be added to bring their concentrations back up to those resulting from the original recipe.

Supernate would be decanted from the drum to accomplish the removal of nitrate. A revised supernate would then be prepared and added back to the drum. The initial mass of supernate recovered from each drum was encouraging, but insufficient to complete the targeted removal of nitrate. De-ionized water was added to the three drums, the drums were mixed, and then the drums were allowed to settle. Several days of settling time produced a discouragingly small volume of decantable material (the amount varied considerably from drum to drum). Calculations indicated that the amount of nitrate removed was still inadequate. One drum was given a second wash immediately, while the other two were allowed to settle for a longer period of time.

Both paths were ultimately fruitful. The Tank 40 simulant solids must settle very slowly in the hindered settling regime. The adjustment of two drums was temporarily discontinued in order to perform the work in this report. One drum, Drum 3, was checked and found to have had the necessary mass of nitrate removed. Using best available data from samples and the sludge recipe, calculations were made to generate a replacement mixture for the other supernate species. The chemicals were weighed and added, the drum was mixed and sampled, and two 25-liter carboys were filled to support near-term future bench-scale testing (including this study).

Prior to starting the testing in this report, sample data on mixed Tank 40 real waste became available [Wilmarth et al.]. The sample ID’s were ESP-237-1 and ESP-237-2. Dried, unwashed samples were subjected to either Aqua Regia dissolution of CsOH dissolution and analyzed for elementals. Two differences drew the most attention. The first was the presence of nickel relative to iron at a level that would correspond to about 0.43% nickel in Table A.3 above (simulant column). The second was the presence of manganese relative to iron at a level that would correspond to about 3.31% in that table (more than a factor of two increase). A decision was made prior to the testing covered in this report that the Tank 40 simulant should be trimmed to the manganese and nickel levels of the Tank 40 waste sample (relative to iron).

Approximately 24 kg of Tank 40-Drum 3 simulant were so treated. The simulant was trimmed with manganese dioxide that had been precipitated in 1998 (using the first part of the overall simulant preparation recipe) rather than with purchased manganese dioxide. Only a limited quantity of this material was available. The simulant was also modified with $NiCl_2 \cdot 6H_2O$ to provide the nickel mass. The table below compares the approximate expected elemental composition of calcined simulant with the average results of the Mobile Lab duplicate analysis of one sample.

Table A.8 – Fully Trimmed Tank 40 Simulant vs. Expected Composition

	Tank 40 - Expected	Tank 40 Sample
Al	9.28	9.77
Ba	0.26	0.193
Ca	3.17	3.84
Ce	0.00	-
Cr	0.30	0.298
Cu	0.19	0.193
Fe	37.71	37.50
K	0.09	0.027
La	0.00	-
Mg	0.17	0.215
Mn	3.31	3.38
Na	8.89	7.3
Ni	0.43	0.420
Pb	0.42	0.309
Si	1.18	1.50
Th	0.00	-
U	0.00	-
Zn	0.39	0.336
Zr	0.74	0.694

The results are generally excellent. (There is other sample data on calcium in Tank 40 simulant suggesting that it is "low", so collectively the calcium results are probably just indicating uncertainty of the result for calcium in the sludge sample matrix.) Ten kg of the fully adjusted and trimmed Tank 40 simulant was used to prepare Tank 8/Tank 40 blend as described below. The remainder of the trimmed simulant was used to conduct the two Tank 40 scoping runs and one Tank 40 variability study run (1A, 2A, and SB2-2).

Preparation of Tank 8/Tank 40 Blend Simulant

The fully adjusted Tank 40 simulant described above was blended with Tank 8 simulant taken from Drum #1 as described above (of Tank 8, USC's numbering scheme, not ours). The blend targeted 52% Tank 40 and 48% Tank 8 on an air-dried solids basis. Approximately 20 kg of blend was prepared from 10.1 kg of Tank 8 and 10.2 kg of Tank 40 simulants. 19.6 kg of this blended simulant was consumed performing the four blend scoping runs (1B-4B) and three blend variability study runs (SB2-1, SB2-3, and SB2-4). Additional blend simulant was used for samples and for one rheology measurement at 25° C. The table below compares the predicted (target) composition for the blend simulant with the results of a duplicate ICP analysis on one sample by Mobile Lab.

Table A.9 – Comparison of Blend Simulant with Target Composition

	Target	Sample Result
Al	10.5	10.7
Ba	0.28	0.26
Ca	2.98	3.24
Cr	0.31	0.28
Cu	0.18	0.23
Fe	35.0	37.5
K	0.052	<0.01
Mg	0.165	<0.01[1]
Mn	3.44	3.37
Na	8.21	7.32
Ni	1.97	1.94
Pb	0.35	0.26
Si	1.09	1.22
Zn	0.37	0.33
Zr	0.68	0.59

Note 1. This magnesium result is not believed to be true. There was a problem determining the detectability limit for magnesium on the new ICP. The actual concentration is believed to be about 0.09 wt. %.

Very good agreement is observed between the expected outcome of the blending and the sample results. Additional comparisons can be found in Appendix D: *SRAT Product Sample Results*.

Appendix B: Revised Basis for Tank 40 Noble Metals

The following cc.mail was received on August 4, 2000:

```
---------------------------------------------------------------------------------------------------
Author:  Terri Fellinger at SRS
Date:    8/4/00  1:46 PM
Normal
TO: Sharon Marra at SRCCH12
CC: Dan Lambert at SRCCC02
CC: David Koopman at SRCCC05
CC: Lewis Landon at SRCCC08
CC: Bill Wilmarth at SRCCA08
CC: Herbert Elder at SRCCH01
CC: John Fowler at SRCCH02
CC: William Boyce at SRCCA12
Subject: Noble Metal Concentrations for Tank 40 Sludge Slurry
------------------------------- Message Contents
```

Sharon,

Ned and I talked with Bill Boyce and Bill Wilmarth about the ICP-MS analyses for Tank 40. They provided us the data and I did the calculations. Ned performed the review of the calculations. During the review of the calculations, we had a lengthy discussion about Pd. For the previous tanks that we have analyzed in the Shielded Cells, the Pd has always been fission product Pd. This time a question has been raised that, based on the data, there might be a smidge of natural Pd in this Tank. Ned and I were wondering if there could have been an addition of natural Pd either in the Canyon or Tank Farm processes? Until someone can confirm that either way, we agreed to say that the Pd is fission product Pd. Presented below are the noble metal concentrations plus silver concentration for Tank 40. This data is presented as weight percent on a dried sludge slurry basis. If some natural Pd were present, the total Pd concentration would increase to 2.7E-03 wt. %. We could only measure Pd-105. All of the other Pd isotopes are masked by isotopes of Cd and Ru-102 and Ru-104.

Total fission product Ru concentration - 2.11E-03 wt. %
Total fission product Pd concentration - 1.00E-03 wt. %
Total fission product Rh concentration - 6.99E-04 wt. %
Total natural Ag concentration - 1.19E-02 wt. %

If you have any questions, please call me at 5-7745 or Ned at 5-2313.

Thanks,
Terri

Appendix C: Excerpt Material from the University of Georgia Reports on Noble Metals

From Report 10 (of 11), December 1991:

ABSTRACT: "The catalytic activities of the three noble metals, rhodium, ruthenium, and palladium for the evolution of hydrogen from formic acid are compared in Purex and HM sludge simulants containing various amounts of nitrite including nitrite-free simulant. All three metals are catalytically active for hydrogen evolution but in different regimes. Rhodium appears to require nitrite for significant catalytic activity in the sludge simulant media. However, the catalytic activity of ruthenium is high only in the absence of nitrite so that nitrite is a strong inhibitor for the ruthenium-catalyzed formic acid decomposition. Preliminary experiments suggest that the catalytic activity of palladium is promoted by the addition of chloride and is relatively insensitive to the presence of nitrite."

BODY:
"previous…technical repots (sic) indicate negligible catalytic activity of ruthenium…in the IDMS sludge simulant…~0.3 M in nitrite."
"…in the nitrite-free sludge ruthenium is a more active catalyst for formic acid decomposition than rhodium in the presence of nitrite."

"experiments…indicate that palladium is only about ~10% as active as rhodium in the high-nitrite HM sludge simulant."
"…palladium is quite active as a catalyst for formic acid decomposition in the presence of nitrite-free sludge simulant."

"In all of the rhodium experiments hydrogen was produced in a relatively short ‘burst’ and

essentially no hydrogen was produced after the first ~2 hr"

TABLE EXCERPTS:

From Table 2: Hydrogen turnover, units of inverse days, estimated from the slope of the mmoles hydrogen versus time data during the period of steady hydrogen evolution.

	0.04 mmole $PdCl_2$	0.06 mmole $RuCl_3$	0.06 mmole $RhCl_3$
HM Simulant	~0	35	not reported
Purex Simulant	~0	10	90
Nitrite Free	450	900	rapid burst, then ~0

Purex sludge was ~0.06 M in nitrite, HM was ~0.3 M in nitrite.

<u>From Report 7, September 1991:</u>

"Nitrite ion is needed to promote catalytic activity of rhodium"

<u>From Report 6, August 1991:</u>

"Currently available information suggests that the rhodium-catalyzed decomposition of formic acid to give hydrogen…(is a)…heterogeneous process…(involving)…small particles of rhodium metal which lose their activity upon aggregation."
"rates of hydrogen generation with Purex simulant (plus rhodium) show highly variable induction periods and fluctuating hydrogen rates."

<u>From Report 4, June 1991:</u>

summarized: palladium (added as $PdCl_2$) is active in media such as IDMS sludge (pH 11.0 initially)

From Table 2: Hydrogen produced per mole noble metal per day.

	$PdCl_2$	$RuCl_3$	$RhCl_3$
IDMS sludge	8	0	112
3% $HCOOH/NaNO_2$	5	3	118
0.76 M NaCOOH	78	40	2.4

This data is older than that from December 1991. The IDMS sludge is not nitrite ion free. It is not clear whether this was either HM or Purex sludge.

The data above seem to suggest that Rh is an order of magnitude more active than palladium in a typical sludge with nitrite ion present, but palladium is typically present in a higher concentration. The later data from December 1991 seem to suggest that Rh might burn out or deactivate in the absence of nitrite. Both palladium and ruthenium appear to be active once nitrite is thoroughly destroyed.

Appendix D: SRAT PRoduct sample Results

This appendix presents a tabular comparison of SRAT product sample results for Tank 40 and for Tank 8/40 blend tests. The first table compares Tank 40 SRAT product calcined solid elemental wt. % results with the expected and starting sludge sample result values. The calcine factor determined for the samples is also included in the last row labeled CF. IS and SS denote the insoluble solids and soluble solids as wt. %.

Table D.1 – Tank 40 Sludge and SRAT Product ICP Results

	Tank 40 – Expected Composition	Tank 40 Simulant Sample	1A SRAT Product	2A SRAT Product	SB2-2 SRAT Product
Al	9.28	9.77	9.45	9.39	9.62
Ba	0.26	0.19	0.23	0.22	0.19
Ca	3.17	3.84	3.57	3.21	3.75
Cr	0.30	0.30	0.27	0.25	0.29
Cu	0.19	0.19	0.23	0.22	0.19
Fe	37.71	37.50	39.5	37.4	37.3
K	0.09	0.03	0.03	0.05	0.12
Mg	0.17	0.215	<0.01	<0.01	0.21
Mn	3.31	3.38	3.50	3.14	3.52
Na	8.89	7.3	6.95	6.65	7.67
Ni	0.43	0.42	0.42	0.41	0.43
Pb	0.42	0.31	0.35	0.33	0.34
Ru	various	none	0.45	<0.01	<0.01
Si	1.18	1.50	1.43	1.41	1.44
Zn	0.39	0.34	0.33	0.31	0.33
Zr	0.74	0.69	0.67	0.63	0.62
IS	-	13.45	14.35	11.80	11.55
SS	-	3.06	3.52	6.56	7.14
CF	-	0.764	0.745	0.696	0.704

The expected composition column in this table was not adjusted to compensate for the presence of the noble metal oxides, so a small dilution effect should be allowed for when comparing the different columns. Overall it looks as if all the results are about where they ought to be given the history of the measurement accuracy, the representative sampling issues, and so forth. There appears to have been some problem initially with the detection of magnesium. Ruthenium was added to the list as a check on the major noble metal. The expected composition of ruthenium in 1A was 0.66%, or about 1.5 times the reported value. (Ruthenium was added as solid $RuCl_3$ at fairly high purity, so there is high confidence that the predicted ruthenium is actually present in the sludge.) The higher calcine factor for 1A relative to 2A and SB2-2 suggests a greater degree of anion destruction in that run. The total solids content of the 1A product was 17.9 wt. %, whereas the total solids content of the other two SRAT products were 18.36 and 18.69 wt. %. This clearly supports the higher degree of anion destruction during the 1A run, since the acid additions were identical.

This next table, D.2, compares the Tank 8/40 sludge blend sample data to the results for the four scoping runs using blend simulant. Results analyzed at the same time as the 1A and 2A samples above do not show detectable magnesium either. This analytical problem seems to have ultimately been resolved, since, as was the case with SB2-2 above, the magnesium concentrations became non-trivial in later samples.

Table D.2 – Tank 8/40 Scoping Run ICP Results

	Blend Target	Raw Simulant	1B SRAT Product	2B SRAT Product	3B SRAT Product	4B SRAT Product
Al	10.5	10.7	10.6	9.68	10.8	10.8
Ba	0.28	0.26	0.25	0.22	0.21	0.21
Ca	2.98	3.24	3.11	2.89	3.31	3.34
Cr	0.31	0.28	0.28	0.25	0.28	0.29
Cu	0.18	0.23	0.22	0.20	0.19	0.18
Fe	35.0	37.5	37.5	34.5	34.5	36.4
K	0.052	<0.01	0.02	0.01	0.03	<0.018
Mg	0.165	<0.01	<0.01	<0.01	0.18	0.17
Mn	3.44	3.37	3.27	2.98	3.33	3.35
Na	8.21	7.32	7.23	6.94	7.51	7.10
Ni	1.97	1.94	1.92	1.73	1.94	1.95
Pb	0.35	0.26	0.25	0.22	0.22	0.22
Ru	various	none	0.36	0.13	0.16	0.15
Si	1.09	1.22	1.31	1.21	1.31	1.29
Zn	0.37	0.33	0.32	0.28	0.30	0.30
Zr	0.68	0.59	0.60	0.55	0.56	0.58
IS	-	13.20	13.00	11.55	11.40	11.40
SS	-	2.68	4.00	5.29	5.06	5.07
CF	-	-	0.753	0.730	0.757	0.748

The data for 2B were noted as being all roughly at 92% of the values for 1B (analyzed at the same time, suggesting that possibly a piece of data had been misread). The run 3B iron looks a bit low. Otherwise the results seem to be about what should be expected. Ruthenium, as the dominant noble metal, was included in the analysis list as a test to see if accurate ICP results could be obtained. A result of about 0.66 wt. % is expected for 1B, and a result of about 0.26 wt. % is expected for 2B-4B. The measurements show the proper trend, but are low by about a factor of 1.6-1.8. Apparently this species is not properly calibrated in this wt. % range in a sludge matrix. The calcine factor for 1B is larger than 2B. 1B ended up with 17 wt. % total solids, whereas 2B ended up with 16.84 wt. % total solids. The 2B to 3B to 4B trend of reducing acid stoichiometry did not have such a simple impact on the solids data.

The next table, D.3, compares similar quantities as D.2, but for the three variability study blend runs.

Table D.3 – Tank 8/40 Variability Study Run ICP Results

	Blend Target	Raw Simulant	SB2-1 SRAT Product	SB2-3 SRAT Product	SB2-4 SRAT Product
Al	10.5	10.7	10.6	10.6	10.6
Ba	0.28	0.26	0.21	0.21	0.21
Ca	2.98	3.24	3.34	3.25	3.22
Cr	0.31	0.28	0.29	0.29	0.30
Cu	0.18	0.23	0.18	0.19	0.18
Fe	35.0	37.5	35.4	35.6	35.6
K	0.052	<0.01	0.03	0.06	0.11
Mg	0.165	<0.01	0.18	0.19	0.19
Mn	3.44	3.37	3.43	3.45	3.34
Na	8.21	7.32	7.39	7.42	7.50
Ni	1.97	1.94	1.98	1.97	1.99
Pb	0.35	0.26	0.22	0.25	0.21
Ru	various	none	0.17	0.17	0.30
Si	1.09	1.22	1.30	1.31	1.26
Zn	0.37	0.33	0.31	0.31	0.31
Zr	0.68	0.59	0.56	0.57	0.57
IS	-	13.20	11.20	11.80	11.20
SS	-	2.68	5.20	4.70	7.51
CF	-	-	0.747	0.755	0.762

The results look quite good across the board. Expected ruthenium concentrations were 0.26%, 0.27%, and 0.53% for runs SB2-1, SB2-3, and SB2-4 respectively. So, these analytical results are also low by a factor of about 1.5-1.8 as was the case for the ruthenium in the two previous tables. If nothing else, the results confirm that ruthenium was added to each batch and not overlooked. It appears that the blend simulant iron composition range is described by 35.9 ± 1.6. This is less than a ± 5% band to capture 100% of the measurement averages. SB2-1 soluble solids and calcine factor were similar to the corresponding 3B scoping run. The high soluble solids content of SB2-4 was no doubt due to the 290% acid addition.

Appendix E: SME PRoduct Sample results

The table below summarizes the ICP data on the SME product samples from the four variability study runs in wt. %. IS is insoluble solids, SS is soluble solids, and CF is calcine factor.

Table E.1 – SME Product Sample Results by ICP

	SB2-1 Tank 8/40	SB2-2 Tank 40	SB2-3 Tank 8/40	SB2-4 Tank 8/40
Al	3.07	2.62	3.04	2.92
Ba	<0.01	<0.01	<0.01	<0.01
Ca	0.88	0.91	0.89	0.89
Cr	0.043	0.043	0.049	0.046
Cu	0.036	0.052	0.051	0.050
Fe	9.35	9.36	9.31	9.16
K	0.11	0.18	0.11	0.11
Mg	1.24	1.26	1.22	1.22
Mn	0.79	0.79	0.82	0.79
Na	8.08	7.86	7.90	7.95
Ni	0.46	0.07	0.49	0.47
Pb	0.04	0.06	0.03	0.03
Si	25.4	26.0	25.7	26.0
Zn	0.03	0.02	0.03	0.03
Zr	0.14	0.19	0.16	0.18
IS	39.45	42.15	39.60	42.80
SS	5.14	7.14	4.52	4.51
CF	0.923	0.909	0.922	0.932

The lower aluminum and nickel in SB2-2 and the higher zirconium and lead are markers that this is Tank 40 simulant melter feed and not blended Tank 8 and Tank 40 simulant melter feed. Higher soluble solids in SB2-2 relative to SB2-1 and SB2-3 was probably due to the combination of higher acid and lower noble metals. Note the relative change in SB2-4 soluble solids which were quite high after the SRAT cycle. There was significant gas evolution in the SME cycle of this run, which apparently accounts for the drop seen.

The final volumes of the four SME products were always no greater, and generally less, than the volume prior to the first frit addition. In other words if a 6000 gallon transfer was made from the SRAT to the SME, and if the volume of the SME was still 6000 gallons after both frit additions (heel volume neglected), then the wt. % total solids would be no greater, and probably lower, than the results above imply. This is only about 45 wt. % total solids. It should be remembered that the simulant substituted water for uranium and for insoluble sodium. Consequently, the wt. % total solids during real waste processing could be expected to be higher across the Chemical Processing Cell in DWPF.

Table E.2 gives the product anion results by IC. The units are mg/Kg (supernate).

Table E.2 – SME Product Anion Results by IC

	SB2-1 Tank 8/40	SB2-2 Tank 40	SB2-3 Tank 8/40	SB2-4 Tank 8/40
Formate	34,000	51,600	34,600	50,600
Nitrate	19,100	28,300	18,000	9100
Chloride	3660	5200	4310	5520

There is little worth comparing in this data, since the concentration end points for SME dewatering were varied. Any contribution of this data to material balance closure was discussed elsewhere. Values of (F-3N) were calculated from this data for redox estimation purposes in the main report.

Appendix F: Supplemental Data From the Test Runs

Not all plots prepared in support of some of the statements made in the text were given in the main body of the report. Additional plots are given in this appendix. The first figure is a composite gas generation/consumption plot analogous to Figures 14 and 18 given in the main text for runs SB2-1 and SB2-4. This plot is for SB2-3, the run with HM levels of noble metals.

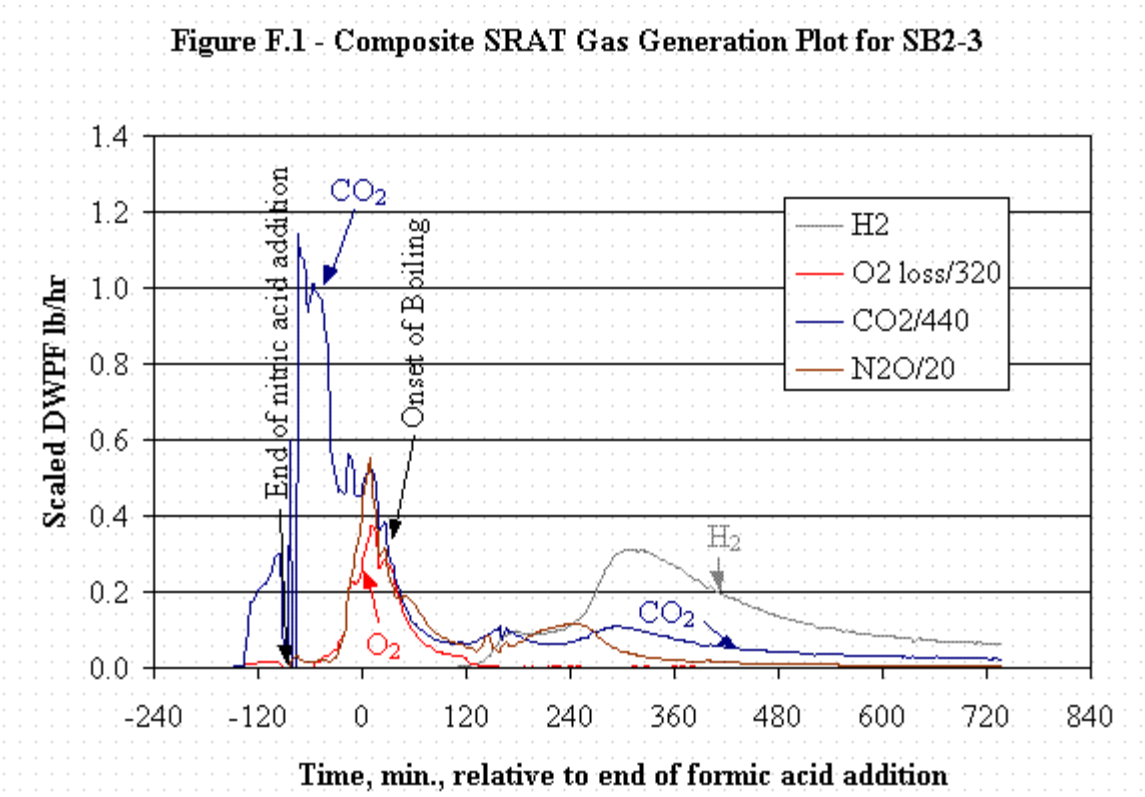

The correlation of oxygen consumption with some, but not all, of the periods of peak carbon dioxide and nitrous oxide generation was again observed. In the later part of the SRAT cycle, the carbon dioxide and hydrogen seem to be tracking. The molar generation rate of CO_2 is roughly 6-7 times greater than the molar generation rate of H_2 during the last half of the SRAT cycle.

The next figure is the corresponding plot, similarly scaled for scoping run 4B at 110% acid. Notice the relative lack of gas generation activity from 120-840 minutes in this figure compared to the plot above and to the plots for SB2-1 and SB2-4 given in the main text. This was attributed both to the presence of less total acid, but also to the lack of nearly complete nitrite ion destruction and corresponding increase in catalytic activity. Complete nitrite ion destruction was not defined as <1000 ppm in this context, but as <10 ppm. This was extrapolated to be a readily achievable upper bound on nitrite ion concentration in the 125% acid runs, given the observed rate of decline in nitrite while it was still measurable.

Figure F.2 - Composite SRAT Gas Generation Plot for 4B - 110% acid

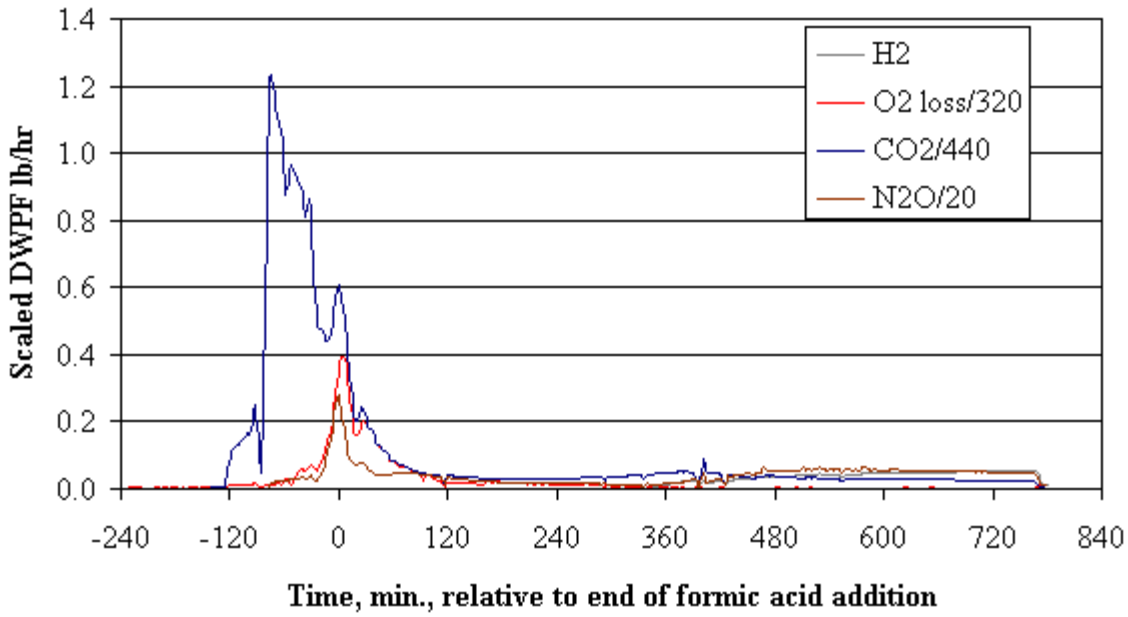

The ratio of CO_2 to H_2 as molar generation rates in the latter part of the SRAT cycle ranged from about 9 - 21 and seemed less constant than in some of the runs with more acid.

The next plot, Figure F.3, is for scoping run 2B, at 137.5% acid.

Figure F.3 - Composite SRAT Gas Generation Plot for 2B - 137.5% acid

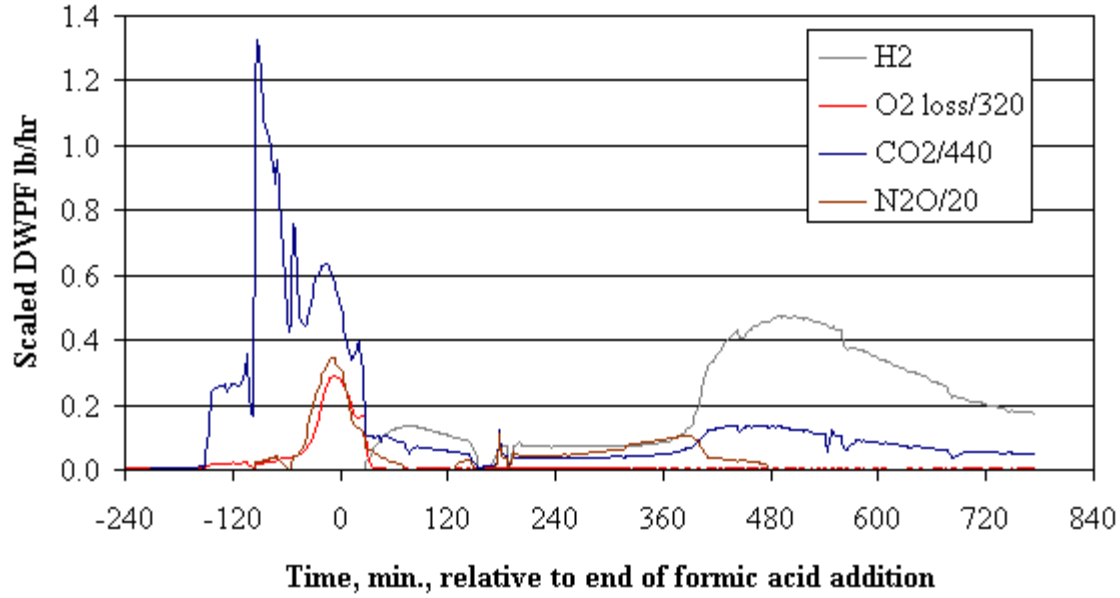

Again the oxygen consumption was seen to be tracking some of the CO_2 features and some of the N_2O features, e.g. at about -50 minutes all three jump together, peak out, and start to fall together. From about 360 minutes on the hydrogen and carbon dioxide rates track, but the molar generation rate ratio is about 6 to 1 CO_2 per H_2.

A pseudo-first order rate constant was derived for scoping run 4B (8/40 blend with 110% acid stoichiometry). This run was the only run with enough non-zero data to make a meaningful calculation. The data are shown in the figure below. Only a very simple kinetic model was used, and no account was taken of the volume reduction that occurred during dewatering (about 10%).

Figure F.4 - Nitrite Consumption at 110% acid in 4B

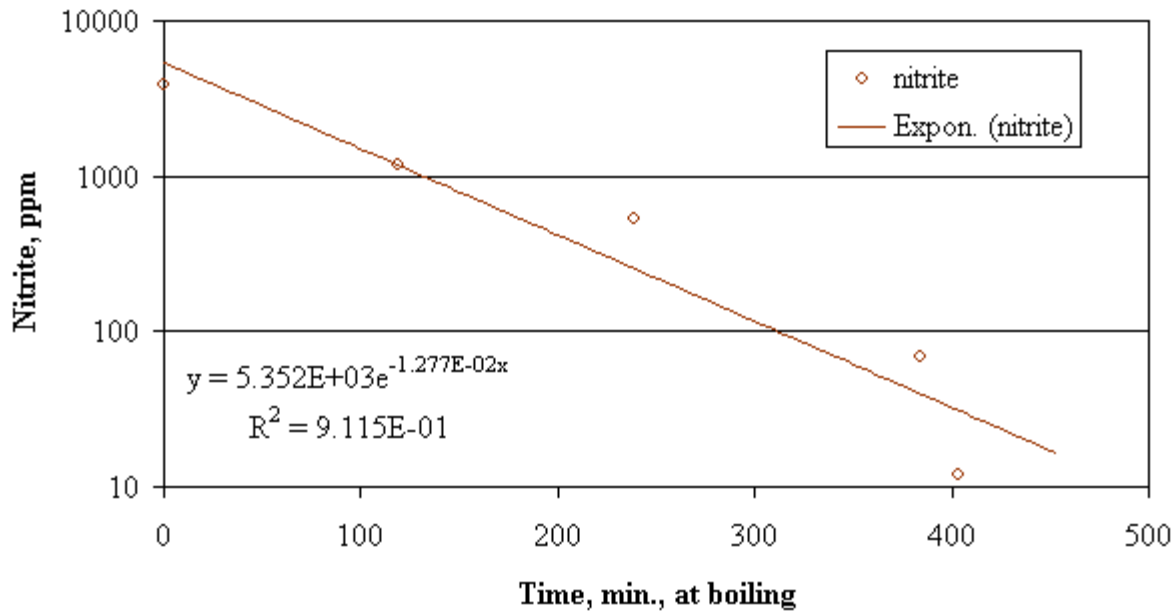

The test was shut down for the night between the 380 and 400 minute samples. Differences in these two samples are supposed to give an idea of how much happens to the SRAT material during the shutdown period (ideally nothing). Mobile Lab performed these measurements and would generally not report the values below 100 as numbers, but as <100 ppm. An exception was made for this data. The derived first order rate constant is about 0.013/minute. This is almost three times greater than the value obtained during GFPS testing with Tank 42 simulant at 137.5% acid last summer (which was 0.0049/minute [Koopman]).

This data was interpreted to mean that 110% acid with Tank 8/40 blend represented a higher effective acid content than 137.5% acid with Tank 42 simulant – from a nitrite ion destruction perspective. (Similarly, the pseudo-first order rate constant at 125% acid with Tank 8/40 blend is probably > 0.02/minute. Taken altogether it appeared that an acid stoichiometry somewhere less than 110% would be needed to duplicate the low nitrite destruction rate seen in the Tank 42 testing.) This nitrite ion perspective was supported by the hydrogen generation rate data. There was a higher hydrogen generation rate in the Tank 8/40 blend testing at 110% acid than there was in the Tank 42 testing in the GFPS at 137.5% acid. More investigation into the differences between these simulants from an acid calculation stand-point is recommended.

Formate ion consumption can be approximately analyzed in a similar fashion. Pseudo-first order rate constants were obtained (as a function of formate ion concentration) for scoping runs 1A, 1B, 2B, 3B, SB2-1, and SB2-4 and are summarized in the table below.

Table F.1 – Formate Consumption Pseudo-First Order Rate Constants

Run	Rate constant, inverse minutes	pH of supernate	Correlation, R^2
1A (Tank 40, 137.5% acid)	0.0026	9.7	0.977
1B (137.5% acid)	0.00071	7.5	0.865
2B (137.5% acid)	0.00043	6.5	0.960
3B (125% acid)	0.00022	6.5-7.4	0.876
SB2-1 (125% acid, nominal)	0.00021	6.8-7.8	0.580
SB2-4 (290%, etc.)	0.00076	6.3-6.5	0.803

Formate loss and loss rate was greatest during scoping run 1A. The 0.0026/minute is not a typographical or transposition error for 0.00026/minute. The other two Tank 40 runs (2A and SB2-2) had insignificant formate ion changes by correlation. Noble metals fell from 1B to 2B. 2B, 3B, and SB2-1 had identical noble metal loadings. SB2-4 was close to 1B noble metals. Scoping run 4B (110% acid) had an insignificant formate ion change by correlation. Interestingly, SB2-3 with HM levels of noble metals showed an insignificant change in formate ion. The most obvious thing that 2A, 4B, SB2-2, and SB2-3 (the four runs not included in the table) all have in common is a much lower silver content than the six runs tabulated above. Precise figures on all noble metals are given in Table 3 in the main body of the report.

Although the regression correlation for formate ion destruction was not outstanding for SB2-1, the regressed rate constant was similar to that in corresponding scoping run, 3B. Both SB2-1 and 3B had a smaller pseudo-first order rate constant than 2B, presumably reflecting a secondary effect derived from the acid stoichiometry. This effect could be an increased catalytic activity of the noble metals at higher acid stoichiometry. Acidity as measured by the pH of SRAT product supernate did not seem to correlate with the rate constant data, although SRAT product pH is not an accurate measure of pH during the SRAT cycle. Time did not permit a more detailed examination of pH data coupled to the rate constant and liquid concentration data. When no pH range is indicated, the single number given was measured with the same instrument that gave the lower bound of the range data. These were TNX measurements with a portable pH meter calibrated with pH 4 and 10 buffers. The upper bound pH measurements were made by Mobile Lab (7.4, 7.8, and 6.5).

Figure F.5 gives the composite gas generation plot for the SB2-2 SRAT cycle. There is not much to see, since carbon dioxide is the only gas evolved in significant quantities.

Figure F.5 - Composite Gas Generation Plot for SB2-2

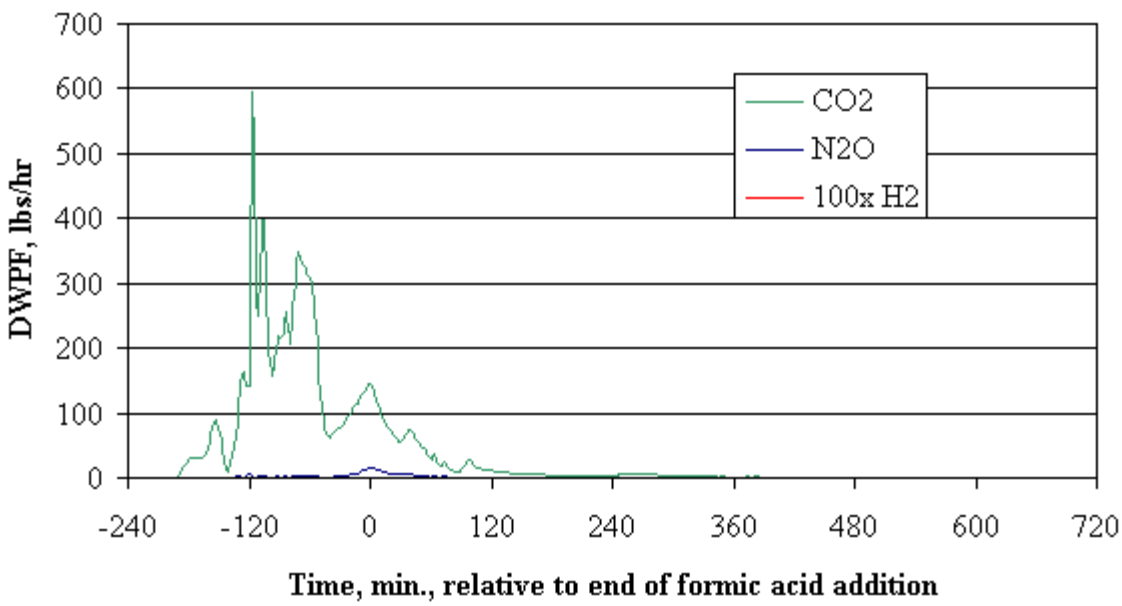

There is the usual simultaneous peak just at the end of acid addition for carbon dioxide and nitrous oxide generation. The onset of boiling came at about +35 minutes. Hydrogen generation was essentially negligible.

Appendix G: Run Details

The ten individual run plans were issued separately as a prerequisite for each scoping and variability study test. The following list documents all ten test runs.

1A: W. E. Daniel, Run Plan for Melter Feed Preparation of Tank 40 in the Defense Waste Processing Facility (DWPF) (U), SRT-PTD-2000-00039, Rev. 0, July 25, 2000.

2A: D. C. Koopman, Tank 40 Scoping Run #2 with Reduced Levels of Noble Metals (U), SRT-PTD-2000-43, Rev. 0, August 5, 2000.

1B: W. E. Daniel, Scoping Run Plan for Melter Feed Preparation of Blended Tank 8 and Tank 40 In the Defense Waste Processing Facility (DWPF) (U), SRT-PTD-2000-00041, Rev. 0, July 27, 2000.

2B: D. C. Koopman, Tank 8/40 Blend Scoping Run #2 with Reduced Levels of Noble Metals (U), SRT-PTD-2000-44, Rev. 0, August 7, 2000.

3B: D. C. Koopman, Tank 8/40 Blend Scoping Run #4 with 125% Acid (U), SRT-PTD-2000-47, Rev. 0, August 9, 2000. (Blend scoping run #4 became 3B and #3 became 4B, because it made sorting the runs by changing acid more natural)

4B: D. C. Koopman, Tank 8/40 Blend Scoping Run #3 with 110% Acid (U), SRT-PTD-2000-46, Rev. 0, August 9, 2000.

SB2-1: D. C. Koopman, Tank 8/40 Sludge Blend Run SB2-1 with Nominal (125%) Acid (U), SRT-PTD-2000-48, Rev. 0, August 14, 2000.

SB2-2: D. C. Koopman, Tank 40 Run SB2-2 with Typical (137.5%) Acid (U), SRT-PTD-2000-49, Rev. 0, August 14, 2000.

SB2-3: D. C. Koopman, Tank 8/40 Sludge Blend Run SB2-3 with Nominal (125%) Acid and HM Noble Metals (U), SRT-PTD-2000-51, Rev. 0, August 22, 2000.

SB2-4: D. C. Koopman, Tank 8/40 Sludge Blend Run SB2-4 with Maximum Acid and Worst Case Noble Metals (U), SRT-PTD-2000-52, Rev. 0, August 22, 2000.

Copies of the ten run plans were incorporated into the two lab notebooks used to record run data.

DWPF parameters were scaled to fit the 4-liter kettle used for this testing. The following DWPF parameters were assumed as a basis:

1. Sludge is charged to the SRAT at 6000 gallons (13-19 wt. %).
2. There is no heel in the SRAT.
3. The sludge transfer is flushed with 500 gallons of water (conservative-low).
4. Heat-up to 93° C for acid addition occurs at the rate of about 1° C/min.
5. Nitric acid is fed at 50 wt. % and at a rate of 2 gpm.
6. Formic acid is fed at 90 wt. % and at a rate of 2 gpm.
7. The SRAT is de-watered to remove the volume of acid and flush water added.
8. The SRAT is refluxed after dewatering until at least twelve total hours at boiling have passed.
9. The antifoam original and revised bases were discussed in the main report.

10. The nominal, net composition of frit, water, and formic acid added to the SME cycle is 45 wt. % frit and 55 wt. % of a 1.5 wt. % solution of formic acid in water.

The scale-factor for all masses and volumes between DWPF-scale and these test runs was 1/9000 (1/9003, officially). Since formic acid and nitric acid were not available at precisely 90 and 50 wt. %, the scaled flow rates were adjusted upwards, so that the delivery rate of each acid was $1/9000^{th}$ of 2 gpm at the nominal strength. This kept the time to deliver a certain acid stoichiometry constant regardless of acid strength. The "frit slurry" was actually added as three individual components: dry frit, water, and ~90 wt. % formic acid, which total to the correct equivalent scaled mass. This has been the historical practice in ITS, both for bench-scale and $1/240^{th}$ Glass Feed Prep System runs.

The redox calculation has been documented previously, see Lambert and Boley [1998]. This spreadsheet was not modified (other than in the sludge input parameters that are unique to either Tank 40 or the Tank 8/40 blend simulants versus previous sludge simulants).

One of the 4-liter kettles was broken during cleaning between runs, and another was substituted. All glassware was thoroughly cleaned between runs. Several kettle pH probes were ruined over the course of all testing. The best probes found to date can remain reliable for perhaps two full SRAT/SME simulations under the aggressive temperature and process slurry conditions. One probe cracked, but did not lose its integrity. It read normally through the run and post-run cal check. There was some blackening of the agitator blades and shaft noticed following Tank 40 scoping run 1A. Some of this material was recovered dry, and some was presumably recovered in solution after soaking the blades in concentrated nitric acid. Samples of both were submitted for analysis, but no results have been received as yet.

Appendix H: Transmittal of PCCS Calculations by W. E. Daniel and K. G. Brown

The following cc.mail documents the transfer of PCCS results for Tank 40 and Tank 8/40 sludge used in the recipe calculations for the SME cycle of the four variability study runs.

Author: Gene Daniel at SRS
Date: 10/6/00 12:42 PM
Normal
TO: David Koopman at SRCCC05
CC: Kevin Brown at SRCCC08
CC: Sharon Marra at SRS
Subject: Re: Documentation of Sludge Batch 2 Simulant Work
---------- Message Contents

Dave,

The previous e-mail was in response to what Dan wanted which I thought was the same. The following results were derived using the "developmental" PCCS (as described in the previous e-mail) on August 15, 2000. Measurement Acceptable Regions were found for Tank 40 and Tank 8/40 blends as follows:

Tank 40 - Frit 200 MAR

Sludge	Frit	Constraint
0.237	0.763	Current Liquidus
0.188	0.812	Homogeneity

Tank 8/40 - Frit 200 MAR

Sludge	Frit	Constraint
0.252	0.748	Current Liquidus
0.209	0.791	Homogeneity